Variation in Soil Properties and Topographic Roughness of Stabilized Sand Dunes in the Central Great Plains, USA: *Implications for Susceptibility to Reactivation*

By

KEVIN G. McKEEHAN

A thesis submitted for the partial fulfillment of the requirements for the degree of

MASTER OF SICENCE
(GEOGRAPHY)

At the

UNIVERSITY OF WISCONSIN-MADISON

2018

Date of final thesis defense: December 6, 2018

The thesis is approved by the following members of the Final Thesis Committee:
Joseph A. Mason, Professor, Geography
Erika Marín-Spiotta, Associate Professor, Geography
Ken Keefover-Ring, Assistant Professor, Botany and Geography

TABLE of CONTENTS

LIST of FIGURES

LIST of TABLES

ACKNOWLEDGEMENTS

This thesis would not be possible without the assistance of many people, in ways large and small. Foremost, I'd like to thank my advisor, Joseph Mason, for his wise guidance, bottomless patience, flexibility in matters academic and personal, and for answering hundreds of questions, always promptly. He took two different chances on me and never made me feel as though I didn't belong in academia. I would also like to thank the other members of my thesis committee: Erika Marín-Spiotta and Ken Keefover-Ring. Dr. Marín-Spiotta provided me with scientific guidance at key moments, important suggestions, and the use of her laboratory. Dr. Keefover-Ring supplied me with early encouragement during my time here at the University of Wisconsin-Madison.

Several others in the Department of Geography need to be recognized for their contributions to this research and my advancement. I would like to thank the Trewartha Graduate Research Award committee for providing me with the funds to conduct field research in Nebraska. Further, I am gratefully indebted to the two graduate student coordinators during the last few years: Sharon Kahn, who got me started, and Marguerite Roulet, with whom I finished. Ann Olsson helped me with the carbon and nitrogen experiments and in learning laboratory protocols. Laura Szymanski provided crucial advice along the way. In addition to those individuals, many people at this fine university provided important assistance, including Lisa Naughton, Matthew Turner, A-Xing Zhu, Jack Williams, Lucas Zoet, Shaun Marcott, Meghan Kelly, and Zhe Yu Lee, and many others. The University of Wisconsin-Madison is a special place and I am eternally appreciative for what I have learned here and to be forever connected to this institution.

Finally, but not in the least, I'd like to thank my parents, Gene and Vickie McKeehan, for their unwavering support of this dream. Likewise, I'd like to thank my sons, Finley and Kellan, who helped me in the field, and for Noah who very much wanted to go. I'd also like to offer my deepest appreciation to Dr. Menglin Wang for support in ways that cannot be overestimated.

ABSTRACT

With a warming global climate, regional climates will undergo changes to their temperature, precipitation, and wind regimes. Consequently, the potential exists for these shifting climatological conditions to affect dunefields across the globe. Sand dunes are found in two states – active and stable, or unvegetated and vegetated, respectively – and the activation of previously stable dunes could have serious ramifications for communities and ecosystems. Yet, the mechanisms of dune reactivation and stabilization are not fully understood.

In research presented here, the links between dune and soil variables and dune status are explored within four dunefields in the state of Nebraska on the central North American Great Plains. Specifically, the links between soil particle size, loss-on-ignition (LOI), cation exchange capacity (CEC), soil carbon and nitrogen, and dune surface roughness, which is interpreted as a proxy for relatively recent dune activity, are examined from soil samples taken in the field and GIS analyses. Results show that dunes suspected of a more recent activity because of their rougher surface topography, contain fewer fine particles in surface soils and have low levels of the other soil variables, indicating relatively weak pedogenesis. Likewise, dunes that are surficially smoother and therefore assumed to have been more stable in recent times, have surface soils containing more fine particles, more soil organic carbon, nitrogen, LOI, and a greater CEC. These results suggest pedogenic-geomorphic feedbacks which may incline stable dunes toward increased stabilization and recently active dunes toward future reactivation. For example, frequently reactivated dunes create a choppy, rough landscape which may experience particularly high shear stress during strong winds, making the dunes susceptible to reactivation and less likely to undergo more significant pedogenesis including development of finer texture and accumulation of more soil carbon. This tendency toward stabilization or reactivation has resulted in dunefields with contrasting soil development and surface topography across the study area, despite similar environmental settings.

Variation in Soil Properties and Topographic Roughness of Stabilized Sand Dunes in the Central Great Plains, USA: *Implications for Susceptibility to Reactivation*

A Research Thesis by Kevin McKeehan

December 19, 2018

CHAPTER 1: Introduction and Literature Review

Introduction

With a warming global climate, regional climates will undergo changes to their temperature, precipitation, and wind intensity regimes. Consequently, the potential exists for these shifting climatological conditions to affect dunefields across the globe. Sand dunes are found in two states – active and stable, or unvegetated and vegetated, respectively – and the activation of previously stable grassland dunes could have serious ramifications for communities and ecosystems (Barchyn and Hugenholtz, 2013a; Schmeisser et al., 2009; Thomas et al., 2005). Yet, the mechanisms of dune reactivation and stabilization in grasslands is not fully understood (Barchyn and Hugenholtz, 2013b; Siegal et al., 2013). Research has shown dune status is dependent upon wind strength, drought duration, and several other factors (Barchyn and Hugenholtz, 2013b; Kocurek and Lancaster, 1999). Clearly, climate is a dominant factor (Hugenholtz and Wolfe, 2005; Mason et al., 2011, 2009; Miao et al., 2007; Xu et al., 2015) along with disturbance (Bo et al., 2013; Meir and Tsoar, 1996) in controlling dune activity, but dune and soil geomorphology are linked to dune status in important ways that are not fully comprehended.

In research detailed in this paper, the links between dune and soil variables and dune status are explored. Previous studies have found that important soil and dune characteristics with regards to dune status are soil moisture, soil texture, dune morphology, dune age, and type and composition of vegetation cover (Barchyn and Hugenholtz, 2013b; Siegal et al., 2013; Werner et al., 2011). This study focuses on some of these same variables with respect to the A, AC, and C horizons in

dune soils, including any paleosols – soil particle size, loss-on-ignition (LOI), cation exchange capacity (CEC), soil carbon and nitrogen and dune surface roughness, which is interpreted as a proxy for relatively recent dune activity, particularly in the form of blowout development.

In the dunefields of the Great Plains, some areas display a distinctly "choppy" surface topography at spatial scales from 10s of m^2 up to about 1 km^2, while adjacent parts of the same dunefield are characterized by smoother surfaces. Closer examination, especially with high-resolution LiDAR-based elevation data, reveals that the "choppiness" is largely due to complexes of blowouts and small parabolic dunes. Choppier, rougher surface features clearly suggest recent local aeolian reworking of the dune surface. Where the surface is smoother, the topography reflects either dune reactivation in the more distant past or the topography of larger dune forms. Even smooth dune forms could contain localized roughness that could represent older blowouts and small dunes that have been made less distinct by local redistribution of soil by bioturbation, rainsplash, or slopewash.

The basic hypothesis underlying this study proposes that finer soil textures, significant organic carbon and nitrogen accumulation, and greater CEC and LOI, together indicating modestly advanced pedogenesis, would be observed on smoother dunes with less indication of recent activity. Conversely, it was expected that areas exhibiting a rougher dune surface will display minimal to very weak soil development, including a coarser texture, a lack of organic carbon and nitrogen accumulation, and low CEC and LOI. This hypothesis is based on the assumption that longer-term dune stability provides more time for soil and plant community development, which would have fostered the conditions allowing soil organic carbon and nitrogen accumulation. Moreover, once colonized by grasses, the vegetated dune surface would trap fine aeolian dust dominated by silt and clay particles, which would contribute to higher CEC along with the accumulation of more organic matter.

Importantly, this hypothesis implies that persistent dune stability should enhance productivity of the grassland ecosystem and allow vegetation growth to more effectively compete with aeolian erosion and deposition, by increasing availability of nutrients and water (plant water availability was not measured in this study but is assumed to increase with silt and clay content). In other words, dune stability should lead to conditions favoring persistence of stability in a positive feedback. The opposite would be true of more active dunes, which due to their lack of stabilizing soil features would have a persistently low threshold for reactivation. As a result of reactivation, silt-sized dust particles would quickly be re-entrained by the wind, maintaining a coarse soil particle size, lower CEC, and less moisture retention. Frequent reactivation would also limit organic carbon and nitrogen accumulation and limit LOI.

In work conducted in dunefields in the central North American Great Plains and presented here, the hypothesis of the study was largely supported, with exceptions. Areas of suspected relatively recent dune activity exhibited significant differences in the targeted variables from those areas where the most recent dune activity may have occurred earlier in the Holocene. Regional dunefields may exhibit significant differences in sedimentary characteristics, echoing recent studies examining the geochemical provenance of aeolian sand in dunefields and downwind loess in the central Great Plains (Muhs, 2017; Yang et al., 2017). These differences may influence the rate and magnitude of pedogenesis on the dunes, potentially complicating identification of relationships between dune stability and pedogenesis. To encompass at least some of the possible range of sedimentary variation, samples were extracted from sites in four distinct dunefields in the US state of Nebraska – the Nebraska Sand Hills, the Imperial Dunefield, the Lincoln Dunefield, and an area termed here as the Sioux Dunefield. These four dunefields, which are largely inactive at present, but have been active several times since the late Pleistocene, are spatially separate, spread over an area of nearly 65,000 km^2, but they are often grouped together in meta-analyses (Halfen and Johnson, 2013).

The results presented here reveal potential differences between these dunefields with regards to variables representing soil development. Each of the four dunefields exhibited a distinct pattern of variation by horizon for soil particle size, LOI, CEC, and organic carbon and nitrogen. This suggests possible effects of different parent materials, related to different provenance, and/or differing regional histories of dunefield activity and pedogenesis. These two findings – that 1) soil and surface differences exist between more active and more stable dunes and that 2) dunefields in relative regional proximity are potentially distinct – might enable a better understanding of the mechanisms that control aeolian system and dunefield state, as proposed by Kocurek and Lancaster (1999) and Barchyn and Hugenholtz (2013b). The results here possibly detect patterns and variable relationships in these four grassland dunefields. As stabilized grassland dunefields, such as those found on the Great Plains, are sensitive to drought and reactivation, linking soil and dune characteristics to dunefield state and recent history of reactivation could assist researchers to understand how these landscapes will respond to climate change in the future and perhaps make sensitivity predictions.

Literature Review

The reactivation of stabilized grassland sand dunes as the result of a warming global climate is a significant concern. The active movement of massive amounts of sand is a destructive force to communities and ecosystems (Barchyn and Hugenholtz, 2013a; Knight et al., 2004; Loope et al., 1999; Schmeisser et al., 2009; Thomas et al., 2005; Wang et al., 2016), while a warming global climate presents challenges for soil resources (Adewopo et al., 2014). The destructive forces of aeolian sand in arid and semiarid lands have altered agricultural processes, displaced peoples, destroyed infrastructure, and caused ecosystem migrations and adaptations. In some semiarid regions, where stabilized sand dunes are found, global climate models show the potential for warming this century, possibly driving dune reactivation in those landscapes (Feng and Fu, 2013).

These sensitive semiarid regions include grasslands of stabilized dunes which were once active during drought conditions in the Holocene and/or Late Pleistocene and, consequently, could be reactivated in response to increased warming and aridity in the future. The grasslands of southern Africa's Kalahari Desert, for example, could transition completely to active dunes by 2099, according to model simulations (Thomas et al., 2005), although the results of other models show a low probability for mass reactivation in the region (Ashkenazy et al., 2012), and still other analyses suggest a variety of responses in arid environments to climate change (Gremer et al., 2015). Regardless of the scale of reactivation in the Kalahari Desert, currently stable grassland dunes there will likely become active at an increasing rate in this century. The results of such a transition would include the degradation of soil, the collapse of agricultural systems, and a decline in air quality due to the effects of airborne dust and aeolian deposition (Thomas et al., 2005). A recent study focusing on the mid-North American continent underscored these threats for the Great Plains. Researchers reconstructed the historic regional megadroughts of the Holocene, which coincided with active sand events in the Great Plains, and identified the extent of drought conditions that led to the collapse of major prehistoric cultures (Cook et al., 2016).

One grassland region comprised mostly of stabilized dunes is the west central Great Plains of North America, specifically the western two-thirds of the US state of Nebraska. This region included the Nebraska Sand Hills and associated nearby dunefields. The Sand Hills, which are the largest stabilized dunefield in North America, and the smaller dunefields nearby are sensitive to changes in temperature, precipitation, and wind potential and, thus, provide geologic evidence of environmental and climatic change during the late Quaternary period (Forman et al., 2001; Mason et al., 2011). Researchers have studied this region closely to determine the nature of Quaternary climates, grassland dune response, and aeolian processes. In times of sustained drought or other conditions limiting growth of dune-stabilizing vegetation during the Pleistocene and Holocene, studies have shown the Sand Hills mobilize into active dunes, while stabilizing in

response to more favorable conditions for plant growth (Ahlbrandt et al., 1983; Halfen and Johnson, 2013; Mason et al., 2011, 2004, 2003).

Signals left in dune sand, paleosols, and associated downwind loess by these megadroughts and wet periods are evidence for the grassland dune sensitivity in the Sand Hills and Great Plains regions. Using optically stimulated luminescence (OSL) and radiocarbon (^{14}C) methods, along with geomorphological observations, evidence of significant droughts throughout and prior to the Holocene can be found in stabilized grassland dune sands (Forman et al., 2008, 2005, Halfen et al., 2016, 2012; Halfen and Johnson, 2013; Hanson et al., 2010, 2009; Mason et al., 2004; Miao et al., 2007; Puta et al., 2013). Dating of eolian sand within stabilized dunes suggested significant dune activation affected the region between 20-25ka (Mason et al., 2011), in the early-mid Holocene, after 9-11 ka (Halfen and Johnson, 2013), and at several later times during the Holocene. Significant drought events across the Great Plains occurred within the last 1,500 years, activating stabilized sand dunes that reflected a response to episodically drier conditions (Forman et al., 2008, 2005; Halfen et al., 2012; Hanson et al., 2009; Mason et al., 2004, 2003). Sand activation occurred during important climatic events such as the Medieval Climatic Anomaly (MCA) (Forman et al., 2008, 2005; Halfen et al., 2012; Mason et al., 2004; Miao et al., 2007; Schmeisser McKean et al., 2015; Schmeisser et al., 2010) and, more recently, the event in the 1930s known as the Dust Bowl (Forman et al., 2008, 2005), although the effects from this latter event were far more pronounced in the southern Great Plains (Worster, 1982) and may not have reactivated dunes in the state of Nebraska (Cronin and Beers, 1937). The arid event 800 to 1,000 years ago coinciding with the MCA was also accompanied by a shift in spring-summer prevailing winds, from moisture-laden southern winds from the Gulf of Mexico to southwesterly dry winds (Sridhar et al., 2006), underscoring the sensitivity these landscapes have to changes in climate. The entire Great Plains region has this susceptibility to drought and climate change. For example, dunefields to the east (Hanson et al., 2009), to the south (Arbogast, 1996; Hanson et

al., 2010; Werner et al., 2011), and farther west in Colorado have histories of Holocene and Pleistocene dune activity as well (Clarke and Rendell, 2003; Muhs et al., 1996). One study from Colorado suggested a geomorphic boundary defined by climate exists between more active northeastern Colorado dunefields and the dunefields of Nebraska (Muhs and Maat, 1993), the latter of which are the focus of this study.

Further evidence for many of these droughts can be found in loess deposits mantling landforms downwind of the Sand Hills. Loess is a generally silt-sized material deposited via aeolian means (Brady and Weil, 2010; Schaetzl and Anderson, 2005), although definitions for loess vary (Follmer, 1996). Silt-sized grains are transported in suspension, potentially high above the ground surface, in contrast to larger, coarser particles, such as sand, which saltates and creeps across the surface (Bagnold, 1941). Initially proposed to be exclusively glacial in origin, loess often is a product of fine material resulting from glacial abrasion and deposited by glacio-fluvial processes (Chamberlin, 1897). Yet, some loess has been classified as "desert loess", a fine material with origins upwind in sand dunes and eroded bedrock (Smalley and Vita-Finzi, 1968). Although the origin of loess downwind from the Sand Hills in central and eastern Nebraska has been disputed in the past (Follmer, 1996; Lugn, 1968; Winspear and Pye, 1995), more recent work demonstrates that most of it is of nonglacial origin, ultimately derived from rocks cropping out in unglaciated areas of western Nebraska, South Dakota, and Wyoming (Aleinikoff et al., 2008; Yang et al., 2017). Thickness and grain size trends demonstrate that much of the loess was last entrained by the wind within the Sand Hills, however, where it was temporarily deposited on its way from more distant sources (Mason, 2001; Mason et al., 2003). This observation implies that the dunes and loess are geomorphically linked, with the loess only likely to have been re-entrained from the dunes and deposited farther downwind if the dunes were active (Mason, 2001), and OSL dating of dunes and loess confirm that episodes of dune activity and rapid loess accumulation were approximately synchronous (Mason et al., 2011; Miao et al., 2007).

Conversely, buried paleosols found between distinct loess and sand layers throughout the Great Plains represent signals of warmer, wetter climatic periods in which grassland sand dunes and loess deposition slowed or ceased. The Brady Soil, a paleosol found throughout much of the loess region of the central Great Plains, represents a wetter interlude in the late Pleistocene to early Holocene, during which the Sand Hills largely stabilized and loess deposition slowed to low rates (Marin-Spiotta et al., 2014; Mason et al., 2011, 2008).

The tendency of stabilized sand dunes in the Great Plains in general, and the Sand Hills region in particular, to respond to climatic warming and drought events by reactivation is important for this study and in the context of predicted atmospheric conditions for the remainder of this century. Some regional climate models focusing on the mid-North American continent predict a rise in mean annual temperature (MAT) and aridity in the region (Feng and Fu, 2013; Galatowitsch et al., 2009; King et al., 2015; Ray et al., 2008). Unfortunately, precise predictions for the Sand Hills region of the Great Plains are difficult to ascertain, as the granularity of some models is relatively coarse. Nevertheless, some generalized predictions are useful background this thesis. One study compared the results from climate prediction models for the late 21st Century with the megadrought conditions during the MCA and found the southern and central Great Plains would likely enter a period of severe episodic drought surpassing the MCA conditions by the year 2050 (Cook et al., 2015). A study focusing on climate change to the northeast of the Sand Hills found a likely rise in MAT of 3°C with a nominal increase in mean annual precipitation (MAP) (Galatowitsch et al., 2009). The study found the most analogous present-day climate for the US state of Minnesota in 2070 to be the current climate regime of northeastern Kansas and northern Missouri. Research focusing on the far western edge of the thesis study area also found a rise in average summer and winter temperatures for northeast Colorado by 2050 (Ray et al., 2008).

Other, more granular models supported a moderate rise in aridity for the Great Plains (Feng and Fu, 2013; King et al., 2015).

If these studies were to come to fruition, climate trends might tend toward episodic drought or could perpetuate a climatic bifurcation of Great Plains region. Currently, the state of Nebraska sits astride a climate divide roughly along the 98th-100th meridians, with the eastern plains located in the humid continental climate zone and the western extent in a semiarid climate zone (Hanson et al., 2009; May, 2003). With climate models predicting a rise in MAT and MAP for areas just east of the Sand Hills and a decrease in precipitation in the western extremities of the study area, it would seem possible the temperature and precipitation gradient running longitudinally through the state will deepen, with the Sand Hills and nearby dunefields potentially straddling this gradient. Such changes also would herald a likely alteration of the current local ecosystem of the Sand Hills and disturb agricultural yields, according to modeling (Ko et al., 2012; Williams et al., 2007). Currently, the Sand Hills and dunefields of this study are astride unique ecotones between the mixed and tallgrass prairies of eastern Nebraska's loess plains and the sandsage prairies of the state's far western scrublands (Dunn et al., 2016). The primary plant communities of the Sand Hills and the nearby dunefields have been designated as Sand Hills and sandsage grasslands and include species uniquely adapted to high sand contents in soil and dunefield morphology.

For these reasons, the Sand Hills and associated nearby dunefields of this study provide the opportunity to research stable grassland dune systems. Yet, the causes of dune reactivation in stabilized grassland dune systems are still not fully understood (Barchyn and Hugenholtz, 2013b; Siegal et al., 2013), but several factors are linked and influence each other. Dune reactivation has been postulated to be a function of climate, disturbance, and/or soil characteristics (Barchyn and Hugenholtz, 2013b). Attempts to understand the importance and interaction of these factors

has led to the formulation of theoretical models that attempt to conceptualize dune formation, movement, morphology, and status as a system (Bagnold, 1941; Barchyn and Hugenholtz, 2013b; Kocurek and Lancaster, 1999). Bagnold (1941) studied the conversion of aeolian deposits into dunes and proposed a series of sand dune types. Kocurek and Lancaster (1999) viewed the dunefield system on both temporal and spatial scales, explaining the development of a dunefield and its state at a given time as the result of complex interactions between the supply of sediment (often originally from sources distant from the dunefield basin), the availability of the sediment for wind transport (often controlled by vegetation), and the potential of the wind to transport sand. They identified nine categories of dune state based on the local sediment supply, sediment availability, and transport capacity, as well as time lags in sediment influx. Barchyn and Hugenholtz (2013b) conceived of a state factor model focused on current dune state with a goal of forecasting potential for reactivation. They classified four stages of dune state from stable to active based on dune vegetation and a geomorphological examination of dunefield blowouts. This approach has the benefit for this study to be temporally contemporary with an eye cast toward reactivation potential.

Other pertinent research focused less on dunefield system dynamics and more on response to climate. The reduction of vegetative cover on dunes, resulting in dune reactivation, has been linked to prolonged drought or episodic aridity in several studies (Mason et al., 2004; Miao et al., 2007; Muhs and Holliday, 2001; Siegal et al., 2013). The inverse effect was discovered in dunes which had stabilized due to decreased wind potential, leading to the advance of vegetation (Xu et al., 2015), further reinforcing the link between climate and dune activity. Research involving grassland dune systems in Alberta and Saskatchewan found that dunes tended toward a stabilized status within the last 200 years due primarily to rising MAT — possibly through the effect of a longer growing season on the competition between vegetation growth and sand movement — as well as less arid conditions (Wolfe and Hugenholtz, 2009).

Despite these studies linking dune activity to climatic factors including moisture availability, wind strength, and temperature or growing season length, it does not appear likely that simple thresholds defined by, e.g., available moisture or wind strength can fully explain the state of dunefields. A widely-used model to predict dune activity based solely on such climatic thresholds (Lancaster, 1988) sometimes fails to accurately predict the amount of activity on the ground (Hugenholtz and Wolfe, 2005; Muhs et al., 2003; Werner et al., 2011). The persistence of bare sand adjacent to stable grass-covered dunes under the same climatic conditions is difficult to reconcile with the concept of simple climatic thresholds separating active and stable states (Yizhaq et al., 2007). A study from the southwestern Great Plains in North America found that local patches of dunes were active at times in the Late Holocene while adjacent aeolian sand sheets were not, indicating the same kind of juxtaposition of stable and active patches in the past (Werner et al., 2011). Research from dune fields in China suggested a lagged response between dune activity and climatic variation (Lu et al., 2005). A study from the Negev Desert in southern Israel found extended droughts to have more impact on arid dunes in the southern Negev than semiarid dunes to the north that received more precipitation, suggesting a complex relationship between climate, vegetation, and geomorphology (Siegal et al., 2013). Yizhaq et al. (2007, 2009) used relatively simple mathematical models of competition between sand transport and vegetation to argue that bistability (coexistence of stable and active states) is a common feature of dune systems.

Vegetation plays a key role in linking climate change to dune activity, in both simple and complex models. Mechanically, vegetation anchors the stabilized surface crust (if present) and soil, while also absorbing part of the wind stress and thereby reducing stress on the sand surface. Observing a link between vegetation and dune activity, a range of studies have found that vegetation variables were influenced by, but worked on a different temporal scale, from climate, driving reactivation and stabilization processes. Sand flux on dunes was shown to decrease with

vegetative cover in an exponential relationship (Lancaster and Baas, 1998). A Nebraska Sand Hills study found vegetation type was a more influential factor in controlling dune stability than short-term fluctuations in precipitation, as the latter varied compared to the steady resilience of prairie grasses (Sridhar and Wedin, 2009). Yet, a study from Australia found vegetation had the capacity to respond rapidly to changes in precipitation and that sand movement and vegetative cover were inversely related (Hesse and Simpson, 2006).

Vegetation diversity and type – primarily the colonization of C_4 grasses, which are more efficient with water usage in drier conditions and in this case also had relatively deep roots – proved key in the stabilization of previously active dunes in a Canadian prairie (Shay et al., 2000). A longer-stabilized site with finer-grained sand and somewhat more silt (5% vs. 0%) in the upper 5 cm was dominated by C_3 grasses with shallower root systems, however. While Shay et al. (2000) seem to have interpreted this observation as indicating eventual replacement of C_4 by C_3 grasses as part of a general pattern of succession on these dunes, it can also be seen as evidence of the influence of even small variations in soil texture on dune plant communities. Another study observed that the ratio of live to dead vegetation on a dune is also important to dune stability, as vegetative coverage alone was not a good indicator of whether a dune remained stabilized during drought conditions (Siegal et al., 2013). Vegetative cover could remain extensive and unchanged, the study found, but if the percentage of dead vegetation increased beyond a certain threshold, the dune destabilized and reactivated despite the cover.

Additionally, vegetation was linked in some dune studies to soil characteristics, which have been suggested as further controlling variables on dune activity. This is an area of research this thesis aims to inform. Previous research is not in complete agreement on the effects of soil variables such as moisture, nutrients, and particle size on dune activity, or how exactly these soil variables are related to vegetation attributes. For example, a study of dune activity in the Great Plains

found older, stabilized dunes had undergone relatively thorough pedogenesis, specifically through addition of finer-grained silt or clay particles that may have originated as aeolian dust (Werner et al., 2011). Vegetation and soil mechanics moved the trapped fine-grained particles into the soil, burying them, resulting in relatively higher soil moisture retention. This also enhanced soil nutrients and the dunes stabilized over time. Conversely, the study concluded that dunes lacking these finer-grained soil particles are more likely to become active during significant drought events, even if the response is lagged (Werner et al., 2011).

Other studies support aspects of these findings from Werner et al (2011). A study reporting the results of a controlled experiment from China found vegetated dunes could trap and accumulate fine-grained dust (Yan et al., 2011). The amount and percentage of fine-grained silt and clay trapped increased with the percentage of vegetative cover on the dune. Further, the trapped fine-grained material also increased the concentrations of beneficial soil nutrients such as nitrogen and phosphorus. Another study from China found more fine-grained particles in dunes stabilized by shrubby vegetation and less in "mobile dunes" (Wang et al., 2005). The active dunes from this study were nearly completely sand. At minimum, 99.6% of the active dunes were comprised of particles >50 μm, while more stable dunes had between 0.26–36% particles <50 μm. Likewise, a study from a sand prairie in Manitoba, Canada, found compatible results. Shay et al. (2000) examined soil particle size in the A and C soil horizons on bare sand dunes, intermediate landforms, and long-stabilized aeolian sands and found a modest increase in fine particle content from bare sand through to the stable prairie sites in the top 5cm of soil. The bare sand dunes in the study contained no measurable silt or clay particles, while the mixed intermediate sites contained a tiny, barely measurable amount, and the sand prairie contained a modest 5%. None of the sites sampled contained measurable silt or clay in the C horizon.

While this small but potentially significant accumulation of fines is consistent with the conclusions of Werner et al. (2011), Shay et al. (2000) also found that observed soil moisture was greatest at their bare dune site but decreased at recently stabilized sites. Observed soil moisture was least at the long-stabilized site with greater silt and clay near the surface, likely due to the greater total vegetation cover there as well greater dominance of shallow-rooted C_3 grasses. Similarly, a study in southwestern Saskatchewan found higher percentages of fine-grained material and lower percentages of sand-sized particles in stabilized dunes versus active dunes (Hugenholtz and Koenig, 2014). This study also noted depletion of soil moisture in stabilized grassland dunes relative to those that were still active, attributed to greater uptake by vegetation.

The finding of lower moisture in stabilized dunes with greater silt and clay content than in bare, active dunes may initially seem to conflict with the conclusions of Werner et al. (2011), however, this observation largely reflects the difference in present vegetation density and degree of depletion of soil water by plant use. If vegetation cover was established on the currently active dunes with their minimal clay content, it is likely that plant moisture stress would be observed earlier there than in the longer-stabilized dunes with some accumulation of fines and organic matter. Shay et al. (2000) measured field capacity water content, the water content immediately after free drainage of a saturated soil and before significant plant water use, at each site they studied. Field capacity water content was significantly higher at their long-stabilized site with higher silt and clay (30% by weight) than at active and more recently stabilized sites (18-19%). Vegetation growing on the long-stabilized site would thus have a substantially greater reserve of moisture during dry periods, consistent with the view of Werner et al. (2011).

Seasonal and local landscape-scale variation of soil moisture may also be important to the persistence of dune-stabilizing vegetation. Forman et al. (2005) cited previous Great Plains research suggesting that soil moisture reductions in winter and spring may be responsible for dune

activation. A study in the Sand Hills linked soil moisture in interdune lowlands to eventual dune stabilization toward the end of the MCA (Schmeisser McKean et al., 2015). In some parts of the Sand Hills, the water table was likely close to the surface even during droughts, because of position within the regional groundwater system and distance from incised streams. As the MCA megadrought relented, Schmeisser McKean et al. (2015) hypothesized that vegetation surviving in those wetter interdunes allowed more rapid colonization and stabilization of nearby dunes than occurred in other parts of the Sand Hills.

Shay et al. (2000) also found much greater contents of organic matter and nitrate, and somewhat higher available K, in the soils at the long-stabilized site than in active dune sand, with intermediate values at recently stabilized sites. CEC was not measured but was likely greater at the long-stabilized site because of higher organic matter and clay content. Content of available P did not show as much variation. These findings suggest that greater availability of some nutrients could favor persistence of stabilizing vegetation on dunes that have been stable for some time and have experienced some effects of pedogenesis and fine dust accumulation. Another study sought to understand cation concentrations in dune systems with both bare sand and vegetated dunes in coastal Brazil (Hay et al., 1981). In that study, no differences were observed between active and stabilized dunes for the cations Na and K, but stable dunes were found to have substantially greater concentrations of Ca and Mg, suggesting again a link between soil development and dune state.

An additional dune variable thought to influence—or reflect—dune state is landform morphology. The morphology of dunes is often clearly connected to vegetation cover and soil characteristics (Barchyn and Hugenholtz, 2013b; Hack, 1941; Hesp, 2002; Hugenholtz et al., 2012; Hugenholtz and Wolfe, 2005; Nield and Baas, 2008; Schmeisser McKean et al., 2015; Siegal et al., 2013; Wolfe and Hugenholtz, 2009). The dunefields of the study areas – the Sand Hills plus the smaller

dunefields to the south and west – exhibit a variety of dune forms. The Sand Hills are comprised of large transverse dunes (barchanoid ridges and megabarchans), with large linear dunes and hummocky sand sheets in the eastern part of the dunefield and large compound parabolic dunes at its western margin (Loope and Swinehart, 2000). Smaller linear or parabolic dunes are superimposed on the larger forms. The Lincoln Dunefield immediate south of the Sand Hills is a mixture of parabolic and linear dunes and hummocky sand sheets. The Imperial Dunefield, which is to the southwest of the Sand Hills, is composed of large compound parabolic dunes (i.e. smaller parabolic dunes superimposed on larger parabolic forms), as too is the Sioux Dunefield far west of the Sand Hills. These dune forms reflect important controls on sand transport when the dunes were active, and they also may have implications for stabilization and reactivation. For example, the geomorphology of parabolic dunes – with their arms pointing upwind – is indicative of a gradual stabilization process involving the anchoring of the parabola's arms via the advent of colonizing (Forman et al., 1992; Hack, 1941; Hanoch et al., 2018; Lancaster and Baas, 1998; Reitz et al., 2010). While the genesis of large compound parabolic dunes is less well-understood, it likely also involves a significant phase of partial vegetation. In contrast, the large transverse dunes of the Sand Hills are typical of fully active, unvegetated desert dunes, suggesting that they were quickly stabilized by vegetation and thus did not become transformed into parabolic forms during the stabilization process. There is also some evidence that the geomorphology of parabolic dunes is indicative of the ongoing presence of relatively higher soil moisture levels or a shallow water table (Wolfe and David, 1997). Interpretation of the linear dunes common in the Sand Hills as both superimposed and free-standing dunes is more complex, because both fully active and partially vegetated linear dunes are observed in other settings (Pye and Tsoar, 2009).

Recent dune activity, especially patchy surficial activation in the form of blowouts, may also leave geomorphic signals in form of choppy, rough landforms. A study of parabolic dunes in the Great Sand Hills region of Canada found the activity of mostly stabilized dunes there left behind a

"varied and often complex terrain" (Wolfe and David, 1997). Conversely, a study from the Negev Desert found the geomorphology of vegetated linear dunes smoothed over time, flattening and elongating (Roskin et al., 2014). In testing the hypotheses of this thesis it is assumed that surface roughness of dunefields is correlated to relatively recent, patchy surficial dune activation, resulting in a choppy landscape. These choppy dunefields should also exhibit soil properties which generally reflect a temporally shorter pedogenic period, because of more frequent disturbance or loss of surface soils through reactivation. This surface roughness can be expressed using different metrics of terrain, such as the standard deviation of elevation, standard deviation of slope, and other topographic metrics (Grohmann et al., 2011).

Studies have explored related dune attributes such as dune type, aspect, and slope and how these variables can influence the mobility and the development of geomorphic features such as blowouts (Barchyn and Hugenholtz, 2013a; Hugenholtz and Wolfe, 2005). Blowouts are concave depressions where bare sand is exposed by erosion on an otherwise stabilized dune surface, with associated mounds of sand on one or two sides of the depression where the blown-out sand has accumulated. These features are important in understanding dune stabilization and reactivation (Barchyn and Hugenholtz, 2013a; Wolfe and David, 1997). Blowouts occur at the point of a vegetation disturbance, where the wind burrows a depression into a stable dune, and, given wind strength and the weakening of other controls, can override the stability of the local dune or migrate downwind, disturbing other stable dunes. The process undoubtedly creates localized surficial roughness and could be captured with a close investigation of dune topography.

Several studies have examined how dune geomorphology has affected other important stabilization and reactivation variables, such as vegetation and soil properties. A study from the Negev Desert found the reactivation and stabilization of dunes dependent on the intersection of vegetation and geomorphic position, specifically the dune location of live grasses (Siegal et al.,

2013). Differences were found, the study noted, in vegetation coverage between dune crests, stoss and lee slopes, and interdunes. The degree of pedogenesis on dunes in Kansas appeared to be related partly to geomorphology, with well-developed Alfisols found on older sand sheets and poorly-defined Entisols found on more active dunes (Werner et al., 2011).

All of these factors – climate, vegetation, soil characteristics, and geomorphology – play interdependent roles in the state of grassland dunes in the central Great Plains, with climate the independent variable often driving interactions among the other factors. A fifth variable influencing grassland dune state is disturbance, either from anthropogenic alteration of the environment, or in the form of fire or burrowing animals (Barchyn and Hugenholtz, 2013b; Bo et al., 2013; Meir and Tsoar, 1996; Seifan, 2009). These are important forms of disturbance in some dune fields, but they remain outside of the scope of this thesis research because of the methods chosen. Instead, this thesis will focus on measuring soil properties and testing whether they are related to surface roughness metrics indicative of recent surficial reactivation. If such linkages can be found between surface roughness and soil properties, then conclusions perhaps can be made regarding future potential for dune reactivation or continued stability.

CHAPTER 2: Study Areas and Methods

Study Areas

An ideal location to test the hypothesis of this thesis is in dunefields of central and western Nebraska, United States. In this area west of the 98th meridian, where the climate transitions from a Dfa (moist continental) to a BS (steppe) per Köppen's classification system (May, 2003), there are several mostly stable dunefields, including the largest stabilized grassland dunefield in North America – the Nebraska Sand Hills (Mason et al., 2011). The Nebraska Sand Hills encompass an area of 50,000km^2 on the North American Great Plains, a sea of grass atop a vast deposit of eolian sand. Surrounding the Sand Hills are several smaller dunefields with unique origins and characteristics. Thus, collecting soil samples from the Sand Hills and an assortment of other regional dunefields that share some similarities to, but are apart from, the Sand Hills should provide a representative basis from which to test the hypothesis.

In addition to samples from the Sand Hills, samples from three other dunefields were collected (Figure 1). Samples were drawn from sites in the Imperial and Lincoln dunefields, south of the Sand Hills and the Platte River system, where some previous research was conducted examining either the provenance of the parent material or dating dune activity via optically stimulated luminescence (OSL) (Forman et al., 2005; Muhs, 2017; Muhs et al., 2000, 1996). A third dunefield to the west of the Sand Hills was chosen, as little research had been done in the 300km between the Sand Hills and the Casper and Ferris dunefields to the west. Within this region are several small dunefields, such as Wyoming's Lone Sand Hill (42.446408, -104.082583). Most of these dunefields are unnamed, but a site was selected approximately 30km north of the Nebraska town of Morrill, which is in the North Platte River Valley near the Wyoming border. This site is within a dunefield located in central Sioux County, referred to in this thesis as the Sioux Dunefield.

While the climate transitions from a Dfa (moist continental) to a BS (steppe) over western Nebraska overall (May, 2003), the actual climate classification based on observed 1981-2010 data is more complex. None of the study sites are designated in the semiarid BS classification as the mean annual precipitation (MAP) for all locations exceeds 10x each site's P-threshold, a precipitation coefficient based partly on the mean annual temperature (MAT), although the Sioux site farthest west is nearly arid enough to qualify. Based on the recent interpretations of Köppen's climate classification formulae (Peel et al., 2007), all sites fall into the D climate class, a midlatitude, continental climate featuring variability and lacking a temperate nature. In general, MAP and MAT increase from northwest to southeast, with the driest and hottest climate belonging to the Sioux study site. While the other sites received between 500-600mm yr^{-1} in precipitation on average, precipitation near the Sioux site is roughly only two-thirds of that (Nebraska State Climate Office, 2018). Likewise, the Sioux site's MAT is nearly 1°C colder than the next coldest study site (Milepost 81, taken at Cox Reservoir) and 2.5°C colder than the warmest site (Imperial). Thus, in terms of climate, the Sioux Dunefield is somewhat an outlier from the other study sites in this thesis, although all sites share a precipitation and temperature pattern similar to the climograph in Figure 2 for Valentine, Nebraska – a cold, dry winter, with a warm and relatively wet summer.

As climate transitions over the study areas, so too does vegetation. As a rule, as precipitation decreases east to west across Nebraska, so to do the average height of the prairie grasses. The tallgrass prairie in the wetter eastern third of Nebraska gives way to the mixed grass prairies of central Nebraska's loess lands, while the shortgrass steppe occurs on fine-grained soils farther to the west. The sandy soils of dune fields in the central Great Plains are occupied by two specialized prairie systems – the "Sandhills" and sandsage prairies (Dunn et al., 2016). The Sandhills prairies inhabit the Sand Hills dunefield, while the sandsage prairies correspond to the

dunefields south and west of the Sand Hills, including the Imperial, Lincoln, and Sioux County dunefields. As a result, two distinct grassland plant communities are present across the five study areas.

Sand Hills Lord Ranch Site

Owing to the size and importance of the Sand Hills, two sites were chosen in the Sand Hills for investigation. The Lord Ranch site (Lat.: 42.61088, Lon.: -100.65524) was selected based on an examination of aerial imagery, which suggested the ranch was home to choppy, semi-active, but mostly stable, dunes. Its climate is classified as Dwa – humid continental with dry winters (Table 1). Meteorological data from Valentine's Miller Field 28km north-northeast of the study site shows the Lord Ranch site likely receives slightly more than 500mm of precipitation annually, has hot summers and cold winters, with a MAT of 8.7.

Some studies have identified a unique plant community comprising of just the Sand Hills (Dunn et al., 2016). This uniqueness is linked to the higher sand content of the soils and the geomorphically high relief of Sand Hills dunes, which drives changes in vegetation. The region's sands have high hydraulic conductivity, which increases with depth (Wang et al., 2008) and, consequently, results in relatively little precipitation running off the stabilized dunes (Dunn et al., 2016), except during rare intense rainstorms or possibly where biocrusts occur (Sweeney and Loope, 2001). Thus, the species often found in the Sand Hills have moderately deep roots (Johnsgard, 1995, p. 70). Dunes here also have high upland relief, along with pronounced swales and blowouts. This localized relief, often expressed as surface roughness, produces localized plant assemblages, with Little bluestem (*Schizachyrium scoparius*) present throughout, sand bluestem (*Andropogon hallii*) anchoring stable dune ridges, and blowout grass (*Redfieldia Flexuosa*) colonizing large blowouts (Dunn et al., 2016; Johnsgard, 1995, pp. 68–76). Sand bluestem and prairie sandreed (*Calamovilfa longfolia*), in particular, are often found on "choppy sand" in the Nebraska Sand

Hills (Dunn et al., 2016). Most of these grasses are amenable to grazing, especially the little bluestem, and evidence at the Lord Ranch site suggests livestock were a recent presence as cow tracks crisscrossed the landscape. Yet, as bison were once plentiful across the Great Plains, it is not known how much cattle have impacted the Sand Hills (Dunn et al., 2016).

The central Sand Hills, including both the Lord Ranch and Milepost 81 sites, are dominated by large transverse dunes with small dune forms superimposed on them (Loope and Swinehart, 2000; Sridhar et al., 2006). The Sand Hills dune sand in general appears to have a complex origin in an array of sources including bedrock formations to the northwest and Pliocene and modern fluvial and aeolian sands (Muhs, 2017). Studies of regional prevailing winds show a bidirectional aspect (Schmeisser et al., 2010; Sridhar et al., 2006). Seasonality explains this bidirectional pattern as southerly to southeasterly winds prevail in summer while somewhat stronger northerly to northwesterly winds are common in winter. The net sand transport direction (resultant drift direction) is toward the south or southeast because of the greater strength of the winter winds (Schmeisser et al., 2010; Sridhar et al., 2006), and the form of the large transverse dunes reflects that transport direction. Smaller linear dunes, often superimposed on the large transverse forms, commonly have a west-southwest to east-northeast orientation reflecting a stronger component of wind from the southwest than is observed at present (Sridhar et al., 2006). That wind component was apparently enhanced during Late Holocene dry periods when the linear dunes developed (Schmeisser et al., 2010; Sridhar et al., 2006). Blowouts and small parabolic dunes that reflect the most recent reactivation of the dune surfaces have orientations consistent with the modern wind regime; that is, they provide evidence of greater transport toward the south or southeast, but with some sand also carried out of blowouts toward the northwest or north. Samples were taken within a large dune complex from three locations along three transects – transect CH-1A ran along a

small 10m dune, transect CH-1B was along the face of a blowout, and transect CH-1C was along another 10m dune (Figure 3).

Sand Hills Milepost 81 Site

The second of two Sand Hills sites in this study is a well-researched, large roadcut 51.5km southwest of the Lord Ranch. The site, known as Milepost 81 (Lat.: 42.2405, Lon.: -101.032577), is located along Nebraska Highway 97 at a 500m long perpendicular cut through one of numerous closely spaced linear dunes superimposed on a larger transverse dune (Figure 4). The roadcut itself is at least 12m high and provides an opportunity to examine thousands of years of eolian deposition and activity (Mason et al., 2011; Miao et al., 2007). Dating of sand grains using OSL techniques has shown the dune at Milepost 81 was active around ~920, ~2400, and ~13,500 years before present. The former date coincides with the Medieval Climatic Anomaly (MCA), while the latter age, from below the base of the linear dune, is within the Pleistocene. The linear dunes at this site have orientations consistent with the change in wind directionality during Late Holocene dry periods such as the MCA that was inferred by Sridhar et al. (2006). The top several meters of the roadcut is associated with linear dune formation and migration during the MCA as well as more recent surficial reactivation, and samples were taken along three transects (MP81-1A, MP81-1B, MP81-1C) approximately 6+ meters laterally from the dune crest.

The climate and vegetation of this site is similar to that of the Lord Ranch site, although meteorological data from a weather station 26.5km to the west at Cox Reservoir recorded more annual precipitation with almost 600mm on average (Table 1).

Imperial Dunefield Site

Two study sites were located south of the massive Sand Hills region. The southernmost is a site in the Imperial Dunefield (Lat.: 40.69003, Lon.: -101.68626), which is located in Chase and Perkins counties between Frenchman and Stinking Water creeks. It is approximately 1,000km^2 in size, or

2% the size of the Sand Hills. Like the Milepost 81 site, research has been conducted within and near this dunefield. Some of this work concerned OSL dating of dune deposits to pinpoint the dates of dune activity. Work conducted 8km northeast on the Cornelius Dune, part of the Imperial Dunefield, found dune activity occurred at ~540, ~3000, and ~14,700 years before present (Mason et al., 2011). The samples from that study yielding an OSL date of ~540 years before present were taken at a soil profile depth of 1m; all samples for thesis at the Imperial site were taken at a depth ≤1.1m, meaning that if the entire Imperial Dunefield was active at this time, then the samples used for this thesis study would be partially from this late Holocene event. Approximately 70km south of the Imperial study site, OSL dating from a different study on the edge of the Imperial Dunefield returned similar Holocene dates. According to that study, dune activity at the southern tip of the Imperial Dunefield near the Republican River occurred at ~70, ~80, ~420, and ~540 years before present (Forman et al., 2005). These dates suggest a regional dune reactivation event across the Imperial Dunefield around 1460 AD in response to the Little Ice Age. It further suggests some reactivation during the Dust Bowl event of the 1930s AD.

These Imperial dune reactivation dates are different than events dated at the two Sand Hills sites, suggesting the Imperial Dunefield may have different drivers and sensitivities from the Sand Hills. A series of studies examining the provenance of the dunefields in the region found that the Sand Hills had a complex origin involving bedrock formations to northwest, along with sands from the Pliocene Era and fluvial sources (Muhs, 2017; Muhs et al., 2000). That same study showed the provenance of the Imperial Dunefield was no more straightforward, but different, with inputs from South and North Platte River sands, bedrock formations to the west, and even the Sand Hills.

Climate and vegetation also differ slightly for the Imperial Dunefield study site as compared to those sites in the Sand Hills. The Imperial site is the warmest in this thesis, with a MAT >10°C and the highest minimum mean monthly temperature (-3.5°C for January). The climate is classified as

a Dfa, humid continental. The site is located in the sandsage plant community (Dunn et al., 2016; Kaul and Rolfsmeier, 1994), named for the abundance of the shrub sandsage (*Artemisia filifolia*). Several of the same species inhabit the Imperial Dunefield that inhabit the Sand Hills, including grasses from the bluestem and grama families. And like the Sand Hills, species in the Imperial Dunefield region have adapted to the "choppy" nature of periodically reactivated dunes, particularly sand lovegrass (*Eragrostis trichodes*), prairie sandreed (*Calamovilfa longfolia*), and windmillgrass (*Choris verticillata*) (Dunn et al., 2016), although little bluestem is found abundantly throughout the area.

Previous studies have classified dunes in the Imperial Dunefield as compound parabolic dunes (Loope and Swinehart, 2000). Aerial images from the study site selected for this thesis confirms the parabolic nature of dunes in this area, especially northwest of the sites (Figure 5). Samples representing the Imperial Dunefield were extracted from three sites each along three transects (IMP-1A, IMP-1B, IMP-1C) which were sited along 330 Avenue in northern Chase County, where several fresh roadcuts were located. To the east and south of the sites are cultivated areas. To the northwest visible from 330 Avenue is a large dune complex with high relief. On some maps, the Imperial Dunefield is identified as the Wray-Imperial-Lincoln (WIL) Dunefield, which lumps three dunefields together stretching from central Colorado to central Nebraska.

Lincoln Dunefield Site

Between the Sand Hills region and the Imperial Dunefield is the Lincoln Dunefield, which is perched south of the Platte River system near the city of North Platte (Lat.: 41.0867, Lon.: -100.9257). The dunefield is approximately 3,500km^2 in size – larger than the Imperial Dunefield and 7% of the size of the Sand Hills. Unlike the Sand Hills, however, a robust collect of OSL data does not exist from the Lincoln Dunefield. The only OSL dataset from the area was collected from the Wach site at the far southern end of the dunefield. Dune activity here dated to 7500, 10700,

and 13600 years before present (Mason et al., 2011). While few OSL dates have been collected from this dunefield, there is research into its origin (Loope and Swinehart, 2000; Muhs, 2017; Muhs et al., 2000; Swinehart and Loope, 1992; Winspear and Pye, 1995). The Lincoln Dunefield is sometimes referred to as part of the Wray-Imperial-Lincoln (WIL) Dunefield, but studies have shown geochemical differences between these three geographic features. While Winspear and Pye (1995) identified it as the "Dickens Dunefield" in their work, most workers refer to the region as the Lincoln Dunefield or Lincoln County Dunefield.

Separated from the Sand Hills only by the Platte River Valley, researchers initially suggested the Lincoln Dunefield had been an active aeolian arm of the Sand Hills that had dammed the North and South Platte rivers during dry climatic periods (Muhs et al., 2000; Swinehart and Loope, 1992). Since then, grain size and provenance analyses have shown the Lincoln Dunefield's origin is unique from the Sand Hills (Muhs, 2017; Winspear and Pye, 1995). It seems likely now that Lincoln Dunefield sands are derived from North Platte River sands, as the geochemical indicators match almost exactly (Muhs, 2017). Thus, unlike the complex origins associated with the Sand Hills and the Imperial Dunefield, the Lincoln Dunefield's origin is straightforward seemingly; sand entrained in the North Platte River from upstream in the basin was deposited on the river's south bank then transported southward across the Platte River Valley and over the South Platte River, until being deposited on the south side of the valley. While geochemically clear, Muhs (2017) suggests the actual geomorphic processes had to be more complex, despite the absence of inputs from sands derived from the South Platte River system, which are geochemically different from North Platte River sands, or the Sand Hills. Nevertheless, the data are clear and suggest that sands originating from the North Platte River basin were instrumental in the formation of the Lincoln Dunefield.

According to data from the nearby North Platte Experimental Farm, the climate for the Lincoln Dunefield is Dwa, humid continental with a dry winter and a hot summer. The dunefield sits at a juncture of the sandsage and mixed-grass prairie ecotones and features many of the same species that are found in the Imperial Dunefield, including bluestems. In comparison to the other study areas, however, the Lincoln Dunefield is less choppy, its surface smoother. Loope and Swinehart (2000) found the Lincoln Dunefield to be a mixture of hummocky sand sheets and complex transverse dunes, but linear dunes similar to those of the Sand Hills are clearly present in parts of this dunefield. The location from which samples for this thesis were taken is clearly of low relief (Figure 6) and is likely in the sector designated as a hummocky sand sheet. Samples were extracted from three profiles each on three transects (LI-1A, LI-1B, and LI-1C) along Range Road just north of the Outlet Canal.

Sioux Dunefield Site

The last study site is the one on which the least amount of research has been conducted. Situated in central Sioux County, this unnamed dunefield is 55km long and 15km wide stretching from extreme eastern Wyoming's Lone Sand Hill, with its 100m of vertical relief, into Nebraska. As this dunefield is unnamed and located mostly in Sioux County, this study will refer to it as the Sioux Dunefield. According to two meta-analyses of Great Plains dune research, no research has been conducted on aeolian activity for any dunefield between the Sand Hills region and the Casper Dunes in central Wyoming (Halfen et al., 2016; Halfen and Johnson, 2013). Loope and Swinehart (2000) did classify the dunes in this region as compound parabolic with a northwest-to-southeast orientation. That study also made note of a dune dam along Sheep Creek, as seen in early 20th Century topographic maps, but no other known OSL or geomorphic research has been done in this area.

The Sioux Dunefield site is the most remote of the study areas in this thesis (Lat.: 42.260681; Lon.: -103.914394). It is at least 260km from all other study sites. It is also the highest in elevation (~1,425m) and the coldest and driest in terms of climate, with a MAT of 7.6°C and a MAP of 365mm. It is also the only site classified as Dwc under the Köppen system, with a humid continental climate, dry winters and equally hot summers and cold winters. The vegetation of the Sioux Dunefield also differs slightly from the other sites. Part of northwestern Nebraska is classified as the short-grass steppe ecotone, meaning that it is dominated by different species of grass, chiefly buffalograss (*Bouteloua dactyloides*), blue grama (*Bouteloua gracilis*), and threadleaf sedges (*Carex filifolia*) (Dunn et al., 2016), yet it is often mixed with sandsage plant communities. The sites where samples were collected for this thesis were clearly sandsage assemblages, with sandsage (*Artemisia filifolia*) and the introduced crested wheatgrass (*Agropyron cristata*) and cheatgrass (*Bromus tectorum*) present in abundance, the latter two of which are more common in northwestern Nebraska than in other areas of the state.

Samples for the Sioux Dunefield were taken from two nearby, but different geomorphic locations, which may present issues with the data (Figure 7). Samples were taken from one transect (SI-1A) that appears to be a sand sheet leeward of a large parabolic dune complex. The second site (SI-1B) was near the intersection of Morrill Road and Murphys Road on the windward side of a dune complex. Both sites are approximately 20km north of the North Platte River Valley.

Table 1: Climate Date for Research Study Areas

Study Site	Closet Weather Station	MAP (mm) (Mean Annual Precip.)	Summer P Wettest / Driest	Winter P Wettest / Driest	P-Threshold	MAT (°C) (Mean Annual Temp.)	Monthly T Hottest / Coldest	Climate Class
Imperial Dunefield	Imperial	513.6	84.3 (June) 66.8 (Aug.)	13.2 (Feb.) 11.7 (Jan.)	34.6	10.3	23.6 (July) -3.5 (Jan.)	Dfa
Lincoln Dunefield	North Platte Experimental Farm	528.32	93.7 (June) 60.7 (Aug.)	12.7 (Feb.) 8.4 (Jan.)	33.4	9.7	23.4 (July) -3.7 (Jan.)	Dwa
Sand Hills Lord Ranch Site	Valentine Miller Field	513.1	90.4 (June) 55.3 (Aug.)	12.2 (Feb.) 6.6 (Jan.)	32.4	9.2	23.6 (July) -4.7 (Jan.)	Dwa
Sand Hills Milepost 81 Site	Cox Reservoir (34km NW of Mullen on Calf Creek)	591.3	100.8 (June) 58.7 (Aug.)	16.5 (Feb.) 11.9 (Jan.)	31.4	8.7	22.7 (July) -4.1 (Jan.)	Dfa
Sioux Dunefield	Agate Fossil Beds National Monument	365	61.2 (June) 39.9 (Aug.)	7.6 (Feb.) 5.1 (Jan.)	29.6	7.8	21.4 (July) -4.7 (Dec.)	Dwc

Figure 1: Research Study Areas

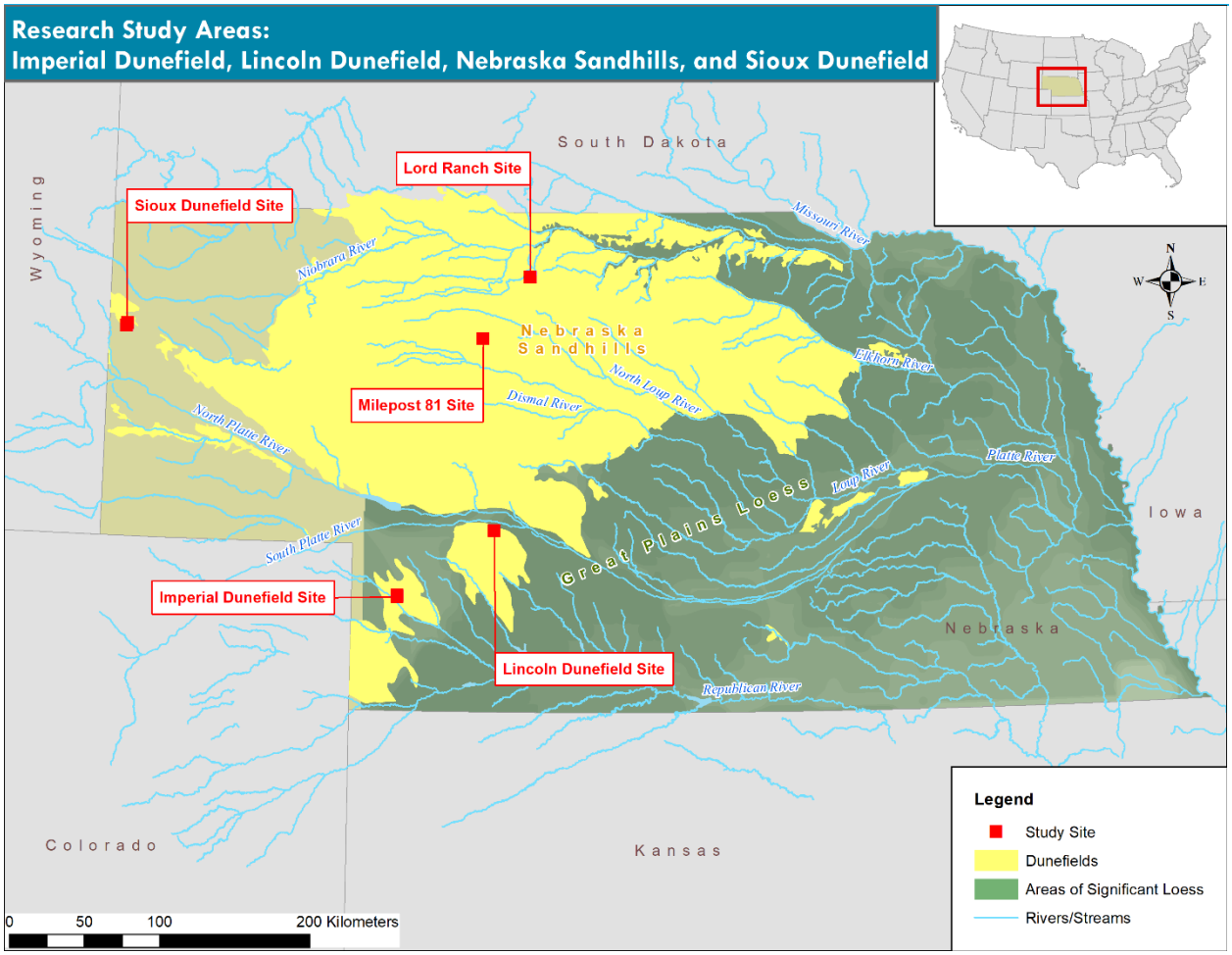

Figure 2: Typical Climograph for Sand Hills Region (NOAA 2018) (https://w2.weather.gov/climate/xmacis.php?wfo=lbf)

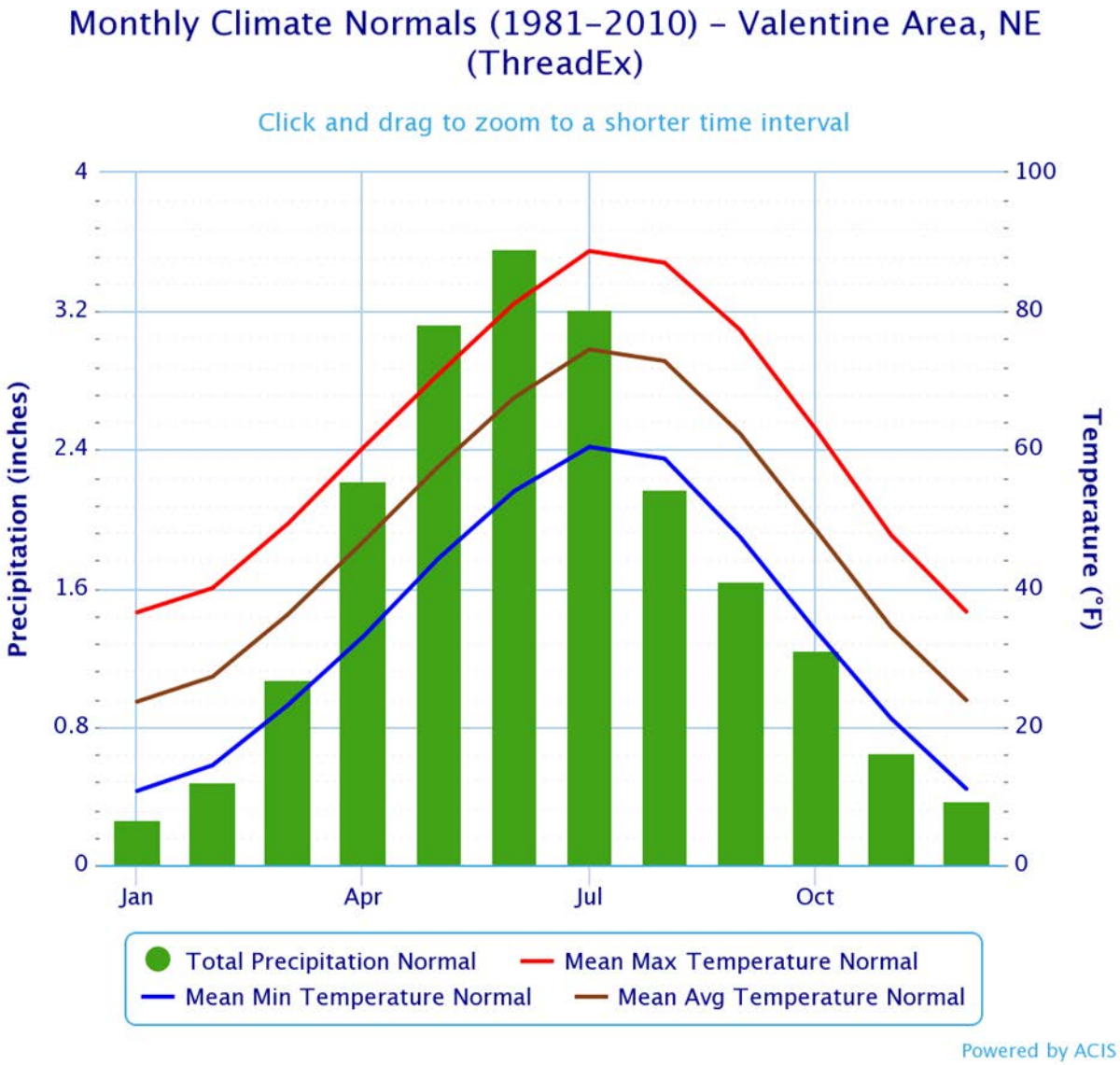

Figure 3-7: Research Study Sites

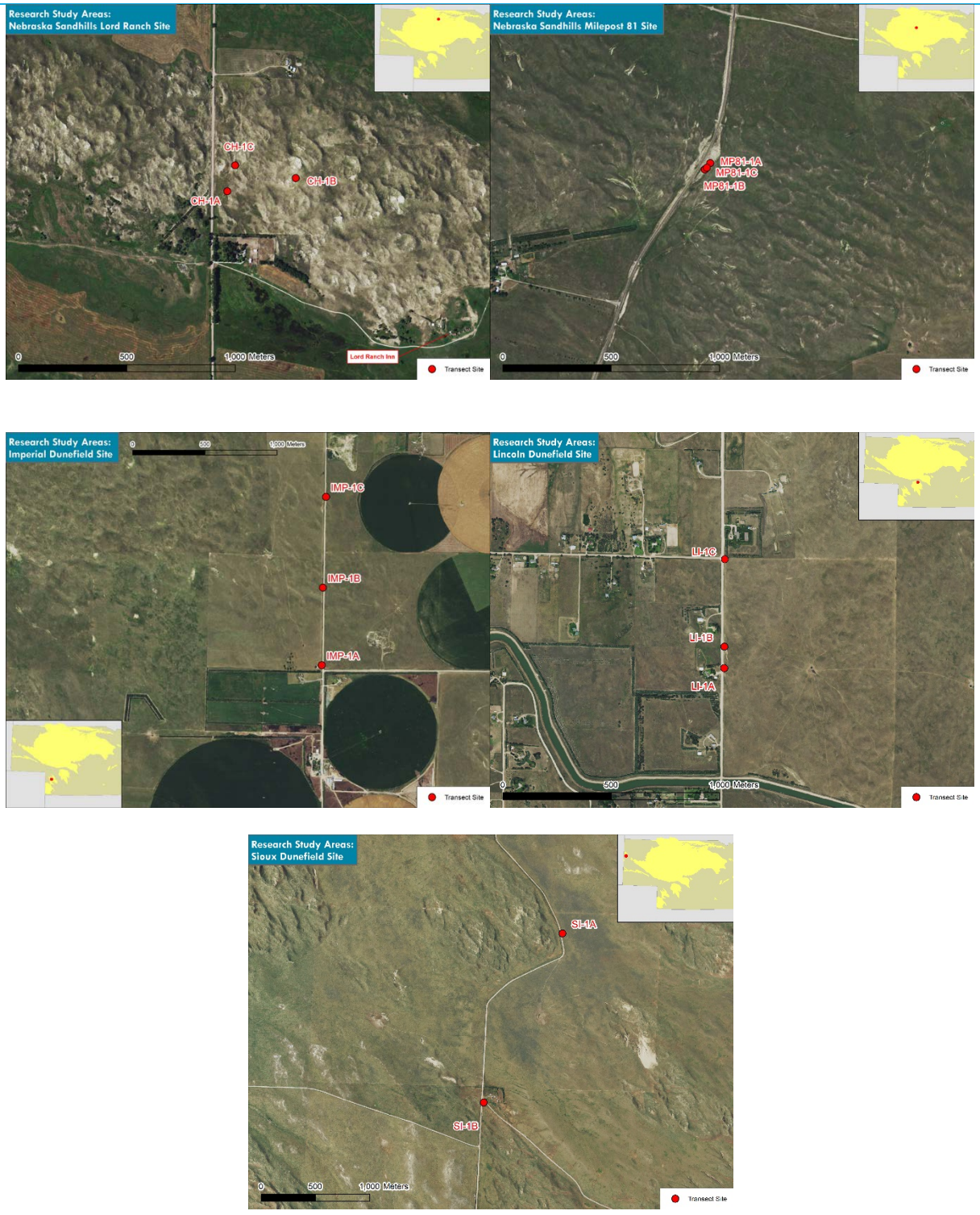

Methods

Variables that are important indicators of soil formation or recent dune activity were measured using samples collected in the field or from elevation data using geographic information system (GIS) procedures. Soil samples were taken from the five sites in the study area specified in Chapter 3 and analyzed using a variety of methods in a laboratory. The results from laboratory and GIS methods were then used in statistical analyses. This section details the methodology used to collect and analyze these data.

Field Collection and Pedology

Soil characteristics were obtained via field sampling, observation, and subsequent laboratory analyses. Field observation and sampling was carried out using roadcuts or other vertical exposures. After cleaning the exposures with a shovel and describing the soil profile, samples were collected by pushing a hand soil probe into the exposure face to extract a 10-cm sample of soil. Specific sampling sites were identified by exploring areas of interest within the study area, which were first identified using aerial imagery in GIS. Grassland dune areas demonstrating a mixture of choppy and smooth dunes – suggesting landscape and dune status variability – were prioritized. Individual sites within these areas of interest were chosen for their accessibility and include a mixture of fresh roadcuts and other exposures in dunefields with accommodating landowners.

At each of the five study sites, a consistent methodology was established to collect samples. Three transects were established at each site, with the exception of the Sioux Dunefield, where two transects were employed due to severe weather conditions in the field. Along each transect, three soil profiles were sampled; the distances between these profiles varied randomly along the transect, with the exact distances determined using a random number function within a Microsoft Excel spreadsheet. Thus, for Transect IMP-1A at the Imperial Dunefield, the three soil profiles were spaced at distances of 2.3, 5.7, and 12.3 meters from the head of the transect, distances

which were calculated randomly. This process of sampling was utilized at each transect sample site.

The soil profiles to be sampled along each transect were cleaned with a shovel or trowel to create a freshly exposed face. The pedological elements of the soil profile were then recorded along with attributes of the landscape in field notebooks and with cameras. Soil horizon colors were recorded using the Munsell System (Anonymous, 1969). Selected soil horizons were also evaluated for carbonate content in the Lincoln and Imperial dunefields using 10% HCl. For each soil profile, samples were taken from the A, AC, and C horizons if present, plus from any paleosols, discontinuities, dune banding, and lamellae observed in the top meter of the profile, if it was deemed necessary. Finally, samples for lab analyses were collected from each horizon by inserting a hand soil sampler probe 10 cm horizontally into the exposed face and placing the collected soil in airtight bags. The samples were air-dried and crushed to pass a 2-mm sieve before lab analyses.

Soil Particle Size

One method was employed to measure soil particle size, which can be used to classify soil type, identify soil series, infer soil moisture capacity and, potentially, recent dune activity. For this research, soil particle size measurements were made via a Malvern Instruments Mastersizer 2000MU laser particle size analyzer. Although the laser diffraction method of measuring soil particle sizes tends to underestimate the amount of the clay (<2μm) particle-size fraction (Mason et al., 2003; Werner et al., 2011), the method was used here as the soils sampled were deemed likely to be overwhelmingly sand-sized particles. Thus, the alternative pipette-sieve method, which has traditionally been used to measure soil content, but takes longer, was not used in this research.

Dry samples immersed in about 400 mL of DI water circulating through the particle size analyzer, with sampled added until the light obscuration measured by the instrument was within the acceptable range of 2-20%. To disperse clays and disaggregate the soil, 10 mL of 50 g L^{-1} sodium metaphosphate solution was added to the beaker. The samples were then sonicated (10 mm displacement, mid-range in sonicator power) for six minutes, followed by particle size analysis. The Malvern Instruments software calculated the particle size distribution from the distribution of scattered light using the Mie optical model, with a refractive index of 1.55 and absorption coefficient of 0.1. While the software initially calculates a size distribution with 100 logarithmically spaced bins, for this study the following variables were calculated from those raw data: % sand (2mm-63µm), % silt (63µm-2µm), % clay (<2µm), median diameter, and mean diameter. Using the percentages of sand, silt, and clay, soil textural class was determined for each sample by using a spreadsheet tool produced by the United States Department of Agriculture, Natural Resources Conservation Service (USDA, 2018).

Loss-on-Ignition (LOI)

This study evaluated soil organic matter (SOM) and soil organic carbon (SOC) using two different approaches. The first used the loss-on-ignition (LOI) technique described by Konen et al. (2002). LOI at 360°C largely represents loss of SOM, with only minor loss from other sources such as dehydration of clay minerals; carbonates are not oxidized at this temperature. LOI at 360°C does not oxidize all SOM; but regression models predicting SOC from LOI can be developed for local regions or groups of soils, often with $R^2 > 0.90$ (Konen et al., 2002). Based on those observations, it was assumed that LOI at 360°C should be a useful relative index of SOM accumulation in the soils studied here.

As outlined by Konen et al. (2002), LOI soil samples were weighed, dried overnight at 105°C to remove moisture, then weighed again. After this, the samples were combusted at 360°C for two

hours in a furnace, cooled at 105°C in an oven, then weighed again. LOI was then expressed as a percentage:

$$LOI\% = \frac{oven\ dry\ soil\ weight - combusted\ soil\ weight}{oven\ dry\ soil\ weight}\ X\ 100$$

Soil Carbon (C) and Nitrogen (N)

SOC and total N were measured with an organic elemental analyzer (EA). Because of the close relationship between SOC and SOM, the measured SOC provides a second indicator of SOM accumulation in the dune field soils, while N is key plant nutrient, much of which is contained in SOM. Samples were ground with a mortar and pestle and passed through a 2mm sieve, then placed in tin capsules (or silver capsules if the sample needed to undergo acid fumigation to remove carbonates). All samples from the southern dunefields – the Lincoln and Imperial dunefields – underwent acid fumigation (Ramnarine et al., 2011) in silver capsules. Samples were replicated and analyzed with a Thermo Scientific FlashSmart Elemental Analyzer.

Cation Exchange Capacity (CEC)

The CEC of a soil horizon represents its ability to attract and adsorb positively charged ions, including important nutrients for plants and is often tied to SOC content, texture, and clay minerology (Schaetzl and Anderson, 2005). CEC was measured on samples from one profile out of the three studied in each transect and processed in accordance with the procedure found in Methods of Soil Analysis, 2nd Edition (Rhoades, 1982). Soil samples weighing ~10g were mixed with ~50 mL of ammonium acetate (1N NH_4OAc), shaken, and left to sit overnight in 100mL plastic bottles. This process saturates the soil exchange complex with NH_4^+, displacing other cations. The next day, the samples were placed in filter funnels, vacuum was applied, and excess NH_4^+ was rinsed from the soil with DI water followed by 50 mL of ethanol. A final rinse with 120 mL of 10% NaCl solution displaced $NH_4^+$from the soil exchange complex into the filtrate. The

NH_4^+ was distilled from the filtrate as NH_3 using a Kjeldahl distillation apparatus, and trapped in boric acid solution, where it was quantified using titration with H_2SO_4. The moles of NH_4^+displaced from the sample are assumed to equal total moles of negative charge on soil particles and can then be used to calculate CEC of the sample in $cmol^+ kg^{-1}$.

GIS Analyses

In addition to providing spatial data for the preliminary site analysis, GIS was used to provide answers to key questions of geomorphology. Specifically, digital elevation models (DEMs) constructed from light detection and ranging (LiDAR) files and were used in a number of analyses to answer questions regarding dune geomorphology and surface roughness, both of which can provide evidence on recent dune activation. LiDAR-based and coarser-resolution DEM data both model the Earth's surface and, thus, could be used to analyze the surface of dunefields. The Nebraska Department of Natural Resources (DNR) has LiDAR-based DEMs available at a resolution of 2m for a limited portion of the state. As of October 2018, LiDAR-based DEMs were available from the Nebraska DNR only for the study sites in the Imperial Dunefield and at the Lord Ranch in the Sand Hills. For the remaining three study areas, 10m DEMs were obtained from the Nebraska DNR and used for analysis in those area. As a result, surface data across the study area was available at different resolutions. Analyses involving metrics that did not require statistical comparisons across dunefields were performed in the data available. For example, the variable aspect – which is the directionality of the dune surface from where the soil sample was drawn – was calculated with 2m LiDAR-based DEMs for the Imperial Dunefield and Lord Ranch sites, but with 10m DEMs for all other sites. On the other hand, the analysis of surface roughness, which needed to be compared across dunefields in a statistically consistent manner, could not be performed just with the original data. For these types of analyses, the higher-resolution LiDAR-based data were converted to lower 10m-resolution raster data for comparison purposes. Thus,

for surface roughness or any other variable involving a statistical comparison, the terrain data used was at a resolution of 10m.

Dune Geomorphology

The most straightforward manner of GIS analyses for this study involved measurements of dune geomorphology. These measurements include elevation, aspect, surface slope, and all three curvature metrics. Elevation is embedded in the pixel values of the DEM raster files for each study site. It was recorded for each soil sample profile location in meters. Elevation also formed the foundation of all other GIS analyses, as it is the input value for aspect, surface slope, curvature, and the surface roughness variable.

Aspect is the directionality of the dune surface. An ESRI ArcGIS software tool called 'Aspect' was used to calculate this metric (ESRI, 2018). It does so by determining the orientation of a surface at each pixel from the elevation of all pixels within a planar 3-cell-by-3-cell moving window. The tool returned an azimuth for each study site location, which was then converted into cardinal and intercardinal directions. Aspect is an important metric in dune geomorphology as the orientations of dunes or blowouts are often tied closely with wind direction. One issue with the not only the aspect tool, but many of the GIS analyses is the potential of the process to return anomalous results due to the influence of roads and roadcuts in the LiDAR data. A review of the results showed that this phenomenon did not unduly alter the outcomes of the processes as more-granular 10m DEMs were used for geostatistical analyses.

Surface slope, likewise, was calculated with an ArcGIS tool. The 'Slope' tool evaluates the steepness of surface terrain in degrees by considering the elevation of pixels within a planar 3-cell-by-3-cell moving window. Slope is an important geomorphic variable as steeper slopes oriented in the direction of the prevailing winds tend to expose more of the dune surface to the potential of aeolian erosion or blowouts. Further, steep surfaces may be indicative of surface

roughness and, therefore, potentially key in understanding dune status. As with many calculations, slight variations in surface slope are more likely to be detected with the higher-resolution LiDAR data than with the 10m DEMs, which tend to smooth out a landscape. For this reason, 2m-resolution LiDAR was used to calculate surface slope where available.

Curvature is a surface geomorphology variable which has three related metrics (ESRI, 2018). The 'Curvature' tool in ArcGIS attempts calculate and visualize the slope shape in three dimensions by evaluating the second derivative – or trend of surficial change – within an envelope of pixels. The three metrics returned from the 'Curvature' tool are profile, planform, and total curvature. Profile curvature measures the convex or concave nature of a surface, while planform measures if a surface is converging or diverging. Profile and planform curvatures are rolled into the overall standard curvature metric.

Surface Roughness

While the metrics of dune geomorphology could be important indicators of dune status and relative activity, it is hypothesized that calculating surface roughness is critical to identifying areas of recent dune reactivation. Unfortunately, the calculation method of surface roughness is contested and often scale- and terrain-dependent (Brown and Hugenholtz, 2012; Grohmann et al., 2011). In accordance with the findings of Grohmann et al. (2011), this study focuses on the standard deviation of elevation, slope, and profile curvature. Each of these were calculated by using the neighborhood statistical tool in ArcGIS called 'Focal Statistics'. The 'Focal Statistics' tool can calculate standard deviation of raster pixels within a neighborhood of pixels as defined by the analyst. As these roughness statistics needed to be compared across dunefields, all data employed in these analyses were 10m-resolution raster files, whether originally from a DEM or 2m-resolution LiDAR dataset, the latter of which was degraded to 10m resolution for the purposes of comparison. As a result, the focal statistical neighborhood defined for all of these analyses was 3-cells-by-3-cells, or 90x90 meters.

CHAPTER 3: Results

Soil Analyses

Pedologic Investigation

Table 1(a-e) represents pedologic data collected from the field for each soil profile. These data include horizons present, horizon depth and soil color. For reference purposes, soil order and series from the United States Department of Agriculture (USDA), Natural Resources Conservation Service's (NRCS) Web Soil Survey is included for each profile, as is the soil texture classification taken from field samples. Table 2 contains the mean depth per horizon per dunefield, although the measurement of depth in the last C horizon sampled was not taken to the next visible horizon or the R horizon. As a result, the mean depth for C and C2 horizons should be taken with caution, as these measurements do not represent the entire depth of those horizons. Figure 8 is a series of pie charts representing the soil colors found in each profile by horizon and dunefield.

From these results, a few trends emerge. First, all profiles that were sampled were Entisols, which speak to the inherent long-term instability of dunefields. Moreover, the soil series at the sample sites are either sandy Valentine or its drier derivative Valent. This was not by design, but these are by far the most extensively mapped soil series in dunefields of the Central Great Plains (personal communication, J. Mason). When one examines the soil horizon information more closely, linkages exist between A and buried A horizons; they often exhibit similar horizon thicknesses within a dunefield and share the same or similar soil colors. Likewise, soil colors in the A and C horizons are shared in the AC horizon of each aggregated dunefield soil profile.

Table 2: Pedologic Description of Soil Profiles for Imperial Dunefield Sites

Profile	Horizon	Depth (cm)	Sample Depth	Color Moist	Color Desc.	Texture	Soil Order	Soil Series	Notes
IMP-1A-1	A	0-50	10 30	10YR 4/2	Dark Grayish Brown	Loamy Sand	Entisol	Valent	Roots
	C	50-122	60	10YR 5/4	Yellowish Brown	Loamy Sand			
IMP-1A-2	A	0-37	10 30	10YR 4/3	Brown	Loamy Sand	Entisol	Valent	Roots
	C	37-80	60	10YR 5/4	Yellowish Brown	Loamy Sand			
IMP-1A-3	A	0-44	10 30	10YR 4/3	Brown	Loamy Sand	Entisol	Valent	Roots
	C	44-83	60	10YR 5/4	Yellowish Brown	Loamy Sand			
IMP-1B-1	A	0-13	5	10YR 5/4	Yellowish Brown	Loamy Sand	Entisol	Valent	Roots
	C	13-87	50	10YR 4/6	Dark Yellowish Brown	Sand			Dune bedding @61cm
	Ab	87-113	110	10YR 3/4	Dark Yellowish Brown	Sand			
IMP-1B-2	A	0-18	5	10YR 4/3	Brown	Sand	Entisol	Valent	
	C	18-90	50	10YR 4/6	Dark Yellowish Brown	Sand			Dune bedding @88cm
	Ab	90-119	110	10YR 3/4	Dark Yellowish Brown	Sand			
IMP-1B-3	A	0-21	5	10YR 4/3	Brown	Sand	Entisol	Valent	Sand Sage Vegetation
	C	21-42	25	10YR 4/4	Brown	Loamy Sand			
	Ab	42-62	50	10YR 4/6	Dark Yellowish Brown	Sand			
IMP-1C-1	A	0-21	5	10YR 3/2	Brown	Loamy Sand	Entisol	Valent	
	AC1	21-35	-	10YR 4/4	Brown	-			
	C1	35-77	50	10YR 4/3	Brown	Sand			
	C2	77-120	110	10YR 5/4	Yellowish Brown	Sand			Coarse grains, pebbles, laminated
IMP-1C-2	A	0-15	5	10YR 3/3	Dark Brown	Loamy Sand	Entisol	Valent	
	AC1	15-25	-	10YR 4/3	Brown	-			
	C1	25-90	50	10YR 4/4	Brown	Sand			Roots @62cm
	C2	90-120	110	10YR 6/4	Light Yellowish Brown	Sand			
IMP-1C-3	A	0-21	5	10YR 3/3	Dark Brown	Sandy Loam	Entisol	Valent	
	AC1	21-34	-	10YR 4/4	Brown	-			
	C1	34-87	50	10YR 4/4	Brown	Sand			
	C2	87-120	110	10YR 6/4	Light Yellowish Brown	Sand			Some dune bedding

Table 3: Pedologic Description of Soil Profiles for Lincoln Dunefield Sites

Profile	Horizon	Depth (cm)	Sample Depth	Color Moist	Color Desc.	Texture	Soil Order	Soil Series	Notes
LI-1A-1	A	0-6	5	10YR 4/2	Dark Grayish Brown	Loamy Sand	Entisol	Valent	
	AC	6-32	20	10YR 4/3	Brown	Loamy Sand			Upper and lower boundaries distinctive
	C	32-98	50	10YR 4/6	Dark Yellowish Brown	Sand			
LI-1A-2	A	0-6	5	10YR 4/2	Dark Grayish Brown	Loamy Sand	Entisol	Valent	
	AC	6-47	20	10YR 4/3	Brown	Loamy Sand			Lower boundary distinctive
	C	47-87	60	10YR 4/4	Brown	Sand			
LI-1A-3	A	0-8	5	10YR 4/2	Dark Grayish Brown	Loamy Sand	Entisol	Valent	
	AC	8-49	20	10YR 3/3	Dark Brown	Loamy Sand			
	C	49-75	60	10YR 4/3	Brown	Loamy Sand			
LI-1B-1	A	0-5	3	10YR 3/3	Dark Brown	Sandy Loam	Entisol	Valent	
	AC	5-21	10	10YR 4/3	Brown	Loamy Sand			Lower boundary distinctive
	C	21-75	40	10YR 4/4	Brown	Sand			
LI-1B-2	A	0-4	3	10YR 4/2	Dark Grayish Brown	Loamy Sand	Entisol	Valent	
	AC	4-22	10	10YR 4/3	Brown	Loamy Sand			Lower boundary distinctive
	C	22-65	40	10YR 4/4	Brown	Sand			
LI-1B-3	A	0-6	5	10YR 4/2	Dark Grayish Brown	Loamy Sand	Entisol	Valent	
	AC	6-26	10	10YR 4/3	Brown	Loamy Sand			
	C	26-50	40	10YR 4/4	Brown	Sand			
LI-1C-1	A	0-8	5	10YR 4/2	Dark Grayish Brown	Sandy Loam	Entisol	Valent	
	AC	8-21	10	10YR 4/3	Brown	Loamy Sand			
	C	21-97	40	10YR 4/6	Dark Yellowish Brown	Loamy Sand			Eff. w/HCl
LI-1C-2	A	0-9	5	10YR 4/2	Dark Grayish Brown	Sandy Loam	Entisol	Valent	
	AC	9-39	20	10YR 3/2	Brown	Loamy Sand			
	C	39-68	60	10YR 3/3	Dark Brown	Loamy Sand			
LI-1C-3	A	0-11	5	10YR 4/2	Dark Grayish Brown	Sandy Loam	Entisol	Valent	
	AC	11-40	20	10YR 3/3	Dark Brown	Loamy Sand			
	C1	40-44	42	10YR 3/6	Dark Yellowish Brown	Loamy Sand			
	Ab	44-51	50	10YR 4/2	Dark Grayish Brown	Sandy Loam			Ab horizon has mod. slope
	C2	51-83	-	-	-	-			

Table 4: Pedologic Description of Soil Profiles for Sand Hills Lord Ranch Sites

Profile	Horizon	Depth (cm)	Sample Depth	Color Moist	Color Desc.	Texture	Soil Order	Soil Series	Notes
CH-1A-1	A	0-9	5	10YR 5/4	Yellowish Brown	Sand	Entisol	Valentine	Dune with some bare sand
	AC	9-20	10	10YR 4/6	Dark Yellowish Brown	Sand			
	C	20-100	50	10YR 4/6	Dark Yellowish Brown	Sand			Roots
CH-1A-2	A	0-8	5	10YR 4/4	Brown	Sand	Entisol	Valentine	Dune with some bare sand
	AC	8-22	10	10YR 3/4	Dark Yellowish Brown	Sand			
	C	22-100	50	10YR 3/6	Dark Yellowish Brown	Sand			
CH-1A-3	A	0-9	5	10YR 4/3	Brown	Sand	Entisol	Valentine	Dune with some bare sand
	AC	9-21	10	10YR 3/4	Dark Yellowish Brown	Sand			
	C	21-100	50	10YR 3/6	Dark Yellowish Brown	Sand			
CH-1B-1	AC	0-10	5	10YR 5/4	Yellowish Brown	Sand	Entisol	Valentine	Blowout
	C1	10-86	50	10YR 6/4	Light Yellowish Brown	Sand			
	Ab	86-105	100	10YR 5/3	Brown	Sand			
	C2	>120	-	-	-	-			
CH-1B-2	AC	0-17	5	10YR 5/4	Yellowish Brown	Sand	Entisol	Valentine	Blowout
	C1	17-120	50	10YR 6/3	Pale Brown	Sand			
	Ab	120-150	135	10YR 4/3	Brown	Sand			
	C2	>150	-	-	-	-			
CH-1B-3	AC	0-10	5	10YR 5/4	Yellowish Brown	Sand	Entisol	Valentine	Blowout
	C1	10-150	50	10YR 6/3	Pale Brown	Sand			
	Ab	150-165	160	10YR 4/3	Brown	Sand			
	C2	>165	-	-	-	-			
CH-1C-1	A	0-9	5	10YR 4/3	Brown	Sand	Entisol	Valentine	Dune with some bare sand
	C	9-53	10 50	10YR 5/4	Yellowish Brown	Sand			
CH-1C-2	A	0-7	5	10YR 4/2	Dark Grayish Brown	Sand	Entisol	Valentine	Dune with some bare sand
	C	7-55	10 50	10YR 3/4	Dark Yellowish Brown	Sand			
CH-1C-3	A	0-7	5	10YR 4/2	Dark Grayish Brown	Sand	Entisol	Valentine	Dune with some bare sand
	C	7-83	10 60	10YR 3/4	Dark Yellowish Brown	Sand			

Table 5: Pedologic Description of Soil Profiles for Sand Hills Milepost 81 Sites

Profile	Horizon	Depth (cm)	Sample Depth	Color Moist	Color Desc.	Texture	Soil Order	Soil Series	Notes
MP81-1A-1	A	0-4	3	10YR 4/2	Dark Grayish Brown	Sand	Entisol	Valentine	Dune with some bare sand
	C	4-85	10 50	10YR 4/3	Brown	Sand			Some banding
MP81-1A-2	A	0-12	2	10YR 4/2	Dark Grayish Brown	Sand	Entisol	Valentine	Dune with some bare sand
	C	12-92	20 70	10YR 4/3	Brown	Sand			Light-dark bands @39cm &, 51cm - Lighter band @62 cm, 10YR 5/4 - Lamellae @83cm
MP81-1A-3	A	0-8	5	10YR 4/2	Dark Grayish Brown	Sand	Entisol	Valentine	Dune with some bare sand - Profile at 30° angle
	C1	8-69	20 50	10YR 4/3	Brown	Sand			Banding throughout
	Ab	69-75	70	10YR 2/1	Black	Sand			
	C2	75-90	-	-	-	-			
MP81-1B-1	A	0-9	5	10YR 4/3	Brown	Sand	Entisol	Valentine	
	C1	9-20	15	10YR 3/3	Dark Brown	Sand			
	Ab	20-40	40	10YR 3/1	Very Dark Gray	Sand			
	C2	40-51	-	-	-	-			
MP81-1B-2	A	0-8	5	10YR 4/3	Brown	Sand	Entisol	Valentine	
	C	8-110	20 50	10YR 3/3	Dark Brown	Sand			
MP81-1B-3	A	0-7	5	10YR 4/2	Dark Grayish Brown	Sand	Entisol	Valentine	
	C1	7-52	20 50	10YR 4/3	Brown	Sand			
	Ab	52-53	52	10YR 3/1	Very Dark Gray	Sand			Possibly lamellae
	C2	53-75	-	-	-	-			
MP81-1C-1	A	0-9	5	10YR 4/2	Dark Grayish Brown	Sand	Entisol	Valentine	
	C	9-82	20 62	10YR 4/3	Brown	Sand			Banding 62-82cm
MP81-1C-2	A	0-10	5	10YR 4/2	Dark Grayish Brown	Sand	Entisol	Valentine	Very weak, possibly AC. Some banding.
	C	10-70	20 50	10YR 4/3	Brown	Sand			Banding @ 20cm, no banding below.
MP81-1C-3	A	0-13	5	10YR 4/2	Dark Grayish Brown	Sand	Entisol	Valentine	Profile at 30° angle.
	C	13-110	20 60	10YR 4/3	Brown	Sand			Banding throughout

Table 6: Pedologic Description of Soil Profiles for Sioux Dunefield Sites

Profile	Horizon	Depth (cm)	Sample Depth	Color Moist	Color Desc.	Texture	Soil Order	Soil Series	Notes
SI-1A-1	A	0-4	3	10YR 4/4	Brown	Loamy Sand	Entisol	Valent	Possibly sand sheet
	AC	4-8	8	10YR 5/6	Yellowish Brown	Loamy Sand			
	C	8-30	25	10YR 3/6	Dark Yellowish Brown	Sand			
SI-1A-2	A	0-12	5	10YR 3/4	Dark Yellowish Brown	Loamy Sand	Entisol	Valent	Possibly sand sheet
	AC	12-18	15	10YR 5/6	Yellowish Brown	Loamy Sand			
	C	18-40	30	10YR 3/4	Dark Yellowish Brown	Sand			
SI-1A-3	A	0-10	5	10YR 3/3	Dark Brown	Loamy Sand	Entisol	Valent	Possibly sand sheet
	C	10-40	15 30	10YR 4/6	Dark Yellowish Brown	Sand			
SI-1B-1	A	0-8	5	10YR 3/3	Dark Brown	Loamy Sand	Entisol	Valent	
	C	8-80	20 60	10YR 3/4	Dark Yellowish Brown	Loamy Sand			
SI-1B-2	A	0-13	5	10YR 3/2	Brown	Sandy Loam	Entisol	Valent	Deep roots
	AC	13-39	20	10YR 4/3	Brown	Loamy Sand			
	C	39-72	60	10YR 3/4	Dark Yellowish Brown	Sandy Loam			
SI-1B-3	A	0-10	5	10YR 4/3	Brown	Loamy Sand	Entisol	Valent	
	C	10-45	20 40	10YR 4/4	Brown	Loamy Sand			

Table 7: Mean Soil Horizon Thickness (cm) by Dunefield Site

Horizon	Imperial	Lincoln	Lord Ranch	Milepost 81	Sand Hills (tot.)	Sioux
A	26.7	7	8.2	8.9	8.6	9.5
AC	12.3	26	12.3	-	12.3	12
C*	53.4	44.8	67.5	82.3	74.9	35.7
C1	-	4	106.3	39	72.7	-
Ab	25	7	21.3	9	15.2	-
C2*	-	32	-	12.7	12.7	-

(* - complete depth to R horizon or next horizon beyond last C horizon sampled was not recorded)

Figure 8: Pedologic Color of Soil Profiles (Horizons A through Ab) for All Dunefield Sites

Soil Particle Size Analysis

Results from the soil particle size analyses show some consistency across horizons and dunefields, but also many differences. Overall mean, mode, and median grain sizes demonstrate a coarseness of soil across all dunefields and horizons. All three descriptive metrics for all dunefields were firmly in the sand fraction, with values greater than 63 μm. Likewise, the profiles at each site exhibited similar vertical trends, with grain sizes becoming coarser downward from the A horizon, then trending back toward a finer sand at some depth (Figure 12a-c). Given these trends, it is not surprising that the mean percentage of sand-sized particles increases in all dunefields from the A horizon to the C horizon (Figure 13a-c) and that this comes at the expense of material in the silt-sized fraction. These findings are unsurprising given the nature of dunefields, even stabilized dunefields. Generally, the parent material of dunefield soils found in the C Horizon is sandy, while the presence of vegetation and the process of pedogenesis in the A horizon traps finer soil particles and incorporates them into the soil.

Yet, while these general trends and patterns show the dunefields of the study areas share similarities, there are important differences in the particle size data which have implications for this thesis. While the overall soil particle size across all the dunefields is coarse, the degree of coarseness differs. The Sand Hills study sites exhibited the coarsest particle sizes of all with an overall mean of 214μm (±30) (Table 13). The dunefield's modal particle size slightly exceeds its mean, suggesting its overall particle size distribution is skewed in that direction. But beyond the pronounced coarseness of the Sand Hills sites, other data suggest important dunefield differences. For example, the mean and modal particle sizes by horizon show a relatively wide variance (Table 13, last column), as expressed by the standard deviation values. This feature can also be seen in the range of modal values in the A horizon, with the Sand Hills sites representing a maximum of Mo=207μm (±26) and the Lincoln Dunefield representing the minimum Mo=111μm (±5).

A further illustration of dunefield soil differences can be found in a comparison of the data for the Sand Hills and Imperial Dunefield sites. The Sand Hills site exhibits the coarsest particle size data, but the grain sizes at depth in the Imperial Dunefield approach those of the Sand Hills sites. In the parent material of the C horizon, the mean particle size for the Sand Hills is $\bar{x} = 214\mu m$ (± 33), while the mean particle size for the Imperial Dunefield actually is higher at $\bar{x} = 217\mu m$ (± 15). Yet, in the A horizon, the mean particle sizes for the two sites diverge. For the Sand Hills, the mean particle size for the A horizon was $\bar{x} = 202\mu m$ (± 23), while it was $\bar{x} = 168\mu m$ (± 19) for the Imperial Dunefield. This divergence for the two locations between the A and C horizons might suggest that soil development is more robust in the Imperial Dunefield than it is in the Sand Hills. Additionally, dunes in the Sand Hills might have experienced more frequent recent activity, leading to loss of finer-grained material – and this possibility has implications for this study.

Other interesting findings with regards to soil grain size involve the overall percentage of silt present in the soil (Figure 12b) and the composition of the silt fraction (Figure 12c). On average, fine silt (2-16μm) comprises approximately 50% or more of material in the silt particle size category (2-63μm) at all horizons. Additionally, the average percentage of silt in the soil profiles decreases from the A horizons down to the C horizon, then increases in buried Ab horizons. Depending upon the horizon, these results have different implications. In the A and Ab horizons, the pronounced presence of fine silt and of silt overall suggests a stable vegetated state to the dunes. In this scenario, grasses could be trapping dust particles, with bioturbation such as insect or rodent burrowing working the silt-sized material down into the soil profile, especially in the A horizon, as was discovered in other studies (Werner et al., 2011; Yan et al., 2011). The relative lack of silt in the C horizons suggests the parent material of the dunefields is somewhat "clean" sand and not silty-sandy dunes.

With regards to clay-sized soil particles (<2μm), very little exists in any of these sites. It is possible that the Malvern Instruments Mastersizer 2000MU® laser particle size analyzer, which was used to measure soil grain size, underestimated clay content relative to other methods such as pipette analysis, as was discovered in other studies (Mason et al., 2003). However, the clay percentages range from 2.5% in the C horizon at site SI-1B-2 in the Sioux Dunefield to 0.4% in two C horizons at the Lord Ranch site. Even with a potential underestimation of clay in the results, there is very little clay in these dunefield soils. Samples from the Sand Hills sites have the least clay, followed by the Imperial Dunefield sites. The profiles with the highest clay content are in the Lincoln and Sioux dunefields.

Table 8: Particle Size Data for Soil Profiles in the Imperial Dunefield

Profile	Horizon	Sample Depth	Mean (µm)	Median (µm)	Mode (µm)	Sand%	Silt% Total	Silt% Fine 2-16(µm)	Silt Fine-Total Ratio	Clay%	Texture General	Texture Mean
IMP-1A-1	A	10	177.3	144.8	157.1	79.1	19.4	10.8	0.56	1.4	Loamy Sand	Fine Sand
	A	30	181.4	150.6	155.2	83.3	15.4	9.1	0.59	1.4	Loamy Sand	Fine Sand
	C	60	189.8	150.8	148.8	82.2	16.4	9.8	0.6	1.4	Loamy Sand	Fine Sand
IMP-1A-2	A	10	175.4	148.2	163.1	79.9	18.7	10.5	0.56	1.4	Loamy Sand	Fine Sand
	A	30	194.5	166.6	179.4	85.3	13.5	8.3	0.61	1.3	Loamy Sand	Fine Sand
	C	60	200.8	157.1	151.7	83.1	15.4	9.8	0.63	1.5	Loamy Sand	Fine Sand
IMP-1A-3	A	10	150.2	123.1	143.6	73.1	25.5	12.8	0.5	1.5	Loamy Sand	Fine Sand
	A	30	171.2	145.6	153.8	82.6	16.1	9.5	0.59	1.4	Loamy Sand	Fine Sand
	C	60	205.8	167.7	169.9	84.8	13.8	8.9	0.65	1.4	Loamy Sand	Fine Sand
IMP-1B-1	A	5	164.1	146.6	167.3	80.3	18.3	10.1	0.55	1.4	Loamy Sand	Fine Sand
	C	50	209	193.4	206	94.2	4.9	3.4	0.7	1	Sand	Fine Sand
	Ab	110	222.7	178.6	180.7	86.1	12.7	7.4	0.59	1.2	Sand	Fine Sand
IMP-1B-2	A	5	159.2	145.7	154.4	86.6	12.2	7.7	0.63	1.3	Sand	Fine Sand
	C	50	220.9	199	213.9	93.4	5.7	4	0.7	1	Sand	Fine Sand
	Ab	110	215.6	171.2	168	87.4	11.5	6.9	0.59	1.1	Sand	Fine Sand
IMP-1B-3	A	5	155.8	145.4	155.8	87.3	11.4	7.3	0.63	1.3	Sand	Fine Sand
	C	25	218.7	178.5	180.1	87.6	11.3	6.8	0.6	1.1	Sand	Fine Sand
	Ab	50	188.1	159.6	166.1	85	13.8	8.6	0.62	1.2	Loamy Sand	Fine Sand
IMP-1C-1	A	5	194.4	161.5	180.4	82.2	16.5	9.3	0.56	1.3	Loamy Sand	Fine Sand
	AC1	-	-	-	-	-	-	-	-	-	-	-
	C1	50	208.6	176.2	176.2	92.1	6.9	4.1	0.59	1.1	Sand	Fine Sand
	C2	110	241.7	209.5	244.8	90.6	8.3	6.1	0.74	1.1	Sand	Fine Sand
IMP-1C-2	A	5	157.6	129.8	150	75.8	23.1	9.8	0.42	1.1	Loamy Sand	Fine Sand
	AC1	-	-	-	-	-	-	-	-	-	-	-
	C1	50	225.9	199.1	229.2	90.3	8.6	5.4	0.63	1.1	Sand	Fine Sand
	C2	110	238.3	204.6	223.2	91.4	7.5	5.2	0.7	1.1	Sand	Fine Sand
IMP-1C-3	A	5	130.8	110.6	132	71.2	27.1	12.6	0.47	1.7	Sandy Loam	Fine Sand
	AC1	-	-	-	-	-	-	-	-	-	-	-
	C1	50	221.9	200.7	223.8	92.5	6.5	4	0.61	0.9	Sand	Fine Sand
	C2	110	216.1	188.0	198.5	92.6	6.4	4.1	0.65	1.1	Sand	Fine Sand

Table 9: Particle Size Data for Soil Profiles in the Lincoln Dunefield

Profile	Horizon	Sample Depth	Mean (µm)	Median (µm)	Mode (µm)	Sand%	Silt% Total	Silt% Fine 2-16(µm)	Silt Fine-Total Ratio	Clay%	Texture General	Texture Mean
LI-1A-1	A	5	108.3	101.1	111.8	75.3	22.9	11.2	0.49	1.8	Loamy Sand	Very Fine Sand
	AC	20	138.4	119.4	129.3	77.7	20.5	11.1	0.54	1.8	Loamy Sand	Fine Sand
	C	50	149.8	136.4	136.9	91.6	7	4.1	0.59	1.5	Sand	Fine Sand
LI-1A-2	A	5	117	106.5	115.2	78.4	19.9	11	0.55	1.7	Loamy Sand	Very Fine Sand
	AC	20	136.6	115.4	125	76.5	21.8	11.9	0.54	1.6	Loamy Sand	Fine Sand
	C	60	157	131.7	128.9	88.5	9.9	5.6	0.57	1.5	Loamy Sand	Fine Sand
LI-1A-3	A	5	111	105	117.2	76.2	21.9	12.9	0.59	1.9	Loamy Sand	Very Fine Sand
	AC	20	119.8	104.1	115.7	73.7	24.6	12	0.49	1.7	Loamy Sand	Very Fine Sand
	C	60	151.6	129.9	130.6	84.4	14.3	8.2	0.57	1.4	Loamy Sand	Fine Sand
LI-1B-1	A	3	106.3	94.7	106.1	71.8	26.4	11.8	0.45	1.8	Sandy Loam	Very Fine Sand
	AC	10	109.9	99.9	108.5	75.8	22.7	10.3	0.46	1.6	Loamy Sand	Very Fine Sand
	C	40	155.9	128.1	121.5	88.2	10.1	4.5	0.45	1.7	Sand	Fine Sand
LI-1B-2	A	3	119.5	104	110.8	77.9	20.3	9.9	0.49	1.8	Loamy Sand	Very Fine Sand
	AC	10	164.3	110.3	114	81.7	16.7	8.9	0.53	1.6	Loamy Sand	Fine Sand
	C	40	166	122.3	121.6	89.3	9.1	4.8	0.53	1.6	Sand	Fine Sand
LI-1B-3	A	5	182.4	108.6	113.2	78.4	20	10	0.5	1.6	Loamy Sand	Fine Sand
	AC	10	128.9	110.6	116.1	79	19.4	9.7	0.5	1.6	Loamy Sand	Fine Sand
	C	40	142.9	126.7	124.7	90.1	8.4	4.3	0.51	1.5	Sand	Fine Sand
LI-1C-1	A	5	112.8	93.8	107.5	69	28.9	13.6	0.47	2.1	Sandy Loam	Very Fine Sand
	AC	10	160	105.3	113.8	74.7	23.5	11.4	0.49	1.8	Loamy Sand	Fine Sand
	C	40	128.7	108	117.1	75.1	23	11.7	0.51	1.9	Loamy Sand	Fine Sand
LI-1C-2	A	5	102.9	96.5	112.7	70.9	27.2	12.9	0.47	1.9	Sandy Loam	Very Fine Sand
	AC	20	116.3	106.3	116	76.9	21	11.2	0.53	2	Loamy Sand	Very Fine Sand
	C	60	140.7	118.1	124.5	77.8	20.4	11.5	0.57	1.9	Loamy Sand	Fine Sand
LI-1C-3	A	5	97.3	86.5	101.4	66.2	31.5	13.9	0.44	2.3	Sandy Loam	Very Fine Sand
	AC	20	111.2	101.3	112.4	74.2	23.6	11.5	0.49	2.1	Loamy Sand	Very Fine Sand
	C1	42	154.8	129.8	132.5	81.4	16.8	9.6	0.57	1.8	Loamy Sand	Fine Sand
	Ab	50	113.5	98.3	111	71.3	26.7	13.7	0.51	2.1	Sandy Loam	Very Fine Sand
	C2	-	-	-	-	-	-	-	-	-	-	-

Table 10: Particle Size Data for Soil Profiles at the Sand Hills Lord Ranch Sites

Profile	Horizon	Sample Depth	Mean (µm)	Median (µm)	Mode (µm)	Sand%	Silt% Total	Silt% Fine 2-16(µm)	Silt Fine-Total Ratio	Clay%	Texture General	Texture Mean
CH-1A-1	A	5	220.1	218.7	232	90.3	8.9	5.2	0.58	0.8	Sand	Fine Sand
	AC	10	210.2	211.3	227.7	86.8	12.5	7.1	0.57	0.7	Sand	Fine Sand
	C	50	230.3	228.5	237.2	92.2	7.3	4.9	0.67	0.6	Sand	Fine Sand
CH-1A-2	A	5	211.1	210.9	224.6	88.6	10.7	6.6	0.62	0.7	Sand	Fine Sand
	AC	10	219	217.8	230.7	89.3	10	6	0.6	0.6	Sand	Fine Sand
	C	50	256.4	251.3	258.7	94.6	5	3.4	0.69	0.4	Sand	Median to Course Sand
CH-1A-3	A	5	213	211.4	223.3	89.8	9.6	6	0.62	0.5	Sand	Fine Sand
	AC	10	225.4	226.6	238.1	89.8	9.5	6.2	0.65	0.6	Sand	Fine Sand
	C	50	225.7	221.8	227.5	93.9	5.6	3.9	0.71	0.5	Sand	Fine Sand
CH-1B-1	AC	5	229.7	228.5	238.1	92	7.5	5.1	0.69	0.6	Sand	Fine Sand
	C1	50	256	253.9	263.7	93.1	6.4	4.2	0.66	0.5	Sand	Median to Course Sand
	Ab	100	274	272.7	288.8	89.9	9.5	5.8	0.62	0.6	Sand	Median to Course Sand
	C2	-	-	-	-	-	-	-	-	-	-	-
CH-1B-2	AC	5	233.2	230.6	238.6	92.6	6.8	4.8	0.7	0.6	Sand	Fine Sand
	C1	50	259.3	254.6	261	94.7	4.8	3.2	0.66	0.5	Sand	Median to Course Sand
	Ab	135	238.7	239.8	253	89.6	9.7	6.3	0.64	0.7	Sand	Fine Sand
	C2	-	-	-	-	-	-	-	-	-	-	-
CH-1B-3	AC	5	247.6	243.5	252.7	93.9	5.6	4.1	0.73	0.6	Sand	Fine Sand
	C1	50	265.3	259.9	267.2	95.3	4.3	3	0.7	0.4	Sand	Median to Course Sand
	Ab	160	251	248.1	256.8	93.4	6.1	4.1	0.66	0.5	Sand	Median to Course Sand
	C2	-	-	-	-	-	-	-	-	-	-	-
CH-1C-1	A	5	239.5	239.4	251.3	91.7	7.7	5.1	0.66	0.6	Sand	Fine Sand
	C	10	240.4	238.8	247.6	92.7	6.8	4.3	0.64	0.5	Sand	Fine Sand
	C	50	258.9	258.6	266.4	93.1	6.3	4.5	0.72	0.6	Sand	Median to Course Sand
CH-1C-2	A	5	220.2	220.9	231.1	90.8	8.6	5.7	0.67	0.6	Sand	Fine Sand
	C	10	235.3	235.7	243.1	92.8	6.6	4.4	0.67	0.6	Sand	Fine Sand
	C	50	248.4	247.6	258	92	7.2	4.9	0.67	0.8	Sand	Fine Sand
CH-1C-3	A	5	238.7	238.8	246.2	93	6.5	4.3	0.66	0.5	Sand	Fine Sand
	C	10	245.3	243	250.8	92.9	6.5	4.3	0.67	0.6	Sand	Fine Sand
	C	60	248.1	251	260.6	90.8	8.6	5.7	0.67	0.6	Sand	Fine Sand

Table 11: Particle Size Data for Soil Profiles at the Sand Hills Milepost 81 Sites

Profile	Horizon	Sample Depth	Mean (µm)	Median (µm)	Mode (µm)	Sand%	Silt% Total	Silt% Fine 2-16(µm)	Silt Fine-Total Ratio	Clay%	Texture General	Texture Mean
MP81-1A-1	A	3	181.9	177.6	185.3	92.8	6.3	5	0.79	0.9	Sand	Fine Sand
	C	10	204.2	197	203.3	95.4	3.9	2.9	0.74	0.7	Sand	Fine Sand
	C	50	168.9	165.6	170.4	94.5	4.7	3.6	0.76	0.8	Sand	Fine Sand
MP81-1A-2	A	2	188.8	183.4	191.4	93	6.2	4.7	0.76	0.7	Sand	Fine Sand
	C	20	180.3	174.1	179.8	94.2	5	3.7	0.75	0.9	Sand	Fine Sand
	C	70	168.1	161.6	171.6	91.1	7.6	5.2	0.68	1.3	Sand	Fine Sand
MP81-1A-3	A	5	187	182	189.3	93.3	5.9	4.5	0.75	0.7	Sand	Fine Sand
	C1	20	198.8	193.4	198.4	95.7	3.8	2.6	0.7	0.5	Sand	Fine Sand
	C1	50	207.8	199	204	95.6	3.9	2.8	0.71	0.5	Sand	Fine Sand
	Ab	70	233.7	220	229.4	96.4	3.1	2.2	0.7	0.5	Sand	Fine Sand
	C2	-	-	-	-	-	-	-	-	-	-	-
MP81-1B-1	A	5	160.2	156.9	163.8	91.8	7.3	5.8	0.8	0.9	Sand	Fine Sand
	C1	15	178.5	173.6	177.8	95	4.3	3.1	0.73	0.7	Sand	Fine Sand
	Ab	40	187.4	181.5	187.9	94.1	5.1	3.7	0.73	0.8	Sand	Fine Sand
	C2	-	-	-	-	-	-	-	-	-	-	-
MP81-1B-2	A	5	179	172	181.6	91.7	7.3	5.8	0.79	0.9	Sand	Fine Sand
	C	20	179.3	172.8	177.8	94.7	4.5	3.4	0.75	0.8	Sand	Fine Sand
	C	50	182.8	177.1	180.6	95.8	3.5	2.5	0.72	0.7	Sand	Fine Sand
MP81-1B-3	A	5	213.6	202.1	211.3	94.3	4.9	3.9	0.78	0.8	Sand	Fine Sand
	C1	20	221.4	209	216.4	96.3	3.1	2.2	0.73	0.6	Sand	Fine Sand
	C1	50	182.5	175.2	180.5	95.1	4.1	3.1	0.76	0.9	Sand	Fine Sand
	Ab	52	185.3	178.2	183.3	95.1	4.1	3.1	0.76	0.8	Sand	Fine Sand
	C2	-	-	-	-	-	-	-	-	-	-	-
MP81-1C-1	A	5	189.9	183.7	189.7	94.5	4.7	3.5	0.74	0.7	Sand	Fine Sand
	C	20	196.5	185.8	194.2	94	5.2	3.8	0.74	0.8	Sand	Fine Sand
	C	62	157.8	153.8	158.7	94.7	4.4	3.4	0.77	0.9	Sand	Fine Sand
MP81-1C-2	A	5	184.2	180	189.6	91.5	7.5	5.9	0.79	1	Sand	Fine Sand
	C	20	214.8	206.6	212.7	95.9	3.5	2.4	0.7	0.7	Sand	Fine Sand
	C	50	190.2	183	188.6	95.4	3.9	2.9	0.74	0.7	Sand	Fine Sand
MP81-1C-3	A	5	198.9	190.8	197	94.7	4.6	3.5	0.76	0.8	Sand	Fine Sand
	C	20	207.1	198.7	204.7	95.1	4.3	3.2	0.74	0.6	Sand	Fine Sand
	C	60	186.2	180.5	185.4	95.7	3.6	2.5	0.69	0.7	Sand	Fine Sand

Table 12: Particle Size Data for Soil Profiles in the Sioux Dunefield

Profile	Horizon	Sample Depth	Mean (µm)	Median (µm)	Mode (µm)	Sand%	Silt% Total	Silt% Fine 2-16(µm)	Silt Fine-Total Ratio	Clay%	Texture General	Texture Mean
SI-1A-1	A	3	135	130.8	152.7	80.7	17.9	10.2	0.57	1.4	Loamy Sand	Fine Sand
	AC	8	146.6	142.8	161.2	85.	13.6	8.6	0.63	1.4	Loamy Sand	Fine Sand
	C	25	146.4	143.5	156.1	87.3	11.4	7.7	0.68	1.3	Sand	Fine Sand
SI-1A-2	A	5	155.3	151.6	171.2	85	13.8	9	0.66	1.3	Loamy Sand	Fine Sand
	AC	15	145.5	142	160	84.7	13.9	9.2	0.66	1.4	Loamy Sand	Fine Sand
	C	30	144.3	141.8	155.4	86.8	11.8	8.1	0.69	1.3	Sand	Fine Sand
SI-1A-3	A	5	147.2	143.3	161.6	84.8	13.9	8.5	0.61	1.3	Loamy Sand	Fine Sand
	C	15	149.2	146.5	160.3	87.4	11.4	7.9	0.69	1.2	Sand	Fine Sand
	C	30	147.5	145.8	160.6	86.5	12.2	8.7	0.71	1.4	Sand	Fine Sand
SI-1B-1	A	5	113.4	105.6	124.2	73.5	24.6	12.3	0.5	1.9	Loamy Sand	Very Fine Sand
	C	20	112.6	105.1	120.2	74.8	23	11.7	0.51	2.2	Loamy Sand	Very Fine Sand
	C	60	108.5	103.4	117.1	75.8	22.1	11.4	0.52	2.1	Loamy Sand	Very Fine Sand
SI-1B-2	A	5	105.9	98.2	117.4	70.3	27.7	13.6	0.49	2	Sandy Loam	Very Fine Sand
	AC	20	113.1	106.4	122.4	75.5	22.7	11.1	0.49	1.8	Loamy Sand	Very Fine Sand
	C	60	101.8	97.6	114.4	71.8	25.7	13.8	0.54	2.5	Sandy Loam	Very Fine Sand
SI-1B-3	A	5	106	99.8	116.6	72.4	25.5	12.4	0.49	2.1	Loamy Sand	Very Fine Sand
	C	20	106.2	100.6	116	73.6	24.3	12.1	0.5	2	Loamy Sand	Very Fine Sand
	C	40	105.2	100.1	117.4	72.6	25.4	12.6	0.5	2	Loamy Sand	Very Fine Sand

Table 13: Mean and Modal Soil Particle Size (µm) by Dunefield

Horizon	Imperial	Lincoln	Sand Hills (tot.)	Sioux	Total
A	$\bar{x}$ = 168 (±19) Mo = 158 (±14)	$\bar{x}$ = 118 (±25) Mo = 111 (±5)	$\bar{x}$ = 202 (±23) Mo = 207 (±26)	$\bar{x}$ = 127 (±22) Mo = 141 (±24)	$\bar{x}$ = 163 (±41) Mo = 163 (±42)
AC	-	$\bar{x}$ = 132 (±20) Mo = 117 (± 6)	$\bar{x}$ = 228 (±13) Mo = 238 (±9)	$\bar{x}$ = 135 (±19) Mo = 148 (±22)	$\bar{x}$ = 164 (±49) Mo = 162 (±57)
C*	$\bar{x}$ = 217 (±15) Mo = 197 (±32)	$\bar{x}$ = 150 (±11) Mo = 126 (±6)	$\bar{x}$ = 214 (±33) Mo = 215 (±36)	$\bar{x}$ = 125 (±21) Mo = 135 (±22)	$\bar{x}$ = 191 (±45) Mo = 186 (±48)
Ab	$\bar{x}$ = 209 (±18) Mo = 172 (±8)	$\bar{x}$ = 113 (±0) Mo = 111 (±0)	$\bar{x}$ = 228 (±35) Mo = 233 (±41)	-	$\bar{x}$ = 211 (±45) Mo = 203 (±53)
Total	$\bar{x}$ = 194 (±29) Mo = 177 (±29)	$\bar{x}$ = 132 (±23) Mo = 118 (±9)	$\bar{x}$ = 214 (±30) Mo = 217 (±33)	$\bar{x}$ = 128 (±20) Mo = 135 (±22)	$\bar{x}$ = 180 (±46) Mo = 176 (±49)

(* - includes all sampled C and C1 horizons, but not C2 horizons.)

Figure 9a-d: Boxplot Profiles of Mean Particle Size Data by Horizon by Dunefield

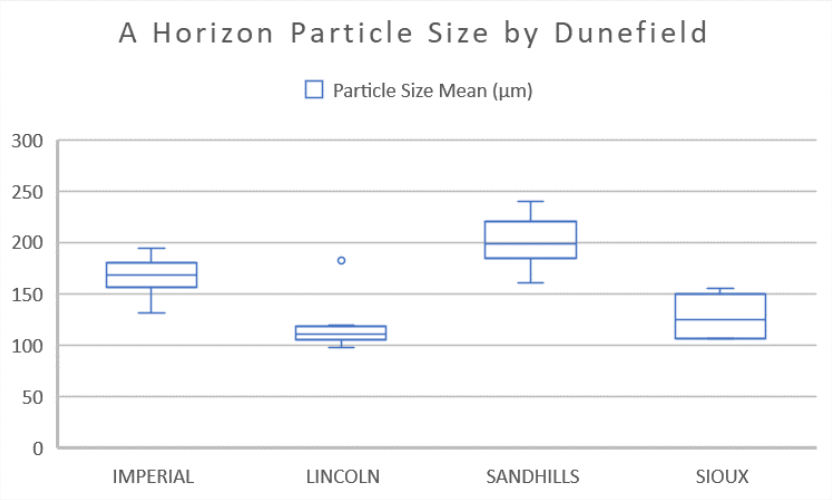

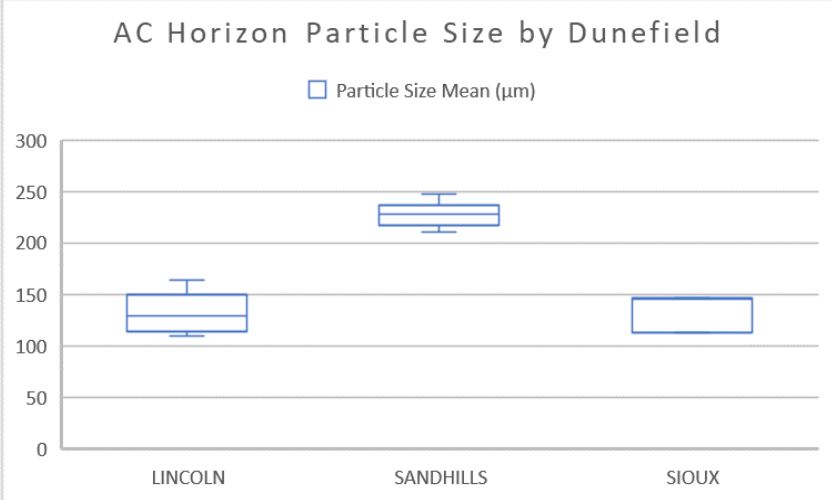

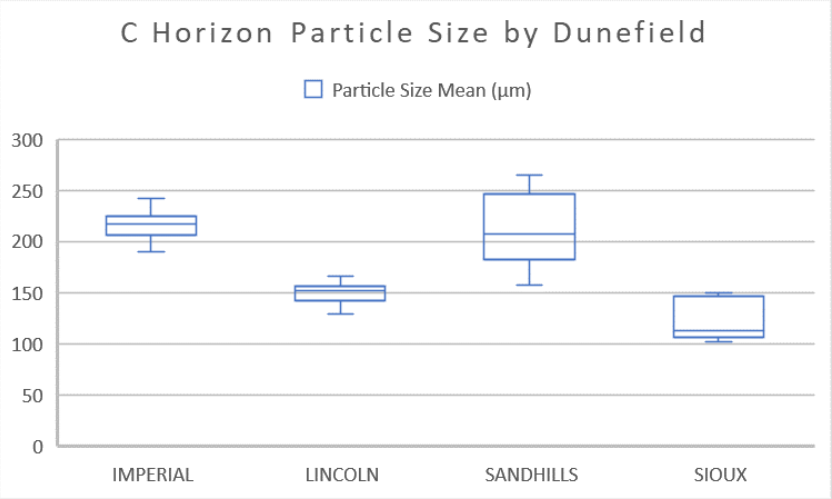

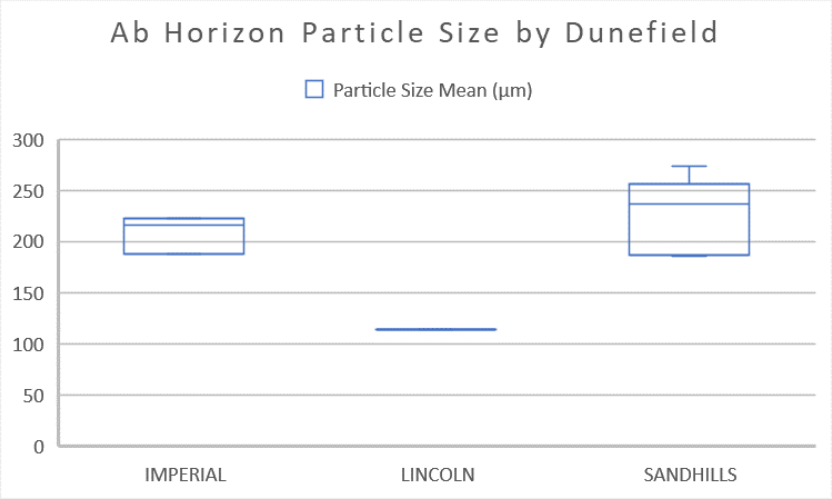

Figure 10a-d: Boxplot Profiles of Modal Particle Size Data by Horizon by Dunefield

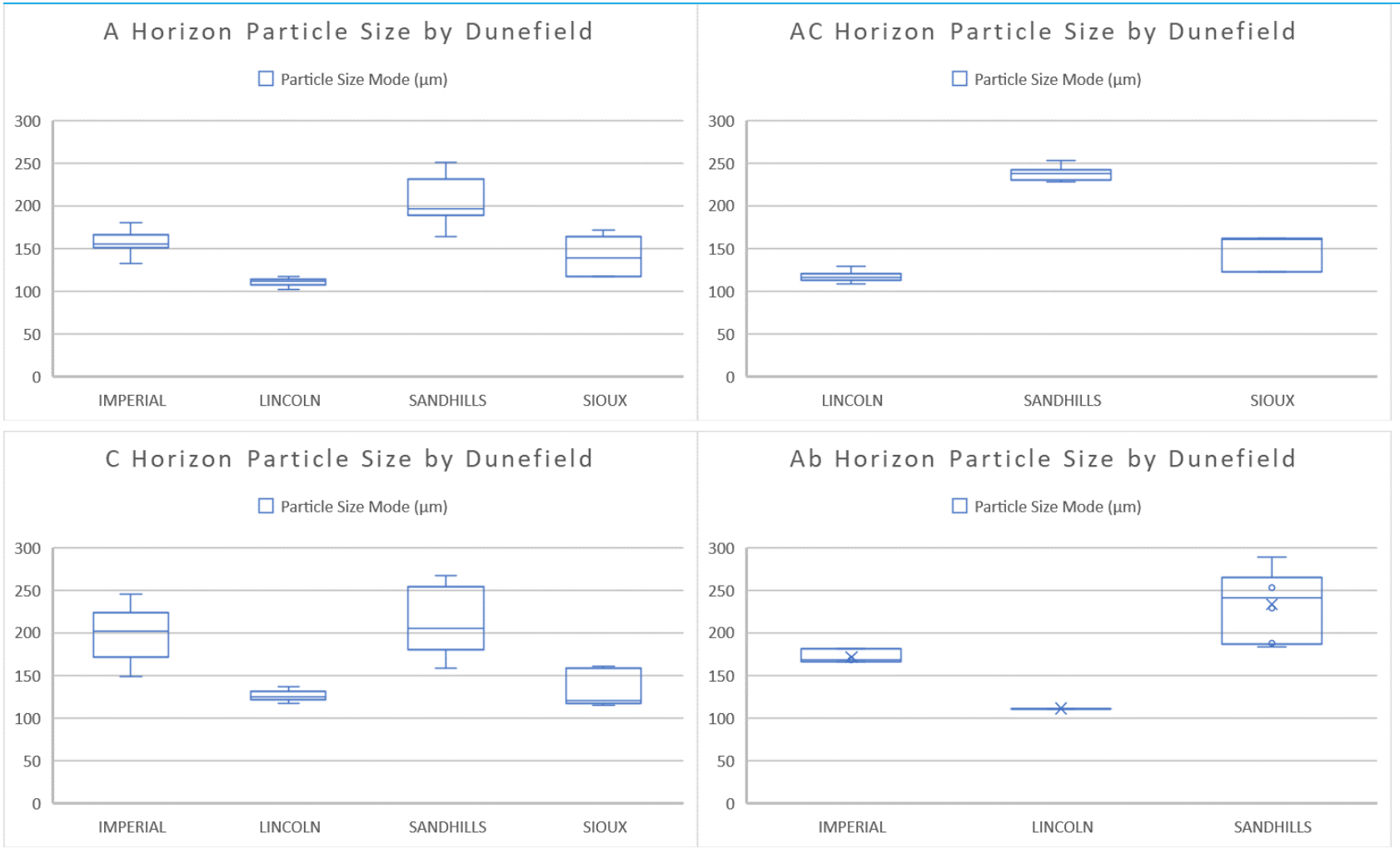

Figure 11a-c: Vertical Profiles of Particle Size Data by Horizon by Dunefield

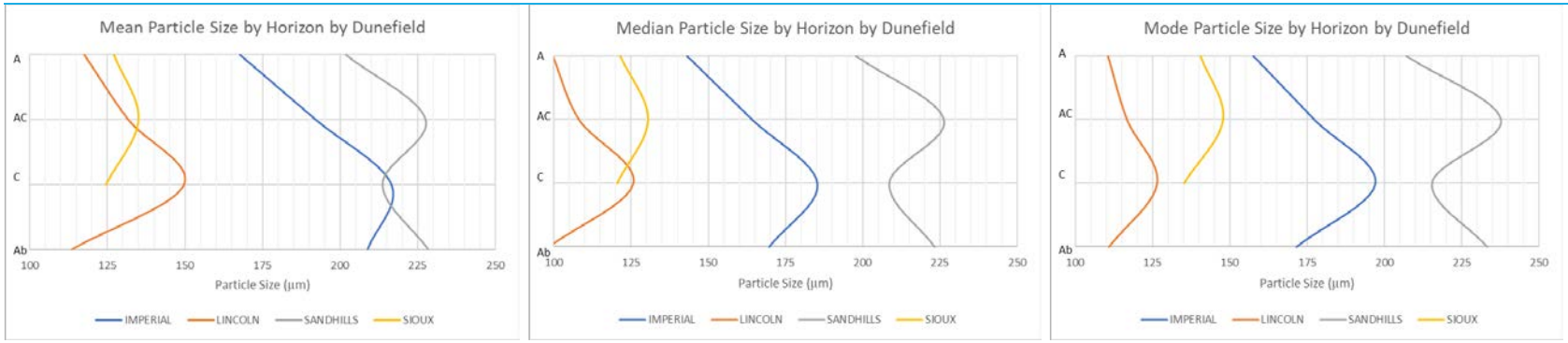

Figure 12a-c: Vertical Profiles of Sand and Silt Data by Horizon by Dunefield

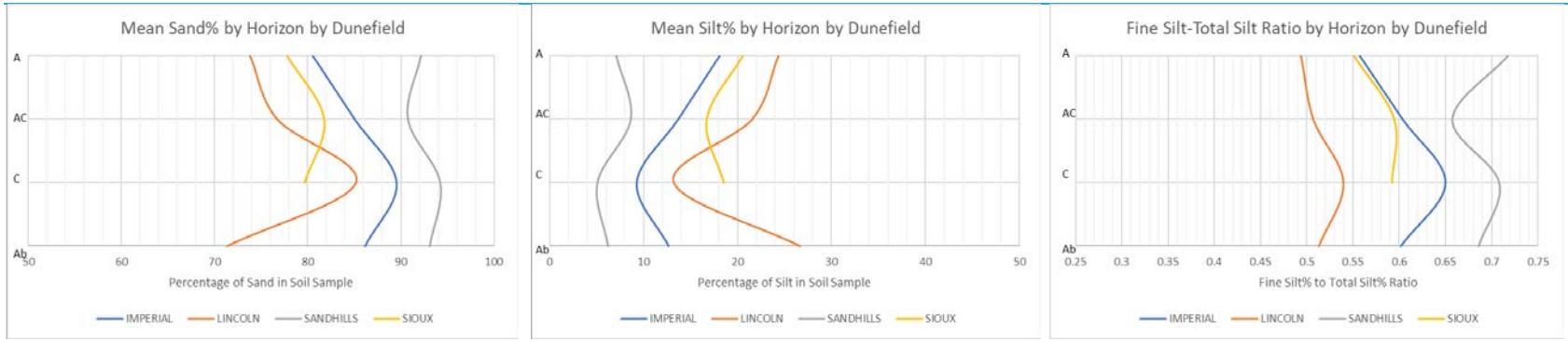

Loss-on-Ignition (LOI)

The results of the loss-on-ignition (LOI) analysis produced an overall pattern to LOI values across all dunefields that was related to pedology, but also illustrated differences between dunefields. Across all dunefields, the loss of soil organic matter (SOM) on ignition decreased overall from the A horizon to the C horizon (Figure 13a), then increased slightly for any buried A horizons present. This general pattern is a trend seen in many of the analyses in this study, including the particle size analysis, where the results have been aggregated by horizon and dunefield. This pattern clearly is tied to pedologic horizon.

Yet, differences exist in the maximum value of LOI% in A horizons, its decrease with depth, and the variance of the results. LOI% values for the Sand Hills sites were relatively low in the A and C horizons when compared with results from the other three dunefields and exhibited very little variance around the low mean LOI (Figure 15a & c). The mean LOI% for A horizons in the Sand Hills was 0.32% (±0.08), while the next lowest mean A horizon LOI% values were 0.77% (±0.35) for the Imperial Dunefield. The Lincoln and Sioux dunefields A horizon LOI% values were both >1%. The three other dunefields exhibited roughly the same mean LOI% values for both A and C horizons, which was higher than in the Sand Hills. The dunefields also differed in the ratio of A horizon LOI% to C horizon LOI%. The metric could be interpreted as a measure of grassland vegetation and pedogenesis, since presumably the parent material of a dunefield soil would be sand and, thus, lacking SOM. For this metric, the results are bifurcated. The ratio of LOI% in the A-to-C horizons is high – greater than 1.75 – for the Imperial and Lincoln dunefields and low – less than 1.5 – for the Sand Hills and Sioux dunefields. This distribution clusters the two southern-most dunefields together (Imperial and Lincoln) and the two northern-most dunefields together (Sand Hills and Sioux).

Table 14a-c: Loss-on-Ignition (LOI) Values for Soil Profiles for the Imperial, Lincoln, and Lord Ranch Sites

Profile	Horizon	Sample Depth	LOI%
IMP-1A-1	A	10	0.72
	A	30	0.26
	C	60	0.59
IMP-1A-2	A	10	0.73
	A	30	0.46
	C	60	0.55
IMP-1A-3	A	10	1.19
	A	30	0.65
	C	60	0.50
IMP-1B-1	A	5	0.79
	C	50	0.28
	Ab	110	0.45
IMP-1B-2	A	5	0.53
	C	50	0.25
	Ab	110	0.38
IMP-1B-3	A	5	0.55
	C	25	0.38
	Ab	50	0.49
IMP-1C-1	A	5	0.65
	AC1	-	-
	C1	50	0.28
	C2	110	0.22
IMP-1C-2	A	5	1.28
	AC1	-	-
	C1	50	0.65
	C2	110	0.32
IMP-1C-3	A	5	1.39
	AC1	-	-
	C1	50	0.35
	C2	110	0.42

Profile	Horizon	Sample Depth	LOI%
LI-1A-1	A	5	0.99
	AC	20	0.83
	C	50	0.39
LI-1A-2	A	5	0.76
	AC	20	0.85
	C	60	0.37
LI-1A-3	A	5	0.69
	AC	20	0.90
	C	60	0.44
LI-1B-1	A	3	1.45
	AC	10	0.98
	C	40	0.46
LI-1B-2	A	3	0.92
	AC	10	0.72
	C	40	0.46
LI-1B-3	A	5	0.93
	AC	10	0.72
	C	40	0.30
LI-1C-1	A	5	1.57
	AC	10	0.90
	C	40	0.80
LI-1C-2	A	5	1.12
	AC	20	0.67
	C	60	0.71
LI-1C-3	A	5	1.36
	AC	20	1.00
	C1	42	0.61
	Ab	50	0.87
	C2	-	

Profile	Horizon	Sample Depth	LOI%
CH-1A-1	A	5	0.52
	AC	10	0.40
	C	50	0.19
CH-1A-2	A	5	0.37
	AC	10	0.48
	C	50	0.10
CH-1A-3	A	5	0.31
	AC	10	0.57
	C	50	0.18
CH-1B-1	AC	5	0.25
	C1	50	0.21
	Ab	100	0.23
	C2	-	-
CH-1B-2	AC	5	0.63
	C1	50	0.83
	Ab	135	0.31
	C2	-	-
CH-1B-3	AC	5	0.13
	C1	50	0.10
	Ab	160	0.26
	C2	-	-
CH-1C-1	A	5	0.29
	C	10	0.27
	C	50	0.19
CH-1C-2	A	5	0.35
	C	10	0.24
	C	50	0.24
CH-1C-3	A	5	0.30
	C	10	0.22
	C	60	0.23

Table 15a-b: Loss-on-Ignition (LOI) Values for Soil Profiles for the Milepost 81 and Sioux Sites

Profile	Horizon	Sample Depth	LOI%
MP81-1A-1	A	3	0.26
	C	10	0.26
	C	50	0.29
MP81-1A-2	A	2	0.30
	C	20	0.29
	C	70	0.52
MP81-1A-3	A	5	0.27
	C1	20	0.22
	C1	50	0.20
	Ab	70	0.21
	C2	-	-
MP81-1B-1	A	5	0.29
	C1	15	0.27
	Ab	40	0.28
	C2	-	-
MP81-1B-2	A	5	0.32
	C	20	0.23
	C	50	0.14
MP81-1B-3	A	5	0.42
	C1	20	0.13
	C1	50	0.21
	Ab	52	0.20
	C2	-	-
MP81-1C-1	A	5	0.22
	C	20	0.22
	C	62	0.19
MP81-1C-2	A	5	0.29
	C	20	0.23
	C	50	0.25
MP81-1C-3	A	5	0.22
	C	20	0.24
	C	60	0.21

Profile	Horizon	Sample Depth	LOI%
SI-1A-1	A	3	0.88
	AC	8	0.71
	C	25	0.60
SI-1A-2	A	5	0.72
	AC	15	0.75
	C	30	0.67
SI-1A-3	A	5	0.78
	C	15	0.67
	C	30	0.51
SI-1B-1	A	5	1.14
	C	20	0.95
	C	60	0.79
SI-1B-2	A	5	1.46
	AC	20	1.01
	C	60	0.99
SI-1B-3	A	5	1.17
	C	20	0.94
	C	40	0.88

Figure 13: Loss-on-Ignition (LOI) Percentage by Horizon by Dunefield
Figure 14: Ratio of LOI% A:C Horizon by Dunefield

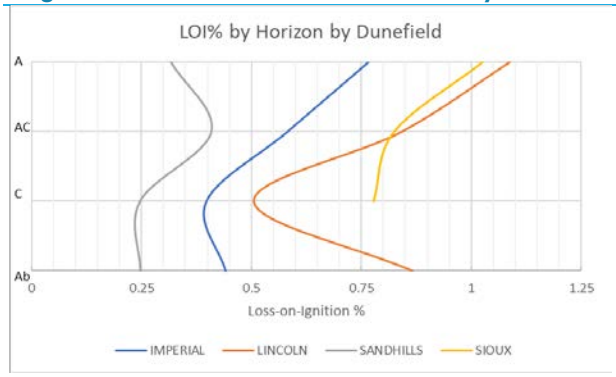

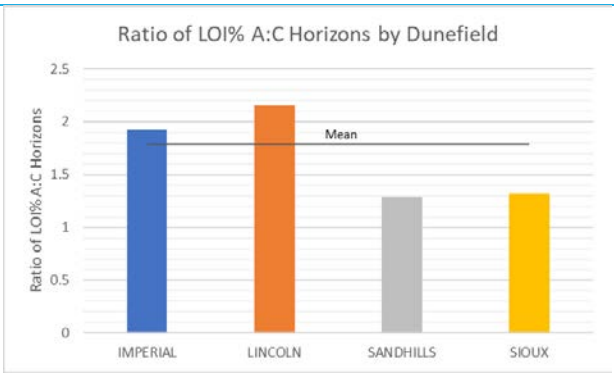

Figure 15a-d: Loss-on-Ignition (LOI) Percentage by Horizon boxplots by Dunefield

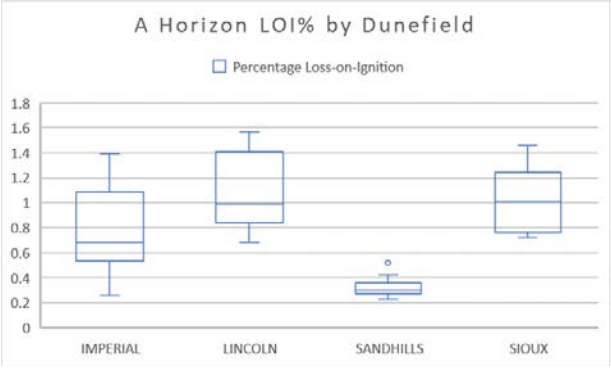

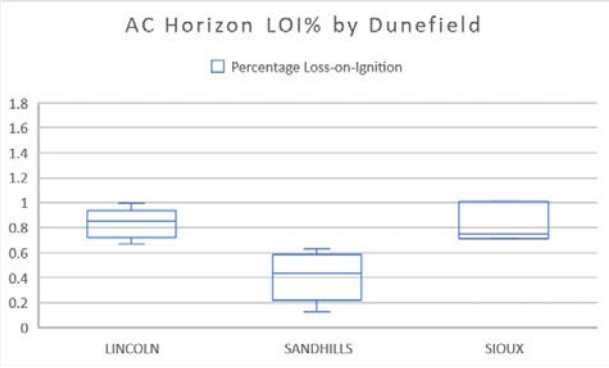

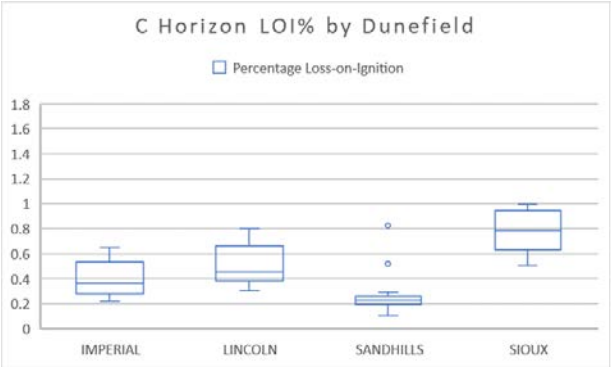

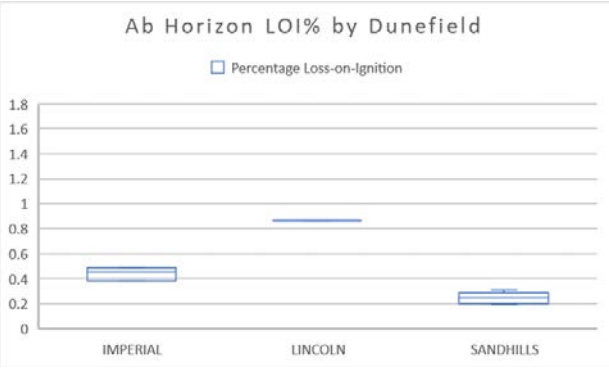

Soil Organic Carbon (SOC) and Nitrogen (N)

Similar to the other soil variable investigations in this thesis, the results of the soil organic carbon (SOC) and nitrogen (N) analyses showed a strong pattern across all dunefields based on soil horizon. On average, SOC and N decreased from the A to C horizons, then increased in any Ab horizons present (Figure 16a-b). Other similarities across all dunefields with regards to SOC and soil N include the C:N ratio (mass ratio, not molar), which was roughly 10:1 in all samples. Yet, this ratio varied slightly by horizon. On average, the ratio decreased from the A to C horizon, then rose in the Ab horizons (Figure 16c), even though the ratio did not deviate greatly from 10:1. SOC and N usually are found in higher abundance at depths where organic matter is added to the soil or was added in the past, in the upper horizons or in paleosols (Jobbagy and Jackson, 2000), although this pattern is not universal and can be controlled by vegetative and anthropogenic influences (Omonode and Vyn, 2006). Thus, this pattern of decreasing amounts of SOC and N from the A to the C horizons – where few roots are present or where soil development has occurred the least – is unsurprising. The rise in SOC and N from the C horizons to any lower Ab horizons also confirms the accuracy of field observations of pedologic profiles, as buried A horizons are likely to have retained some SOC and N prior to the deposition of eolian sand which would have lacked these elements. The somewhat higher content of SOC in buried A horizons than in C horizons above and below them also supports previous findings of the widespread sequestration of carbon in paleosols across the Great Plains (Marin-Spiotta et al., 2014), although the total quantity sequestered is low in these sandy soils.

Despite the presence of these pronounced patterns across all dunefields in the study area, other aspects of the SOC and N analyses demonstrate important differences between dunefields. The Sand Hills sites registered the least amount of SOC and N in every horizon when compared to the three other dunefields (Figure 16a-b). This feature was most distinct in the A horizon, where Sand

Hills sites on average recorded approximately 0.3% less SOC and 0.03% less N than the other dunefields. The SOC and N values for all dunefield C horizons are more analogous, suggesting that sandy parent material carries and developed little organic material and that the differences in the A horizon between the Sand Hills and other dunefields may be attributable to soil development and more stable vegetation. The Sand Hills sites also demonstrated the least amount of variance in its SOC and N values (Figures 18a-d and Figure 19a-d), with a coefficient of variance (CV) of 0.48, also signifying a greater confidence surrounding these values and, thus, the lack of SOC and N in the A horizons of those Sand Hills sites.

As mentioned in the Study Area and Methods Section (Chapter 2), the SOC and N analyses involved the use of a method which employed an organic elemental analyzer (EA). The use of an EA to extract SOC values differs from the LOI method, which can be considered a measure of SOM. Nevertheless, these two methods are presumed to be related. To test this idea and the validity of the SOC and LOI results, a regression analysis was conducted of SOC% and LOI% values for each soil sample site (Figure 17). The results of the regression analysis showed a strong correlation between SOC% and LOI% with an R^2-score of 0.86 . The results demonstrated the applicability of both methods and the relationship between SOC and SOM.

Table 16a-c: Soil Organic Carbon (SOC) and Nitrogen Values for the Imperial, Lincoln, and Lord Ranch Sites

Profile	Horizon	Sample Depth	C%	N%
IMP-1A-1	A	10	0.35	0.04
	A	30	0.26	0.03
	C	60	0.20	0.02
IMP-1A-2	A	10	0.38	0.04
	A	30	0.20	0.02
	C	60	0.20	0.02
IMP-1A-3	A	10	0.66	0.07
	A	30	0.27	0.03
	C	60	0.16	0.02
IMP-1B-1	A	5	0.44	0.04
	C	50	0.07	0.01
	Ab	110	0.16	0.02
IMP-1B-2	A	5	0.28	0.03
	C	50	0.11	0.01
	Ab	110	0.15	0.02
IMP-1B-3	A	5	0.31	0.03
	C	25	0.16	0.02
	Ab	50	0.20	0.02
IMP-1C-1	A	5	0.33	0.03
	AC1	-	-	-
	C1	50	0.10	0.01
	C2	110	0.07	0.01
IMP-1C-2	A	5	0.72	0.07
	AC1	-	-	-
	C1	50	0.11	0.01
	C2	110	0.09	0.01
IMP-1C-3	A	5	0.87	0.08
	AC1	-	-	-
	C1	50	0.10	0.01
	C2	110	0.06	0.01

Profile	Horizon	Sample Depth	C%	N%
LI-1A-1	A	5	0.42	0.04
	AC	20	0.33	0.03
	C	50	0.08	0.01
LI-1A-2	A	5	0.29	0.03
	AC	20	0.36	0.04
	C	60	0.11	0.01
LI-1A-3	A	5	0.31	0.03
	AC	20	0.39	0.04
	C	60	0.19	0.02
LI-1B-1	A	3	0.63	0.06
	AC	10	0.41	0.04
	C	40	0.07	0.01
LI-1B-2	A	3	0.34	0.03
	AC	10	0.29	0.03
	C	40	0.07	0.01
LI-1B-3	A	5	0.42	0.04
	AC	10	0.31	0.03
	C	40	0.05	0.01
LI-1C-1	A	5	0.87	0.08
	AC	10	0.51	0.05
	C	40	0.40	0.04
LI-1C-2	A	5	0.51	0.05
	AC	20	0.30	0.03
	C	60	0.27	0.03
LI-1C-3	A	5	0.71	0.07
	AC	20	0.37	0.04
	C1	42	0.22	0.02
	Ab	50	0.33	0.03
	C2	-	-	-

Profile	Horizon	Sample Depth	C%	N%
CH-1A-1	A	5	0.25	0.02
	AC	10	0.23	0.02
	C	50	0.11	0.01
CH-1A-2	A	5	0.30	0.02
	AC	10	0.20	0.02
	C	50	0.06	0.01
CH-1A-3	A	5	0.18	0.02
	AC	10	0.16	0.02
	C	50	0.08	0.01
CH-1B-1	AC	5	0.17	0.02
	C1	50	0.09	0.01
	Ab	100	0.14	0.01
	C2	-	-	-
CH-1B-2	AC	5	0.12	0.01
	C1	50	0.08	0.01
	Ab	135	0.13	0.02
	C2	-	-	-
CH-1B-3	AC	5	0.05	0.01
	C1	50	0.04	0.005
	Ab	160	0.10	0.01
	C2	-	-	-
CH-1C-1	A	5	0.14	0.01
	C	10	0.14	0.01
	C	50	0.08	0.01
CH-1C-2	A	5	0.14	0.01
	C	10	0.11	0.01
	C	50	0.12	0.01
CH-1C-3	A	5	0.11	0.01
	C	10	0.10	0.01
	C	60	0.11	0.01

Table 17a-b: Soil Organic Carbon (SOC) and Nitrogen Values for the Milepost 81 and Sioux Sites

Profile	Horizon	Sample Depth	C%	N%
MP81-1A-1	A	3	0.11	0.01
	C	10	0.06	0.01
	C	50	0.07	0.01
MP81-1A-2	A	2	0.13	0.01
	C	20	0.09	0.01
	C	70	0.18	0.01
MP81-1A-3	A	5	0.11	0.01
	C1	20	0.06	0.01
	C1	50	0.06	0.01
	Ab	70	0.07	0.01
	C2	-	-	-
MP81-1B-1	A	5	0.12	0.01
	C1	15	0.10	0.01
	Ab	40	0.11	0.01
	C2	-	-	-
MP81-1B-2	A	5	0.14	0.01
	C	20	0.09	0.01
	C	50	0.06	0.01
MP81-1B-3	A	5	0.09	0.01
	C1	20	0.06	0.01
	C1	50	0.07	0.01
	Ab	52	0.08	0.01
	C2	-	-	-
MP81-1C-1	A	5	0.07	0.01
	C	20	0.08	0.01
	C	62	0.07	0.01
MP81-1C-2	A	5	0.10	0.01
	C	20	0.05	0.01
	C	50	0.05	0.01
MP81-1C-3	A	5	0.08	0.01
	C	20	0.07	0.01
	C	60	0.06	0.01

Profile	Horizon	Sample Depth	C%	N%
SI-1A-1	A	3	0.32	0.03
	AC	8	0.25	0.03
	C	25	0.20	0.02
SI-1A-2	A	5	0.33	0.03
	AC	15	0.29	0.03
	C	30	0.21	0.02
SI-1A-3	A	5	0.34	0.03
	C	15	0.25	0.02
	C	30	0.24	0.02
SI-1B-1	A	5	0.50	0.05
	C	20	0.41	0.04
	C	60	0.27	0.03
SI-1B-2	A	5	0.72	0.07
	AC	20	0.42	0.04
	C	60	0.30	0.04
SI-1B-3	A	5	0.46	0.05
	C	20	0.43	0.05
	C	40	0.36	0.04

Figure 16a-c: Soil Organic Carbon% (SOC), Nitrogen%, and Carbon%-to-Nitrogen% Ratio by Horizon by Dunefield

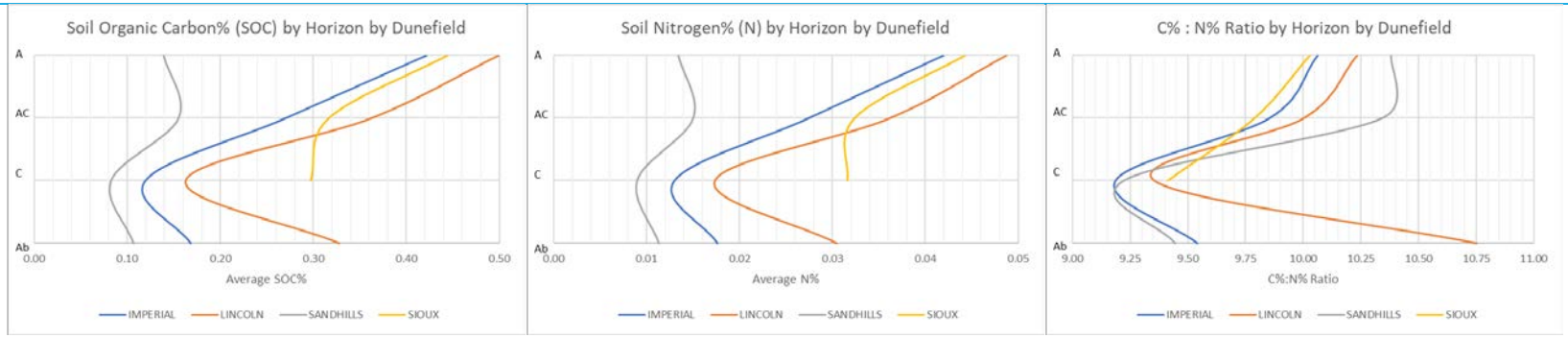

Figure 17: Regression Analysis of Soil Organic Carbon% (SOC) – Loss-on-Ignition% (LOI) Results

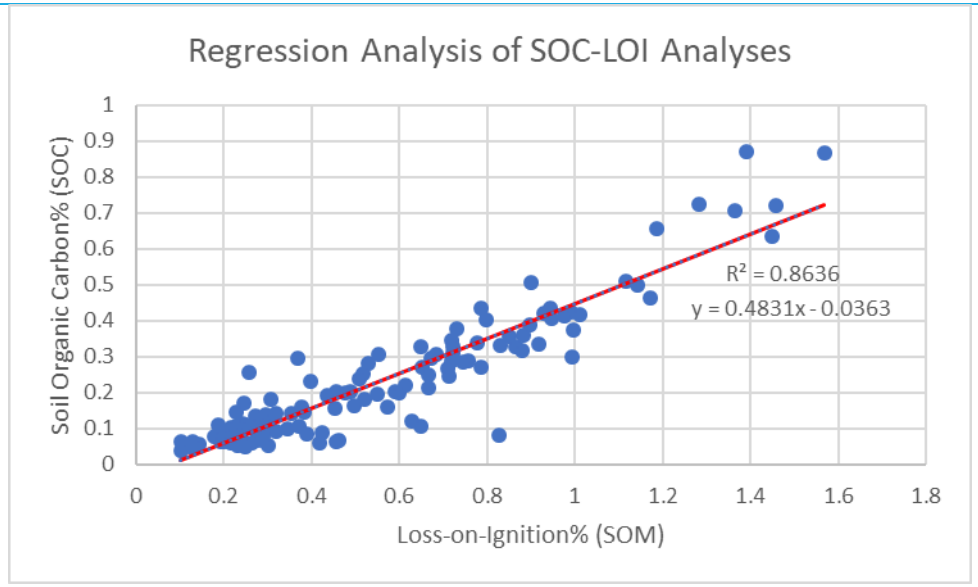

Figure 18a-d: Boxplot Profiles of Soil Organic Carbon% Data by Horizon by Dunefield

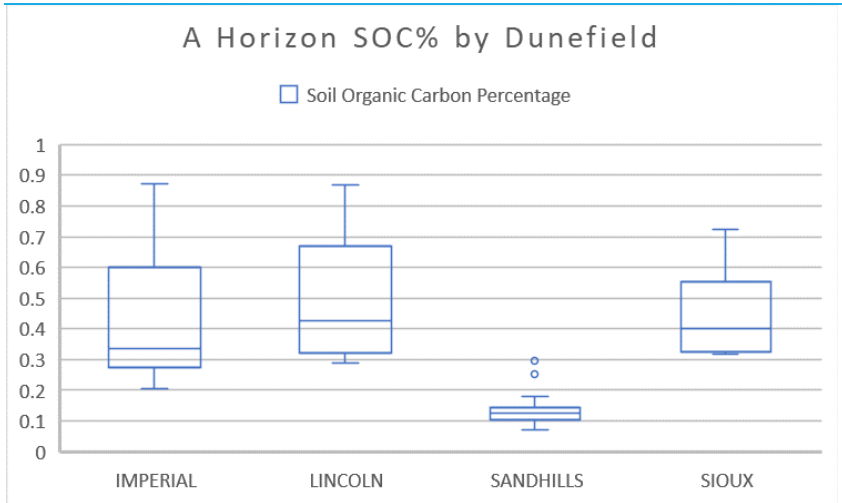

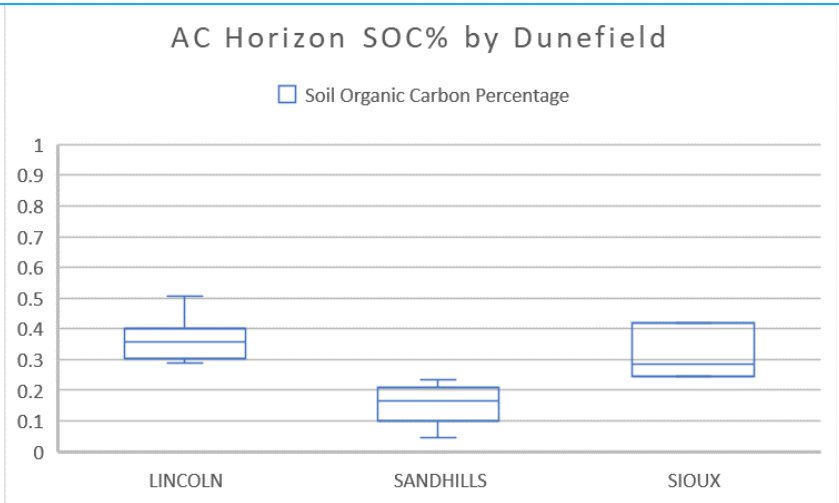

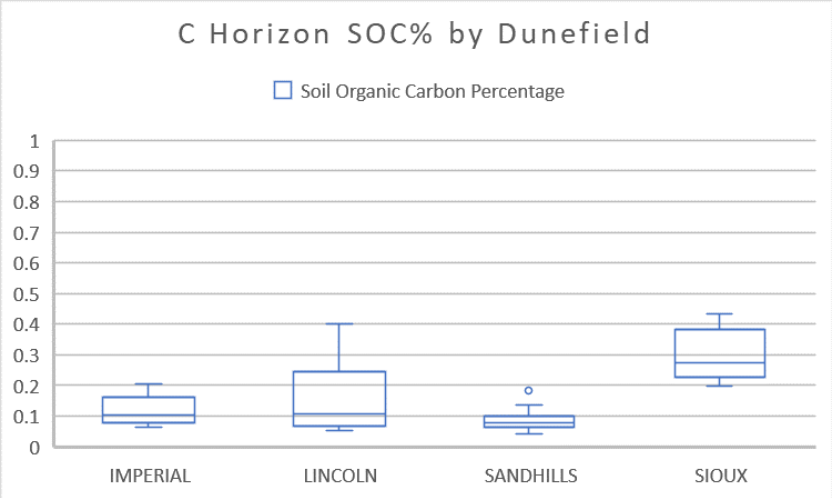

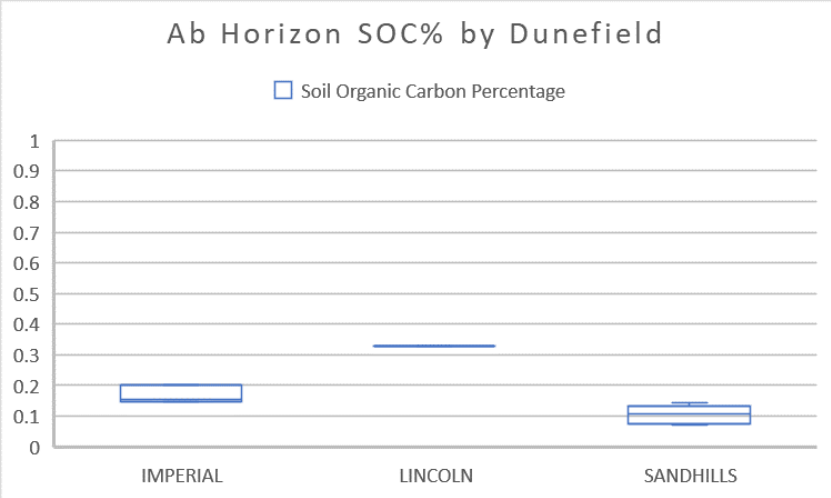

Figure 19a-d: Boxplot Profiles of Soil Nitrogen% Data by Horizon by Dunefield

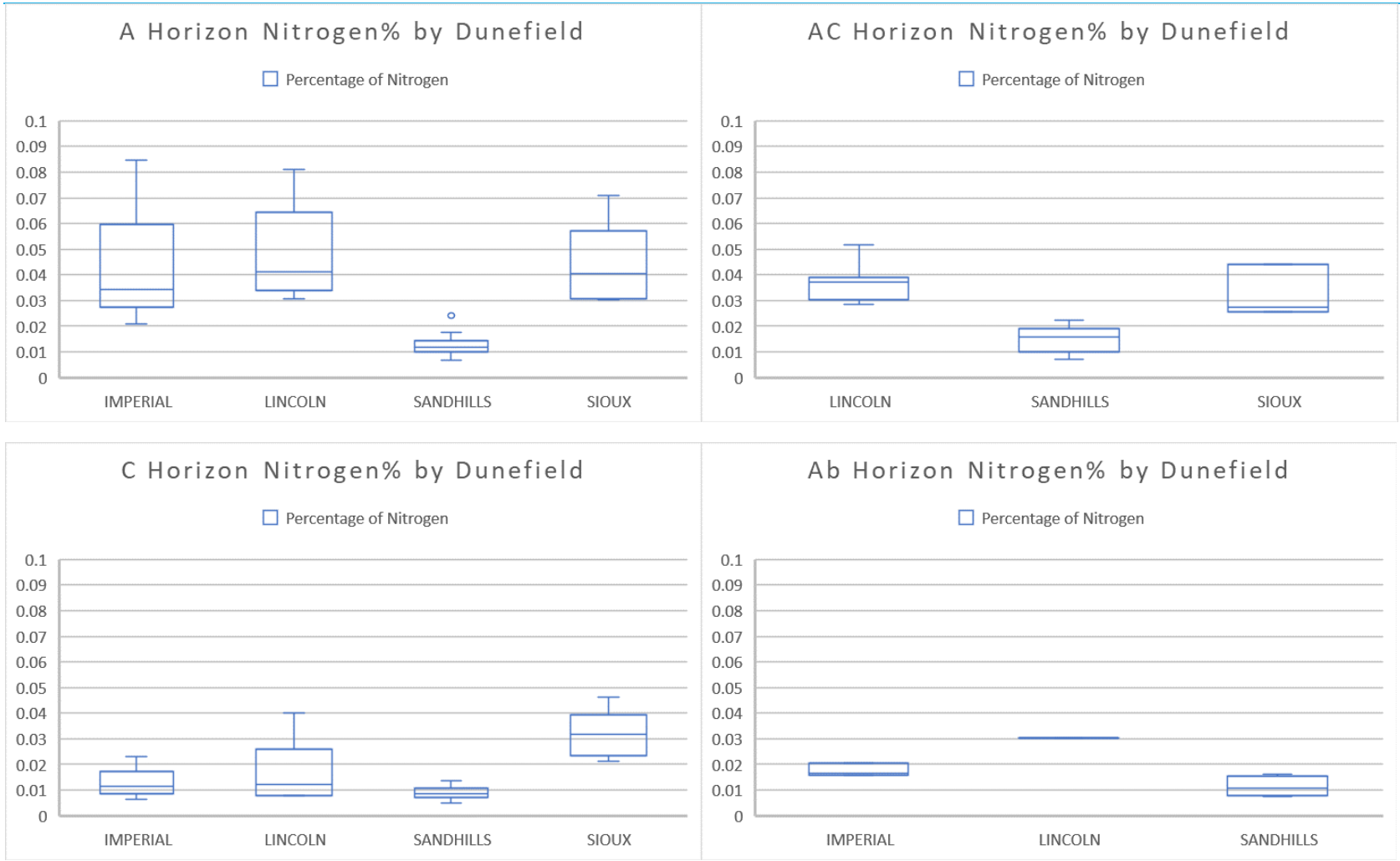

Cation Exchange Capacity (CEC)

Results for soil cation exchange capacity (CEC) did not follow the pedological patterns exhibited in the investigations of particle size, soil organic matter, soil organic carbon, or soil nitrogen. Instead, the average CEC decreased from A through AC to C, and did not increase again in Ab horizons (Figure 20). Results for the Imperial Dunefield were typical, with an average CEC of 6.24 (±0.98) cmol+ kg^{-1} in the A horizon, a CEC value of 4.9 (±0.84) cmol+ kg^{-1} in the C horizon, and a CEC from one data point of 4.04 cmol+ kg^{-1} in the Ab horizon. The analysis may be hindered by a limited sample size, but, with the exception of the Sioux Dunefield, the results for CEC did not generate much variance. The standard deviation of CEC values by horizon in each dunefield other than the Sioux Dunefield was less than 1. The variance of CEC values in the Sioux Dunefield likely can be explained by the low CEC values from one site – SI-A1-3. This site's geomorphology – on a sand sheet downwind from a larger dune – is different from the two other Sioux Dunefield sites.

Despite this, some differences with regards to CEC emerge between the dunefields. The four dunefields can be arrayed in a sequence from least to greatest CEC across all horizons. The Sand Hills exhibited the lowest CEC, followed by the Imperial, Lincoln, and lastly Sioux dunefields. As CEC may be largely due to negative charges on SOM in these clay-poor soils, it is not surprising to see *some* similarities between CEC values and the A horizon SOC content found in carbon and nitrogen analysis (Figures 16a-b, 20). Unfortunately, these results for the analysis of CEC make it difficult to draw firmer conclusions.

Table 18a-c: Cation Exchange Capacity (CEC) Values for the Imperial, Lincoln, and Lord Ranch Sites

Profile	Horizon	Sample Depth	CEC (cmol+ kg-1)
IMP-1A-1	A	10	5.93
	A	30	5.19
	C	60	5.92
IMP-1A-2	A	10	-
	A	30	-
	C	60	-
IMP-1A-3	A	10	-
	A	30	-
	C	60	-
IMP-1B-1	A	5	6.32
	C	50	5.24
	Ab	110	4.04
IMP-1B-2	A	5	-
	C	50	-
	Ab	110	-
IMP-1B-3	A	5	-
	C	25	-
	Ab	50	-
IMP-1C-1	A	5	-
	AC1	-	-
	C1	50	-
	C2	110	-
IMP-1C-2	A	5	7.54
	AC1	-	-
	C1	50	4.37
	C2	110	4.09
IMP-1C-3	A	5	-
	AC1	-	-
	C1	50	-
	C2	110	-

Profile	Horizon	Sample Depth	CEC (cmol+ kg-1)
LI-1A-1	A	5	8.39
	AC	20	6.72
	C	50	6.99
LI-1A-2	A	5	-
	AC	20	-
	C	60	-
LI-1A-3	A	5	-
	AC	20	-
	C	60	-
LI-1B-1	A	3	-
	AC	10	-
	C	40	-
LI-1B-2	A	3	6.70
	AC	10	7.24
	C	40	7.57
LI-1B-3	A	5	-
	AC	10	-
	C	40	-
LI-1C-1	A	5	-
	AC	10	-
	C	40	-
LI-1C-2	A	5	8.30
	AC	20	8.45
	C	60	7.46
LI-1C-3	A	5	-
	AC	20	-
	C1	42	-
	Ab	50	-
	C2	-	-

Profile	Horizon	Sample Depth	CEC (cmol+ kg-1)
CH-1A-1	A	5	-
	AC	10	-
	C	50	-
CH-1A-2	A	5	3.45
	AC	10	3.65
	C	50	3.89
CH-1A-3	A	5	-
	AC	10	-
	C	50	-
CH-1B-1	AC	5	3.13
	C1	50	2.36
	Ab	100	2.25
	C2	-	-
CH-1B-2	AC	5	-
	C1	50	-
	Ab	135	-
	C2	-	-
CH-1B-3	AC	5	-
	C1	50	-
	Ab	160	-
	C2	-	-
CH-1C-1	A	5	3.23
	C	10	2.58
	C	50	2.91
CH-1C-2	A	5	-
	C	10	-
	C	50	-
CH-1C-3	A	5	-
	C	10	-
	C	60	-

Table 19a-b: Cation Exchange Capacity (CEC) Values for the Milepost 81 and Sioux Sites

Profile	Horizon	Sample Depth	CEC (cmol+ kg-1)
MP81-1A-1	A	3	4.31
	C	10	3.17
	C	50	3.75
MP81-1A-2	A	2	-
	C	20	-
	C	70	-
MP81-1A-3	A	5	-
	C1	20	-
	C1	50	-
	Ab	70	-
	C2	-	-
MP81-1B-1	A	5	-
	C1	15	-
	Ab	40	-
	C2	-	-
MP81-1B-2	A	5	-
	C	20	-
	C	50	-
MP81-1B-3	A	5	4.85
	C1	20	3.12
	C1	50	6.03
	Ab	52	-
	C2	-	-
MP81-1C-1	A	5	3.83
	C	20	3.67
	C	62	2.59
MP81-1C-2	A	5	-
	C	20	-
	C	50	-
MP81-1C-3	A	5	-
	C	20	-
	C	60	-

Profile	Horizon	Sample Depth	CEC (cmol+ kg-1)
SI-1A-1	A	3	-
	AC	8	-
	C	25	-
SI-1A-2	A	5	-
	AC	15	-
	C	30	-
SI-1A-3	A	5	7.30
	C	15	8.26
	C	30	5.84
SI-1B-1	A	5	11.28
	C	20	9.07
	C	60	11.77
SI-1B-2	A	5	10.92
	AC	20	9.73
	C	60	10.87
SI-1B-3	A	5	-
	C	20	-
	C	40	-

Figure 20: Cation Exchange Capacity (CEC) by Horizon by Dunefield

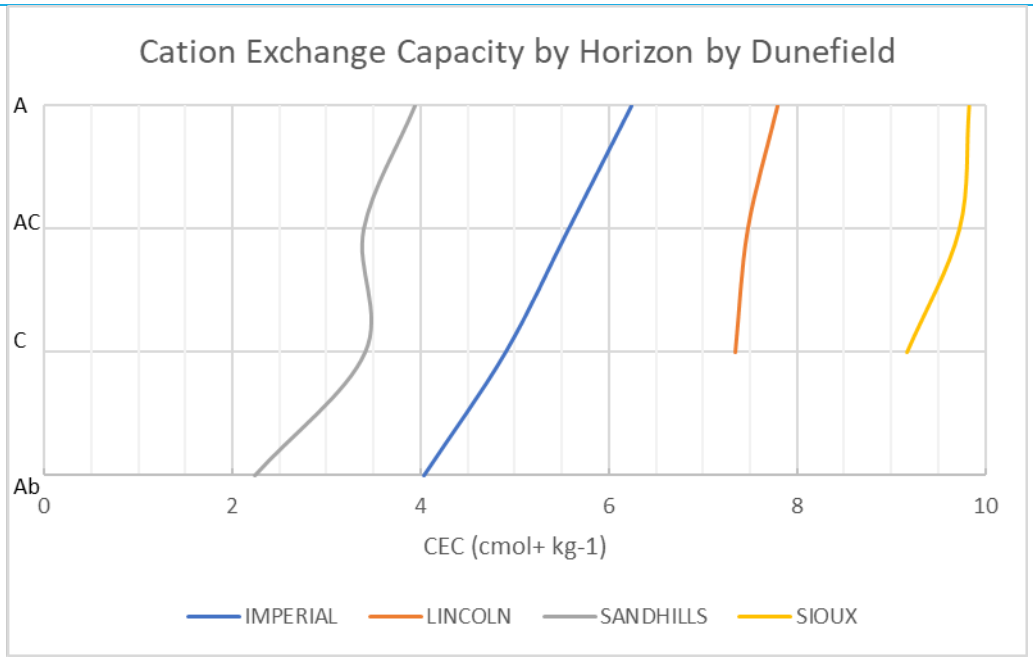

Figure 21a-b: Boxplot Profiles of Cation Exchange Capacity (CEC) by Horizon by Dunefield

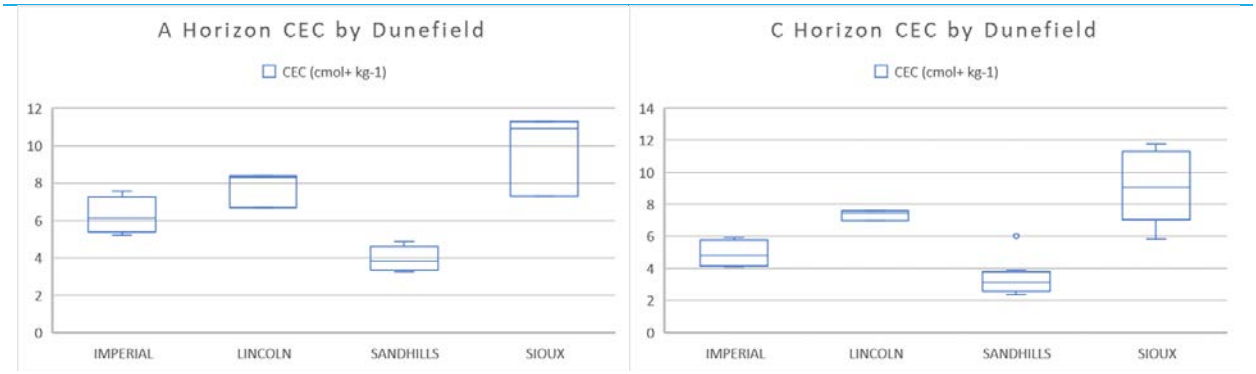

Analysis of Variation of Soil Properties Among Horizons and Dunefields

A recurring trend in the results of soil variable analyses were differences between dunefields and horizons. For example, the mean soil particle size for the Sand Hills sites were coarsest, followed by the Imperial Dunefield (Table 13, Figure 9). Results for mean soil particle size for the Lincoln and Sioux Dunefields were more clustered together and relatively finer – although still sandy and above 100μm in general overall. Furthermore, the values for soil metrics varied with soil horizon down through the profile. To understand whether these differences among dunefields and among horizons within dunefields are statistically significant, a series of analyses of variance (ANOVAs) were performed. Two sets of one-way ANOVAs tested horizon and dunefield separately as factors in the differences in soil variables. A set of two-way ANOVAs tested horizon and dunefields together as factors to ascertain if one factor was more significant in determining differences in soil variable results.

Results from the one-way ANOVAs where dunefield is the factor show that soil properties differ significantly by dunefield, as P-values are very low (Table 20). Dunefield influence was also strong in the two-way ANOVAs (Table 22). This strong geographic influence on soil properties could be explained by differences in frequency of recent reactivation or by variation of the composition of the aeolian sand parent material across the various dunefields. The soil properties in dunefields with choppy, rough surfaces and frequently active dunes may diverge from soil properties in more stable, smoother dunefields. Likewise, provenance studies show that the C horizon parent material in these different regional dunefields have somewhat different sedimentary origins (Muhs, 2017).

Unlike the dunefield ANOVA results, the results for horizon factors were mixed (Table 21-22). The influence of soil profile development, as expressed by pedogenic horizons, appears relatively strong for three metrics regardless of dunefield – LOI%, SOC%, and soil N%. For the

Lincoln Dunefield, horizon is a strong influence on all soil properties tested, with the exception of CEC. This suggests that pedogenesis in the Lincoln Dunefield is more advanced, possibly because of the lack of recent dune activity or because this dunefield contains finer sand that is more conducive to pedogenesis, as indicated by the dunefield's lower modal grain size. Soil profile horizon seems to have a mixed influence of soil properties, varying by dunefield and metric. Again, this mixed result may be indicative of the differential nature of pedogenesis and parent material.

Table 20: Summary of One-Way ANOVA Results with Dunefield as the Factor

Horizon	Particle Size Median		Particle Size Mode		LOI% (SOM)		SOC%		N%		CEC	
Dunefield is factor	*F-Test*	*P-Value*	*F-Test*	*P-Value*	*F-Test*	*P-Value*	*F-Test*	*P-Value*	*F-Test*	*P-Value*	*F-Test*	*P-Value*
A	55.5	<0.001	49.4	<0.001	20.8	<0.001	12.6	<0.001	14.1	<0.001	16.3	0.002
AC	690.1	<0.001	965.6	<0.001	29.9	<0.001	33.6	<0.001	38	<0.001	35.2	0.01
C	39.7	<0.001	31.8	<0.001	39.4	<0.001	34	<0.001	36.6	<0.001	23.8	<0.001
Ab	7.7	0.017	6.8	0.023	78.3	<0.001	26	<0.001	15	0.003	N/A	N/A

Table 21: Summary of One-Way ANOVA Results with Horizon as the Factor

Dunefield	Particle Size Median		Particle Size Mode		LOI% (SOM)		SOC%		N%		CEC	
Horizon is factor	*F-Test*	*P-Value*	*F-Test*	*P-Value*	*F-Test*	*P-Value*	*F-Test*	*P-Value*	*F-Test*	*P-Value*	*F-Test*	*P-Value*
Imperial	18.7	<0.001	8.7	0.001	3.2	0.032	6.4	0.001	6.3	0.002	2.4	0.207
Lincoln	20.1	<0.001	11.5	<0.001	11.2	<0.001	8.8	<0.001	9.2	<0.001	0.3	0.764
Sand Hills	1.7	0.175	1.8	0.157	3.5	0.021	7.8	<0.001	7.1	<0.001	1	0.413
Sioux	<0.1	0.899	<0.1	0.848	5.1	0.038	6.6	0.021	4.6	0.047	0.1	0.713

Table 22: Summary of Two-Way ANOVA Results with Dunefield and Horizon as the Factors

Factor	Particle Size Median		Particle Size Mode		LOI% (SOM)		SOC%		N%		CEC	
Two-Way ANOVA	*F-Test*	*P-Value*	*F-Test*	*P-Value*	*F-Test*	*P-Value*	*F-Test*	*P-Value*	*F-Test*	*P-Value*	*F-Test*	*P-Value*
Dunefield	123.1	<0.001	103.1	<0.001	61.9	<0.001	35.6	<0.001	39.1	<0.001	58.2	<0.001
Horizon	5.7	0.001	3.4	0.019	9.2	<0.001	20.8	<0.001	19.1	<0.001	1.6	0.193

GIS Analyses

Dune Geomorphology

The geomorphic analysis of terrain data utilized GIS tools. Hillshade profiles of each sample site were generated from either 2m LiDAR-based digital elevation models (DEMs) or 10m DEMs, if the former were not available (Figures 22a-26a). The hillshade profiles show that the five study sites chosen for this thesis can be categorized into three different dune morphologies. First, the Imperial and Sioux dunefield sites can be classified as compound parabolic dunes with a clear northwest-to-southeast orientation. Sioux site 1A may be located on a sand sheet downwind of a large parabolic dune complex, while site 1B sits at the foredune of such a complex. Nevertheless, the two Sioux sites and the study locations for the Imperial Dunefield demonstrate the typical hairpin, hemicyclid, and nested morphologies typical of parabolic dunes (Pye and Tsoar, 2009). The second dune classification present in the study area as evidenced by the hillshade analysis is the hummocky sand sheet of the Lincoln Dunefield. Here, the relief is minimal compared with the other sites and the morphology lack a discernable pattern. Finally, the last dune classification present is the complex tranverse dune systems of the two sites in the Sand Hills. These sites are located within a linear train of large-relief dune systems in which blowouts and other dune types can be found, often overlapping each other. This geographic categorization of dune types – with complex transverse dunes comprising the central Sand Hills, parabolic dunes comprising satellite dunefields to the west and south, and hummocky sand sheets peppered throughout – fits the general distribution pattern described in some other studies, including Loope and Swinehart (2000).

In further keeping with these dune classifications, most dune surfaces sampled for this thesis have westward aspects, with an azimuth heading between 200-360° (Table 23). The only two sites with contrary aspects were two sites likely located within sand sheets – Sioux site 1A and Lincoln site 1B. This is logical as a larger proportion of dune surfaces would be oriented windward, as

opposed to the more compact slip faces on the leeward side. Other geomorphic characteristics proved to be less uniform. GIS curvature values show a mixture of concave and convex, and divergent and convergent landforms. Thus, no pattern to the curvature results is evident, but this could be indicative of surficial variability and roughness. However, the curvature analyses often resulted in different outcomes depending upon the dataset used. Where available, analyses using the 2m DEM data were performed (Table 24). These higher-resolution analyses were not used in any advanced comparisons as the 2m DEM data exists only for two locations – the Imperial Dunefield and the Lord Ranch Sand Hills site – but they often resulted in outcomes different from the analyses conducted with the 10m DEM data, even though the DEMs used for these two sites were degraded 2m DEMs. For example, the differences between the standard deviations for both elevation and slope at each transect were almost always greater with the 2m DEM data (Table 24). Likewise, the two analyses produced difference curvature results for sites such as IMP-1A, from flat-convergent with 10m data, to convex-divergent with 2m data (Tables 23-24). At site CH-1B, which was a large blowout ~5m deep, the 2m DEM data perhaps captured the geomorphology better by finding the sample site to be convex and linear, with a flat plan curvature, which seems logical for the face of a blowout. The analysis with the 10m data, on the other hand, pronounced the CH-1B site to be convex-divergent, which seems less reasonable.

Surface Roughness

As discussed in the Study Area and Methods section, different metrics were tested with the aim of understanding surface roughness – a potential indicator of dune status and activity. The standard deviations of elevation, slope, and curvature all could provide valuable insight with regards to surface roughness. These metrics were calculated from 10m DEM data for each of the standard deviations (Table 23), while maps were produced to visualize the standard deviations for elevation and slope (Figures 22b-c—26b-c). These values and maps suggest that the two Sand

Hills sites are surficially the roughest, followed by the Imperial Dunefield sites. The Sioux Dunefield exhibits pronounced roughness near the large parabolic dune complexes, while the Lincoln Dunefield is the least variable in terms of surface roughness. This hierarchy of roughness was also demonstrated with some variation in boxplots visualizing the standard deviations of elevation, slope, overall curvature, and profile and plan curvature (Figures 27-28).

These geomorphic results were subjected along with the findings from other analyses to more advanced statistical investigations, as described in the next subsection. Yet, questions exist regarding the use of these metrics based on local variance of terrain attributes to describe surface roughness. Arguments can be made for any of the metrics, but a regression analysis was used to identify any relationships between the standard deviations of elevation, slope, and curvature (Figures 30-32). While all three metrics appeared to be related – an unsurprising finding based upon the interrelated nature of landforms – the relationship between the standard deviation of elevation and the standard deviation of curvature was the strongest, with an R^2-score of 0.75. This suggests that any statistical analysis testing both the standard deviations of elevation and curvature should be similar, with the possibility that one metric is a slightly better indicator or predictor of surface roughness than the other. Thus, in addition to the standard deviation of slope, both the standard deviations of elevation and curvature were tested in a series of simple linear regression analyses which sought to determine the relationships between surface roughness and soil variables, the results of which are presented in the next subsection.

Table 23: Results of Geomorphic Analyses for All Dunefield Sites from 10m DEMs

Transect	Dunefield	Elevation (m)	Elevation St. Dev. 3x3	Aspect	Slope (degrees)	Slope St. Dev.	Curvature	Curvature St. Dev.	Profile	Profile Description	Plan	Plan Description
IMP-1A	Imperial	1017.9	0.162	Southwest	0.62	0.36	-0.58	0.44	0.08	Flat	-0.51	Convergent
IMP-1B	Imperial	1026.2	0.598	North	2.91	1.15	0.59	1.87	0.14	Concave	0.73	Divergent
IMP-1C	Imperial	1023	1.024	Northwest	5.86	3.54	2.61	1.27	-2.28	Convex	0.33	Divergent
LI-1A	Lincoln	920.8	0.940	West	5.38	1.89	-2.13	1.96	1.89	Concave	-0.24	Convergent
LI-1B	Lincoln	913.8	0.287	Northeast	1.57	1.06	-0.61	0.68	0.15	Concave	-0.46	Convergent
LI-1C	Lincoln	909.5	0.365	West	2.35	0.45	1.22	0.66	-0.46	Convex	0.76	Divergent
CH-1A	Sand Hills	883.7	0.647	West	4.65	2.07	-2.86	1.53	1.61	Concave	-1.25	Convergent
CH-1B	Sand Hills	899.1	1.795	Southwest	12.41	3.24	2.34	4.45	-0.83	Convex	1.51	Divergent
CH-1C	Sand Hills	886.9	1.322	West	8.85	2.72	2.11	3.63	-0.70	Convex	1.41	Divergent
MP81-1A	Sand Hills	1016.8	0.863	West	5.23	2.55	-1.22	2.80	-0.41	Convex	-1.63	Convergent
MP81-1B	Sand Hills	1012.9	0.806	West	4.41	1.75	-1.83	1.86	0.71	Concave	-1.12	Convergent
MP81-1C	Sand Hills	1014.7	1.183	West	8.03	1.04	1.22	1.34	-0.36	Convex	0.86	Divergent
SI-1A	Sioux	1432.3	0.434	East	2.84	0.93	-0.30	0.45	0.30	Concave	0.00	Linear
SI-1B	Sioux	1422.5	0.392	Northwest	2.49	0.85	0.00	0.86	0.23	Concave	0.23	Divergent

Table 24: Results of Geomorphic Analyses for the Imperial Dunefield and Lord Ranch Sand Hills Sites from 2m LiDAR-based DSMs (where available)

Transect	Dunefield	Elevation (m)	Elevation St. Dev. 15x15	Diff. Btw. Elv. S.D. 2m-10m	Slope (degrees)	Slope St. Dev.	Diff. Btw. Slope S.D. 2m-10m	Curvature	Profile	Profile Description	Plan	Plan Description
IMP-1A	Imperial	1018.0	0.240	+0.078	1.02	1.83	+1.47	2.34	-1.31	Convex	1.03	Divergent
IMP-1B	Imperial	1025.6	0.592	-0.006	2.44	5.85	+4.70	-3.81	1.43	Concave	-2.39	Convergent
IMP-1C	Imperial	1023.3	0.946	-0.078	1.95	8.35	+4.81	1.72	0.25	Concave	1.97	Divergent
CH-1A	Sand Hills	884.1	0.771	+0.124	16.37	4.64	+2.57	-9.23	5.86	Concave	-3.36	Convergent
CH-1B	Sand Hills	899.1	1.915	+0.120	26.47	7.70	+4.46	3.94	-3.92	Convex	0.03	Linear
CH-1C	Sand Hills	887.7	1.354	+0.031	22.02	5.03	+2.31	-0.88	-0.42	Convex	-1.31	Convergent

Figures 22a-c: Hillshade, Standard Deviation of Elevation, and Standard Deviation of Slope Maps for the Imperial Dunefield Sites

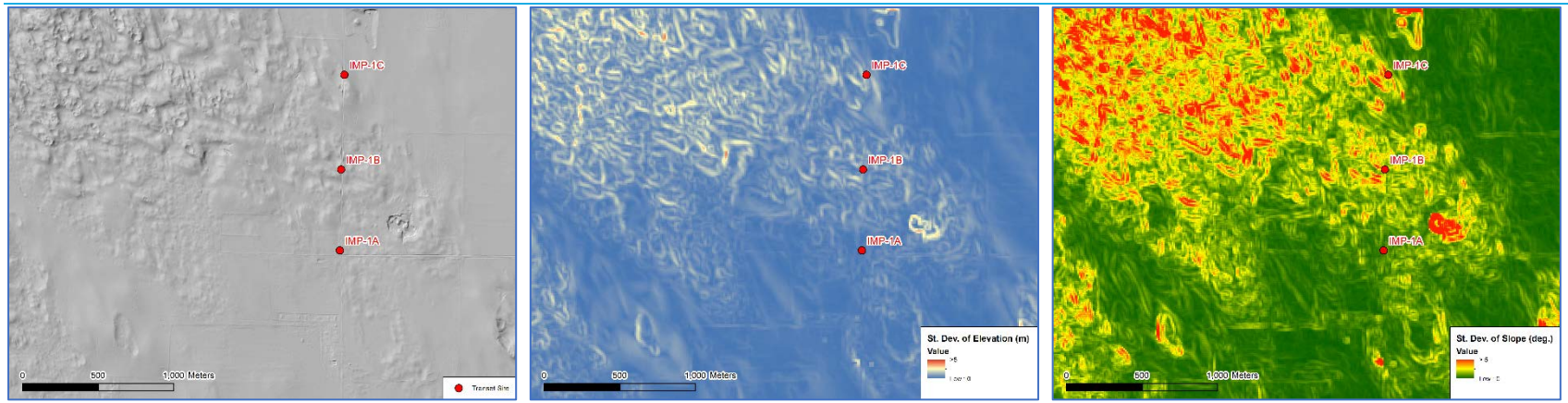

Figures 23a-c: Hillshade, Standard Deviation of Elevation, and Standard Deviation of Slope Maps for the Lincoln Dunefield Sites

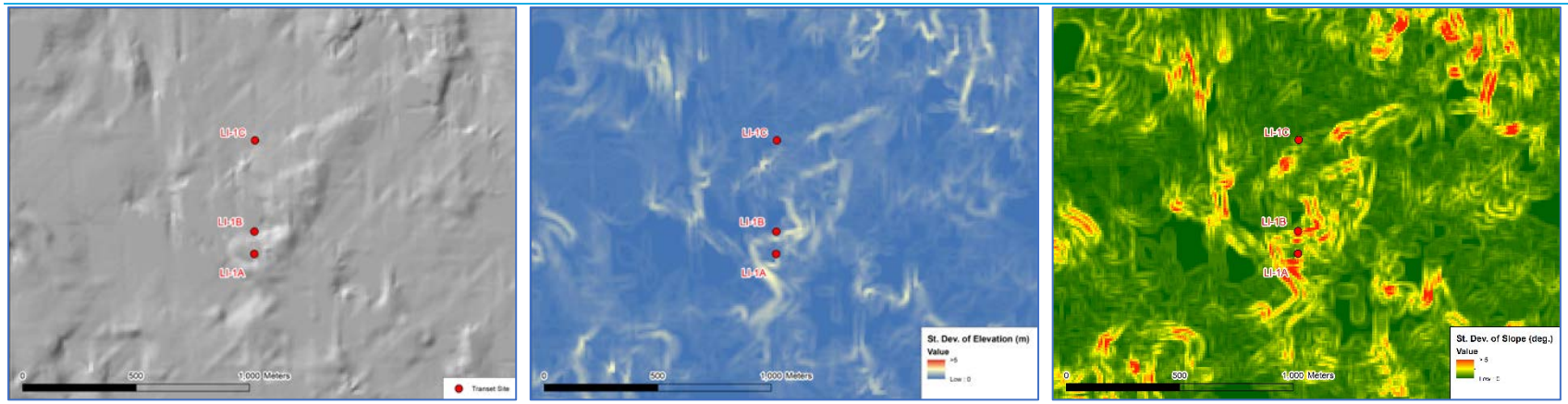

Figures 24a-c: Hillshade, Standard Deviation of Elevation, and Standard Deviation of Slope Maps for the Lord Ranch Sand Hills Sites

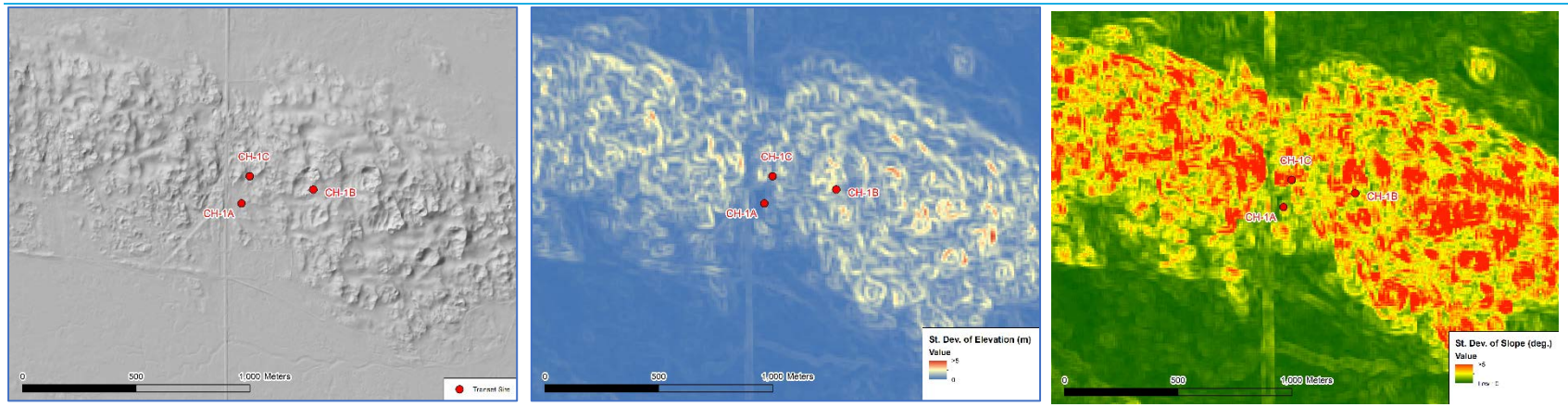

Figures 25a-c: Hillshade, Standard Deviation of Elevation, and Standard Deviation of Slope Maps for the Milepost 81 Sand Hills Sites

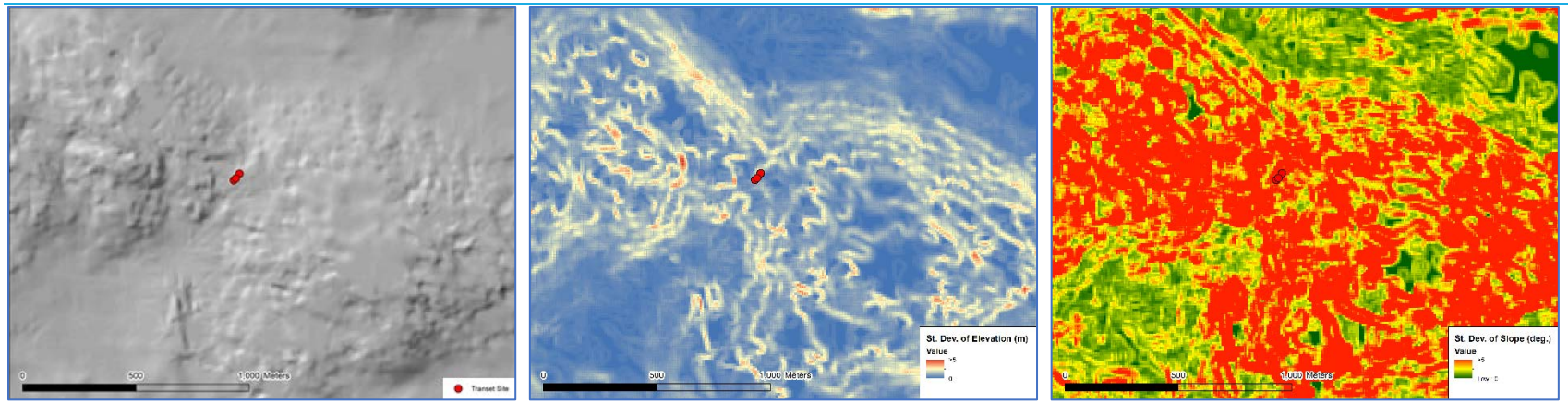

Figures 26a-c: Hillshade, Standard Deviation of Elevation, and Standard Deviation of Slope Maps for the Sioux Dunefield Sites

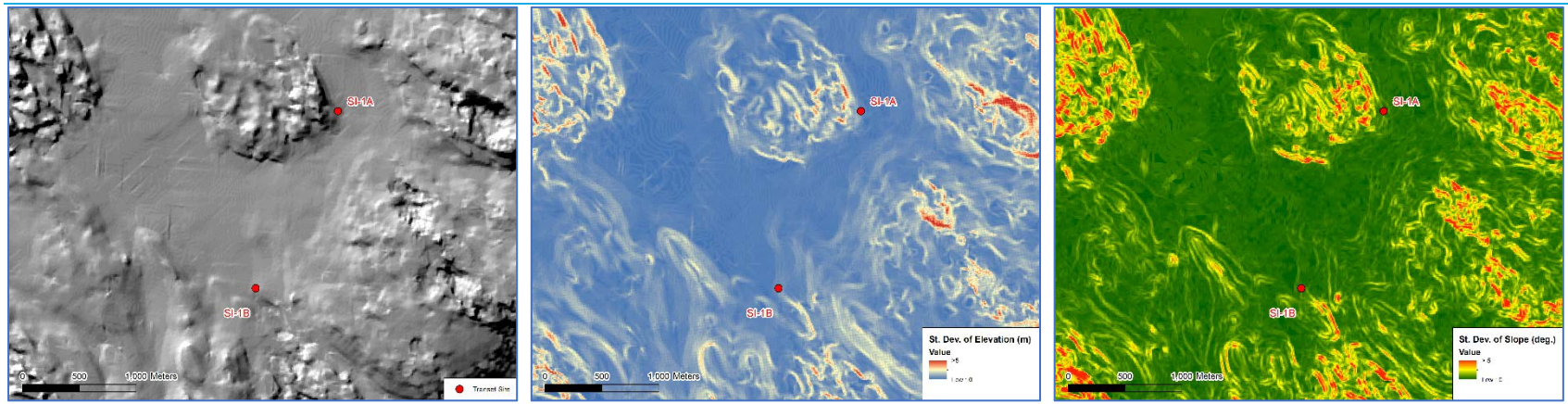

Figures 27a-b: Standard Deviation of Elevation and Standard Deviation of Slope Comparisons by Dunefields, Values for Individual Sites

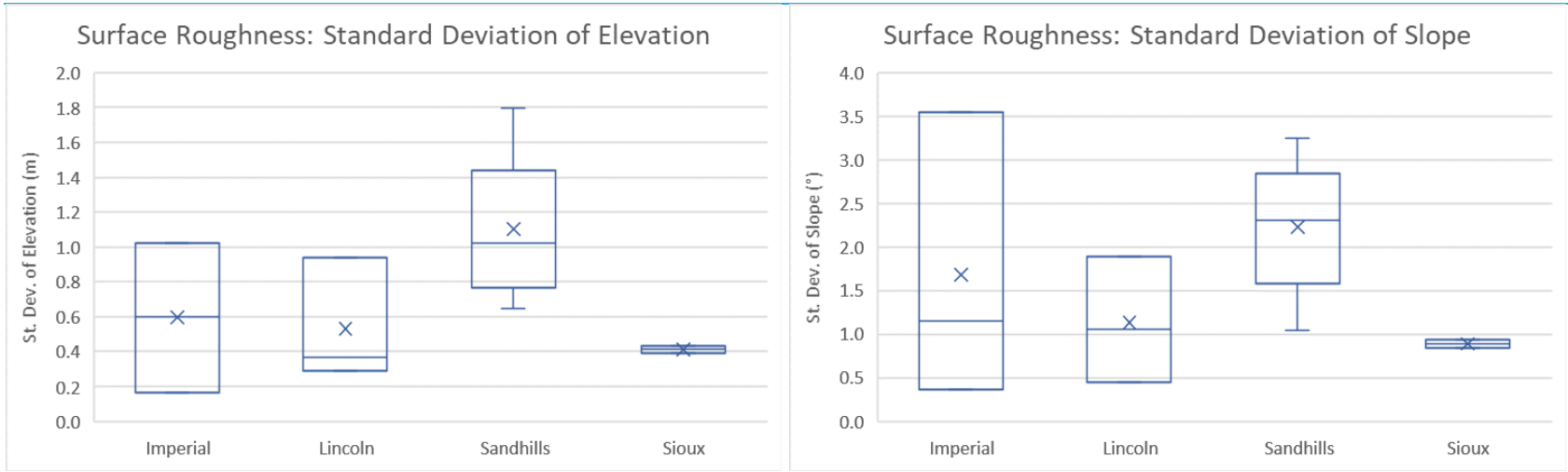

Figures 28a-c: Standard Deviation of the Three Curvature Metrics by Dunefields

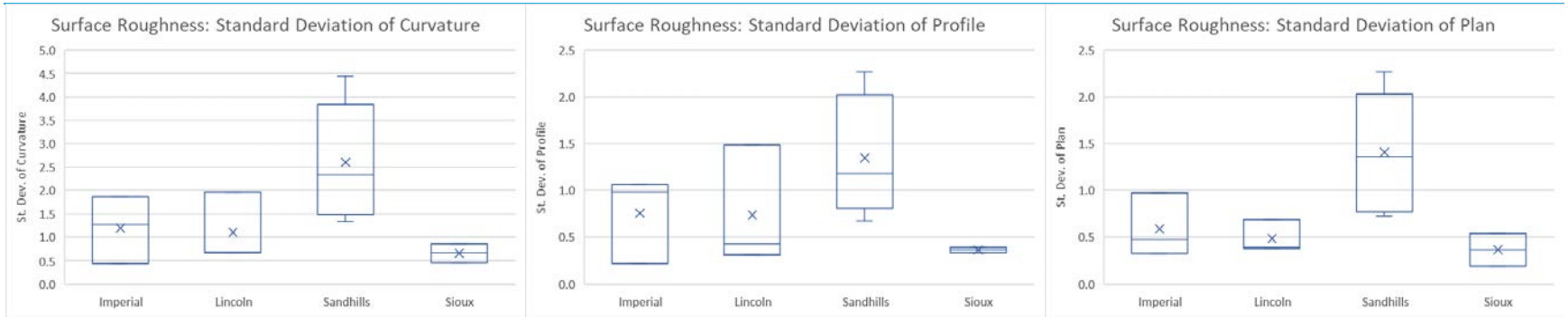

Figures 29a-c: Regression Analysis of Different Surface Roughness Metrics by Dunefields

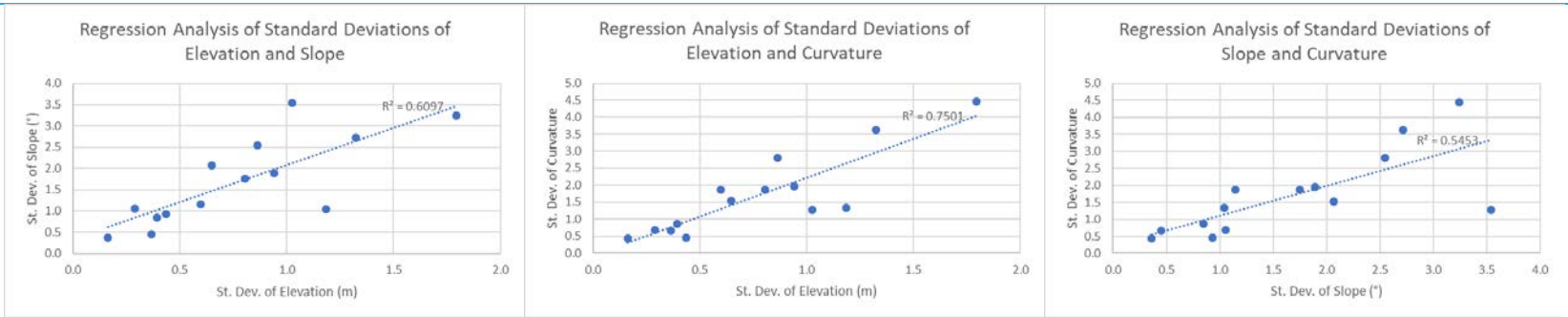

Table 25: Summary of Regression Analyses R^2-Scores

Standard Deviation Metric	Particle Size Mode	Particle Size Mean	Fine Silt%	Sand%	LOI% (SOM)	SOC%	N%	CEC
Elevation	0.474	0.432	0.412	0.371	0.334	0.318	0.327	0.314
Curvature	0.52	0.484	0.431	0.406	0.395	0.392	0.398	0.365
Slope	0.33	0.327	0.221	0.182	0.137	0.088	0.102	0.177

Statistical Analyses of Relationships Between Soil and Topographic Variables

Simple Linear Regression Analyses of Surface Roughness

The hypothesis of this thesis is that dunes with a relative recent history of activity as indicated by surface morphology should have less developed soils, which have properties less conducive to plant growth. If a dune's surface roughness, indicated by standard deviations of elevation, slope, or curvature is indicative of frequent reactivation in the recent past, as this study assumes, then there should be a relationship between surface roughness and soil variables. For example, dunes with a large standard deviation of elevation should also have a coarse mean soil particle size in the A horizon, as dune activity would result in the entrainment and removal of silt-sized particles. To determine if a relationship between surface roughness and soil variables exists, a series of simple linear regression analyses were conducted. For these regression analyses, the indicators of surface roughness at each sample site were set as independent variables. Dependent variables were the results of each soil analysis from the A horizon – soil particle size, soil organic matter as expressed as loss-on-ignition percentage, soil organic carbon, soil nitrogen, and cation exchange capacity.

The results of these simple linear regression analyses show that dunes with a higher standard deviation of curvature have A horizon properties reflecting greater accumulation of SOM and silt in general and fine silt in particular, as well as higher CEC (Table 25). For every soil variable tested, the standard deviation of curvature had a stronger relationship than did the standard deviation of elevation. Likewise, the standard deviation of elevation had higher R^2-scores for every soil measure than recorded for the standard deviation of slope, which had several weak relationships with soil variables, particularly the percentage of A horizon sand, LOI%, SOC%, N%, and CEC. The strongest relationship seen in the data is between standard deviation of curvature and modal particle size. These results suggest coarser modal and mean soil particle size are strongly associated with highly variable, choppy landscapes, which have likely

experienced relatively recent dune activation, while a finer particle size mode and mean are related to smoother surfaces.

Figures 30a-h: Simple Linear Regression Analysis for Standard Deviation of Elevation and Soil Variables

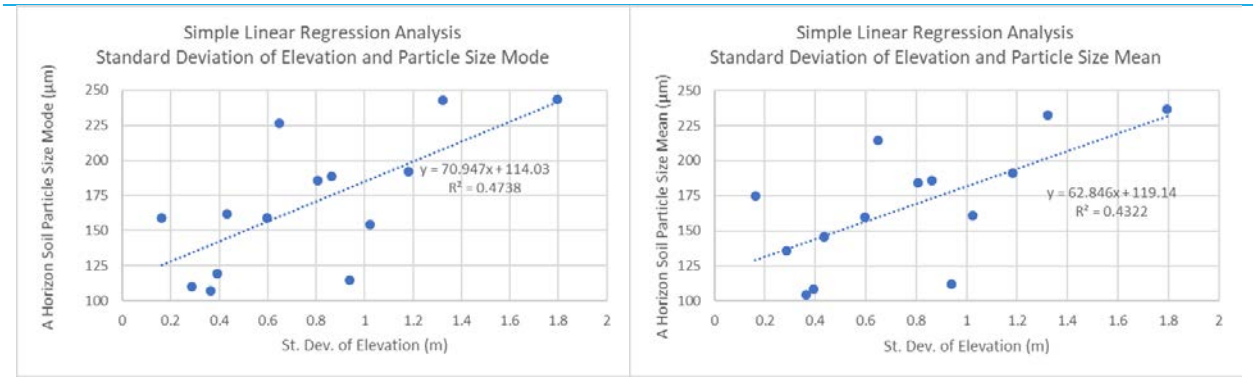

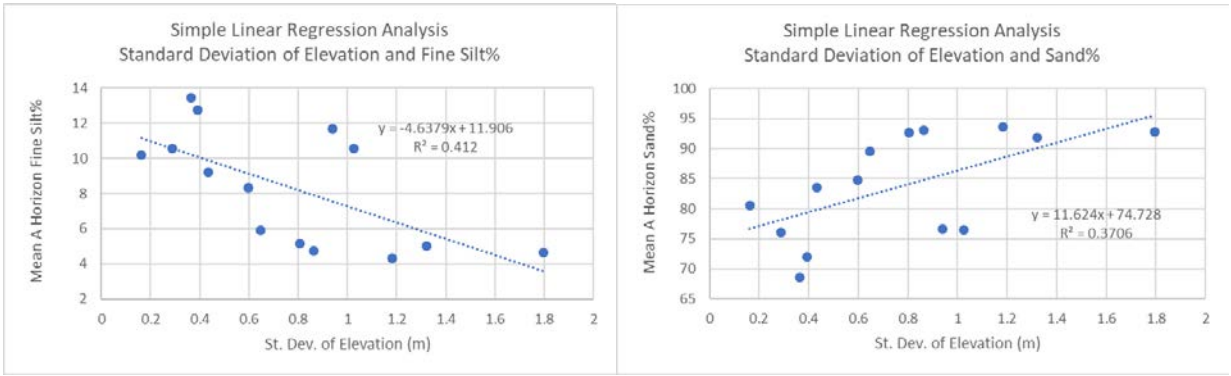

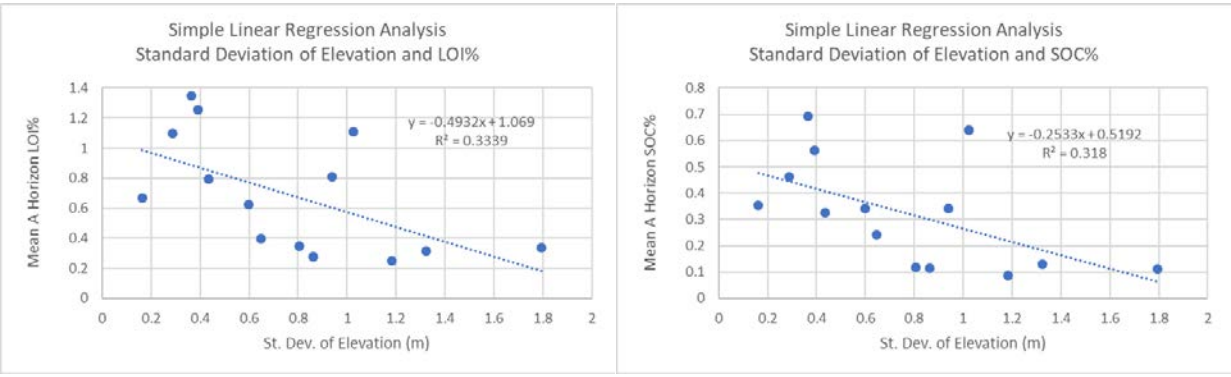

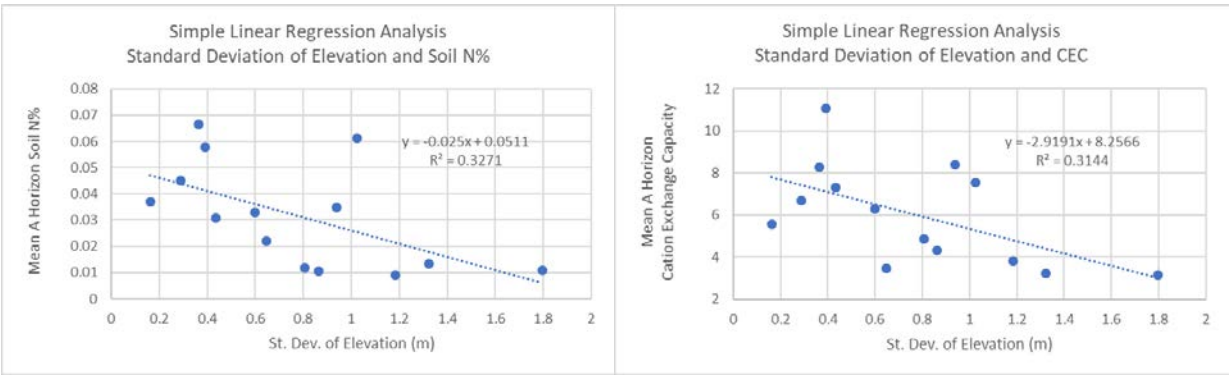

Figures 31a-h: Simple Linear Regression Analysis for Standard Deviation of Curvature and Soil Variables

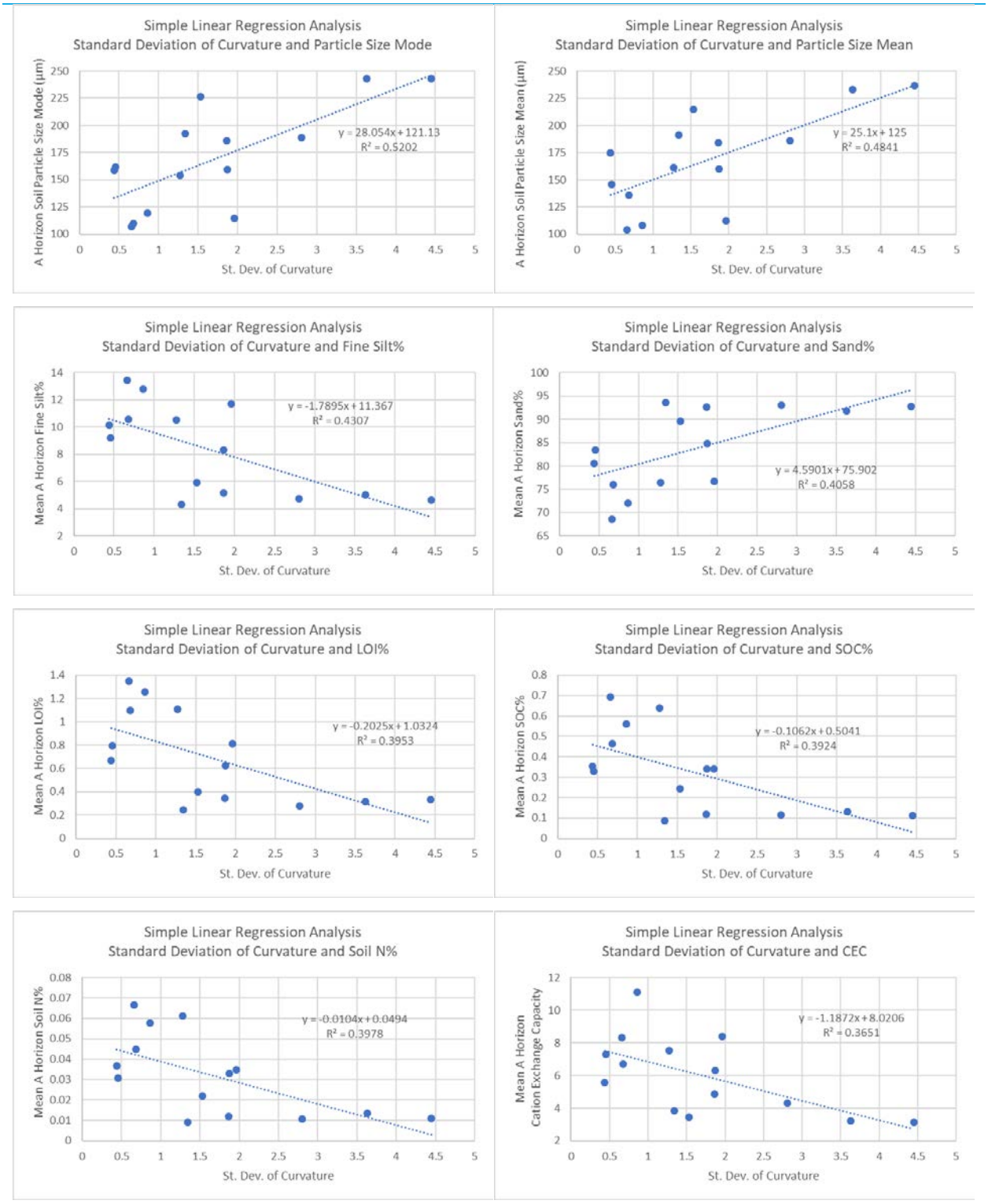

Figures 32a-h: Simple Linear Regression Analysis for Standard Deviation of Slope and Soil Variables

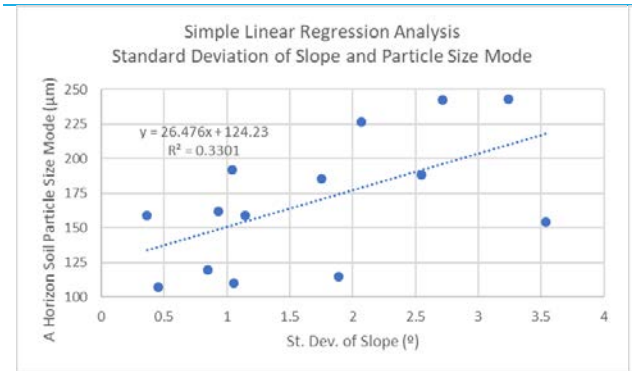

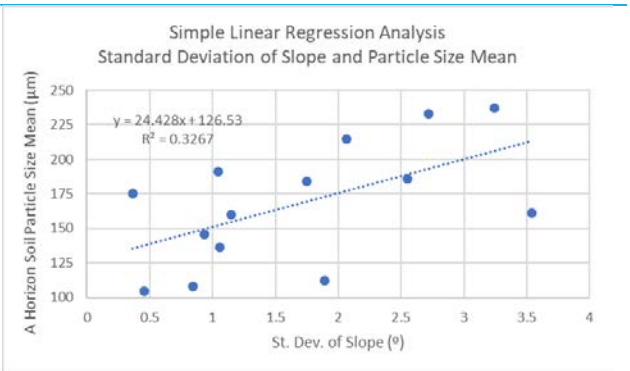

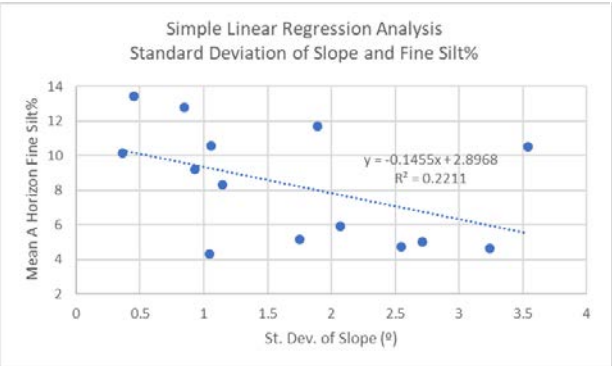

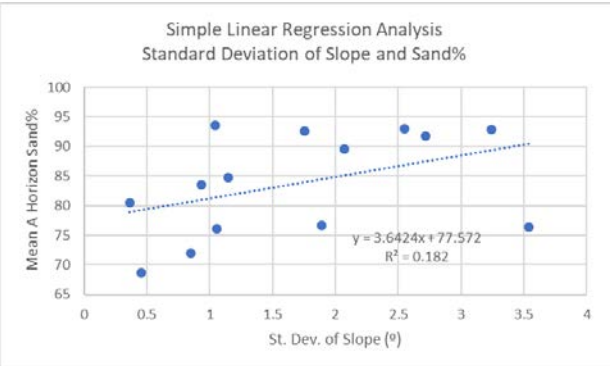

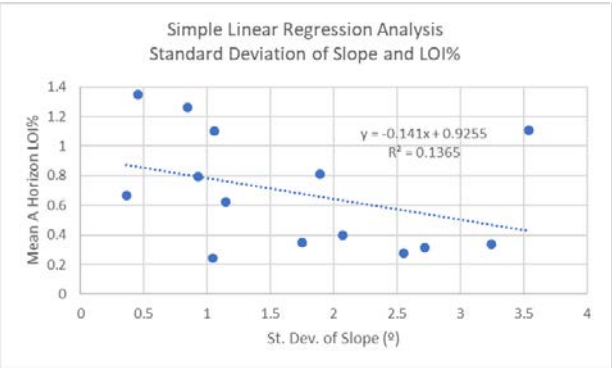

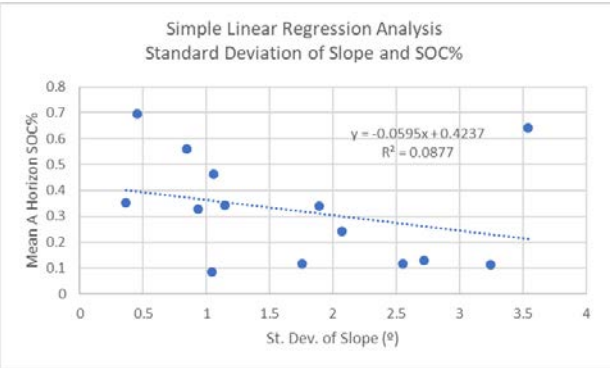

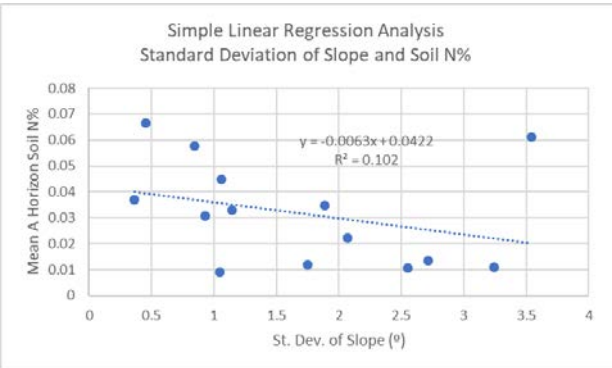

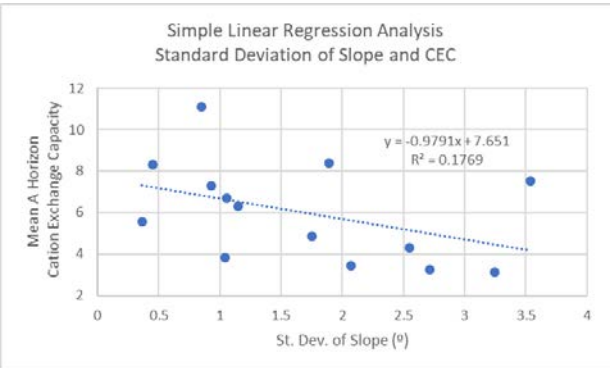

CHAPTER 4: Discussion and Conclusions

Discussion

The results of the soil and geomorphic analyses largely support the hypothesis of this thesis. Greater accumulations of silt-sized particles, SOC, soil nitrogen, SOM, and CEC were found in the A horizons of dunes with topography indicative of longer periods of stability, and thus, pedogenesis. The opposite was true as well; dunes with topography assumed to represent more frequent recent reactivation were found to have minimal accumulation of silt and clay and lower SOC, soil nitrogen, SOM, and CEC in the A horizon. This pattern is evident when the results for sites in the Sand Hills are compared to those obtained in other dunefields. At both the Lord Ranch and Milepost 81 sites bare sand patches and blowouts were observed while in the field, more so than at any other site. Unsurprisingly, the geomorphic analyses of the terrain found the Sand Hills sites to be rougher, as measured by the standard deviations of elevation and curvature, when compared to the other study areas. This indicates that the Sand Hills had been reactivated more recently and likely more frequently, causing a complex and choppy landscape to emerge. Consequently, the Sand Hills sites had lower CEC and less silt and clay, SOC, soil nitrogen, and SOM in the A horizon when compared to sites sampled elsewhere, suggesting a stunted pedogenic period interrupted by sand reactivation and blowouts.

If the Sand Hills sites' topography indicated more frequent recent reactivation, then the Sioux and Lincoln dunefield sites have been the most stable in recent times of those studied here. Both of the latter dunefields were the smoothest in terms of the roughness metrics and had relatively high concentrations of fine particles in A horizons. Both sites had greater accumulations of organic carbon, nitrogen, SOM, and CEC in the A horizon than the Sand Hills sites, with the Sioux Dunefield sites recording over twice the mean CEC in the A horizon as the mean of the Sand Hills sites. The Imperial Dunefield sites were rougher than the Lincoln and Sioux sites, but smoother than the Sand Hills sites. The results for the Imperial Dunefield soil and roughness analyses were

often between those for the Sand Hills and Lincoln/Sioux results, suggesting more recent reactivation than the Sioux and Lincoln dunefields, but less than the dunes in Sand Hills.

The trends in soil properties from the Sand Hills sites through the Imperial dunefield sites to those in the Lincoln and Sioux dunefields clearly resemble trends observed in studies of the changes following dune stabilization. As reviewed earlier in Section 1, stabilized dunes often accumulate fine particles in near-surface layers, probably through dust trapping by vegetation (Hugenholtz and Koenig, 2014; Shay et al., 2000; Wang et al., 2005; Yan et al., 2011). Shay et al. (2000) also found progressive increases in SOM and some nutrients in surface horizons, from active through recently stabilized to long-stabilized dunes. These parallel trends support the inference that the contrasts in particle size and A horizon properties between sites sampled in this study reflect differences in recent history of dune activity, as reflected by dune surface topography.

Taken together, the results of this study suggest a varied and regionalized response to the factors driving dune reactivation and/or stabilization on the west central Great Plains. Based on the progress of pedogenesis and the roughness at each site, it is clear some dunefields—or at least parts of some dunefields—have experienced surficial reactivation more frequently than others, despite being geographically in the same Great Plains region. While there is a danger of extrapolating results from individual sites to make conclusions about entire dunefields, the rough topography of the sampled dunes in the Sand Hills appears to be characteristic of a large fraction of that dunefield, while smoother topography characterizes large areas of the smaller regional dunefields. The sampled site in the Imperial Dunefield suggests more frequent reactivation than those sampled in the Lincoln and Sioux dunefields, but additional work would be needed to test whether the Imperial Dunefield as a whole has characteristics intermediate between the Sand Hills and the other two smaller dunefields. The climate for the four dunefields is largely the same, yet their late Holocene history of reactivation may differ, as the results of the

soil and roughness analyses demonstrate. In fact, the dunefield in the driest climate, where reactivation might be expected to be most frequent – the Sioux Dunefield of far western Nebraska – has the smoothest topography, and the most mature soil development, even more so than the sites in the Lincoln Dunefield. Thus, it appears as though climate cannot explain the apparent variation in frequency of reactivation among these dunefield sites. If that is true, then other factors must account for these differences.

In the dune reactivation model proposed by Barchyn and Hugenholtz (2013b), some type of disturbance is required to initiate the reactivation process. The disturbance can range from long-term changes in climate to short-term storminess, from fire to anthropogenic effects such as locally heavy livestock grazing. It is often difficult to observe the disturbance which sparks the reactivation process, and this study provides little evidence on types of disturbance that could have led to more frequent reactivation in the Sand Hills. However, it is possible to rule out some types of disturbance as likely causes of the increased reactivation in the Sand Hills and, to a lesser extent, the Imperial Dunefield. While rare extreme windstorms or large wildfires might lead to local short-term reactivation, it is unlikely that individual events can explain the observed contrast between dunefields, especially given the extensive areas of rough topography in the Sand Hills as compared to the other dunefields. Moreover, while it is true that evidence of anthropogenic disturbance was observed at the two Sand Hills dunefield sites, there was evidence of human influence on the landscape at all five sites. Cow paths were evident in the dunes at the Lord Ranch along with a windmill and water tank. Mesh netting had been installed in some dunes in the Milepost 81 roadcut in an attempt at stabilization and the entire site was surrounded by ranching operations. Samples from the SI-1B transect in the Sioux Dunefield were taken within sight of an abandoned ranch-style home and corral. Ranches and homes surrounded the Imperial and Lincoln locations. Human impacts are a fact of this landscape in a manner similar to the semi-arid nature of the region's climate. Yet, again, instead of responding evenly to anthropogenic

disturbance, the evidence for recent reactivation varies widely across the five study areas. In addition, livestock ranching in these dunefields only began in the late nineteenth century. While it is difficult to estimate the timescale over which the contrasts between study sites were established, the degree of soil development at the Lincoln and Sioux County dunefields suggests that greater stability there may predate the time of livestock ranching. On the other hand, the grassland dunefields of the Great Plains have been home to bison for more than 100,000 years, which could have had an effect similar to domestic cattle. Clearly more research is needed to understand dunefield response to different types of anthropogenic and nonanthropogenic disturbance, but at this point it is difficult to identify a type of disturbance that would consistent occur more frequently or have greater effects in the Sand Hills than in the other study areas.

There is another intriguing possibility, however, which is that pedogenic-geomorphic feedbacks could maintain more frequent stability or activity in a given area after a short-term but large-magnitude disturbance (a locally severe drought, possibly combined with large fires or overgrazing, for example). Reactivation of a stable dune surface leads to erosion or burial of pre-existing A horizons and loss of any fine particles, SOM, and nutrients that have accumulated there. Even if the surface of the dune is restabilized by vegetation, the surface soil will initially have lower water retention capacity and nutrient availability than the surfaces of dunes that have been stable for some time and have developed A horizons impacts the pedogenic process. Lower available water and nutrients could then limit the resilience of vegetation when exposed to drought or disturbance, making the dune more prone to frequent reactivation and thus limiting long-term development of soils that can sustain more resilient ecosystems. The frequency of reactivation results in blowouts and small parabolic dunes that ultimate create a choppy, rough landscape across much of the entire dunes. Sharp-edge ridge crests characteristic of this choppy landscape may experience particularly high shear stress during strong winds, also favoring recurrent activity. In contrast, a dune that has remained stable for some time, whether by chance

or because of local environmental factors, will develop soils that reduce the susceptibility of the dune-stabilizing vegetation to drought or disturbance (Werner et al., 2011).

If these hypothesized pedogenic-geomorphic feedbacks are effective under a wide range of environmental conditions, they would have important implications for predicting the impacts of future climate change across the region. Rather than a uniform response of dunefields to more severe or sustained droughts, for example, there may be more pronounced response through reactivation in rough dune landscapes with more limited soil development. Conversely, greater precipitation in future decades, as predicted for regions north and east of the study areas and possibly extending into the Sand Hills, may not be sufficient to fully stabilize Sand Hills dunes marked today by rough topography, abundant blowouts, and minimal soil development.

While pedogenic-geomorphic feedback loops offer a compelling explanation for corresponding contrasts in soil properties and dune topography in this study, one complicating issue must be addressed – the impact of parent material on all of the metrics used in this thesis. As explained by Muhs (2017), the Sand Hills, the Imperial Dunefield, and the Lincoln Dunefield all have unique provenances. Unfortunately, no published provenance data exists for the Sioux Dunefield, but it could follow the regional pattern of provenance and have its origins in the surficial bedrock formations to the northwest plus a mixture of other fluvial and aeolian origins. The known unique origins for three of the four dunefields in this study, which are evident in their distinguishing geochemical signatures, offer one viable explanation for the distinct C horizon parent material at each study site. Coarser sand grains are more abundant in the parent material of the soils studied in the Sand Hills, and to some extent in the Imperial Dunefield, as compared to the other two dunefields. A somewhat coarser sand size distribution at the time of deposition could have hampered some processes of pedogenesis in the Sand Hills, and to a lesser extent in the Imperial Dunefield. Importantly, coarser initial sand size would probably not affect the process of silt and

clay accumulation in surface horizons through dust trapping, so not all of the observed variation in soil properties between dunefields can be attributed to different provenance. It should also be noted that in addition to the effects of provenance, sand size may vary significantly within a dunefield because of geomorphic effects; for example, grain size may be finer higher on large dunes. While there is no obvious geomorphic explanation for the coarser sand at the Sand Hills sites, sampling a larger network of sites might reveal one.

Other results uncovered in this thesis work include a better understanding of surface roughness metrics. Several indices of surface roughness were calculated as part of this thesis. Ultimately, the standard deviations of elevation and curvature proved likely to be the most useful in capturing surface variability. Standard deviation of slope, mentioned as a good index of surface roughness in one study in Scotland (Grohmann et al., 2011), did not seen to capture the choppy nature of the landscape. Although not necessarily pertinent for questions of dune status, another important finding of this thesis was the discovery of horizon-specific patterns to the soil analyses results. Results across dunefields showed a horizon-specific pattern that was unmistakable. For example, the percentage of soil organic carbon and nitrogen decreased in each dunefield from the A horizon to the C horizon, before increasing in an buried A horizon, if present. Variations on this pattern repeated across metrics. The pattern was strong enough to be statistically significant in the ANOVAs for which dunefield was a factor. While dunefield was a more of an influence with regard to differences in soil characteristics according to the ANOVA results, horizon was a powerful influence on the differences uncovered as well.

The results of this thesis allow for the possibility of future research in a number of subjects. First, more samples can be taken across a wider portion of each dunefield to confirm the patterns seen here. For example, samples can be taken from smoother areas of the Sand Hills or in other geographic corners of the vast dunefield, while samples could be taken from overtly choppier

landscapes in the other three dunefields. By obtaining more samples and from a variety of dunefield landforms, it could determined if the patterns seen here extend to the entire dunefield or are more localized. Additionally, this same research could be conducted in other parts of the Great Plains, on different coastal dunefields, or any place where dunes exist to determine if the patterns here are applicable to a wider aeolian environment. Any further extensions of this study also might want to better incorporate the analysis of vegetation, specifically the type, coverage percentage and percentage of live and dead vegetation. A different aspect of this study which might require further exploration is the measurement of surface roughness. The literature is inconclusive on which methods provide the best results when evaluating roughness and no research has been conducted on capturing the degree of roughness in aeolian environments. Perhaps instead of relying on existing, and imperfect, metrics to capture surface roughness at the dune-scale, a new quantitative method tested in dunefields could be developed. Once a new method emerges, it could be applied to these study areas and compared side-by-side to the two methods used here – the standard deviations of elevation and curvature.

Conclusions

Dunefields with a recent history of reactivation inferred from rougher topography, such as the Sand Hills and to some extents the Imperial Dunefield, display soil properties which indicate a shorter period of pedogenesis – low silt and clay content, soil organic carbon (SOC), soil nitrogen, loss-on-ignition (SOM), and cation exchange capacity (CEC) in surface horizons The Lincoln and Sioux dunefields, demonstrated the opposite attributes – smoother terrain and relatively high silt and clay content, SOC, soil nitrogen, SOM, and CEC. These findings suggest the possibility of pedogenic-geomorphic feedbacks, where the soil and geomorphic properties of the dunes may drive the landscapes toward frequent reactivation or persistent stability based whether or not they have developed soil properties favoring growth of dune-stabilizing vegetation. For instance, a significant period of stability could allow the accumulation of fine material through dust

deposition, enhancing the soil's ability to retain moisture, as well as buildup of SOM and nutrients that would foster vegetative growth, two processes that could limit reactivation of dunes during dry periods or after disturbance. Conversely, the lack of finer-grained soil material, SOM, and nutrients in recently actively dunes would make reactivation more likely, perpetuating conditions that limit vegetation growth. One caveat to this interpretation is that the degree of soil development and thus susceptibility to reactivation or stability could be somewhat influenced by the provenance of the parent sand material or geomorphic setting within a dunefield. The findings of this study could have important implications for the potential response of dunefields in the Central Great Plains to current and future climate change: Dunes with weak to minimal soil development may be particularly susceptible to persistent reactivation in a climate where severe drought is more common, creating a patchwork of response across the region. Further study is needed to test whether the findings reported here are applicable across other dunefields of the Great Plains and similar regions.

REFERENCES

Adewopo, J.B., VanZomeren, C., Bhomia, R.K., Almaraz, M., Bacon, A.R., Eggleston, E., Judy, J.D., Lewis, R.W., Lusk, M., Miller, B., Moorberg, C., Snyder, E.H., Tiedeman, M., 2014. Top-Ranked Priority Research Questions for Soil Science in the 21 Century. Soil Sci. Soc. Am. J. 78, 337. https://doi.org/10.2136/sssaj2013.07.0291

Ahlbrandt, T.S., Swinehart, J.B., Maroney, D.G., 1983. The dynamic holocene dune fields of the great plains and rocky mountain basins, U.S.A, in: Developments in Sedimentology. pp. 379–406. https://doi.org/10.1016/S0070-4571(08)70806-9

Aleinikoff, J.N., Muhs, D.R., Bettis, E.A., Johnson, W.C., Fanning, C.M., Benton, R., 2008. Isotopic evidence for the diversity of late quaternary loess in Nebraska: Glaciogenic and nonglaciogenic sources. Bull. Geol. Soc. Am. 120, 1362–1377. https://doi.org/10.1130/b26222.1

Anonymous, 1969. Munsell Soil Color Charts: With Genuine Munsell Color Chips. Munsell Color, Grand Rapids, Mich.

Arbogast, A.F., 1996. Stratigraphic evidence for late-holocene aeolian sand mobilization and soil formation in south-central Kansas, U.S.A. J. Arid Environ. 34, 403–414. https://doi.org/10.1006/jare.1996.0120

Ashkenazy, Y., Yizhaq, H., Tsoar, H., 2012. Sand dune mobility under climate change in the Kalahari and Australian deserts. Clim. Change 112, 901–923. https://doi.org/10.1007/s10584-011-0264-9

Bagnold, R.A., 1941. The Physics of Blown Sand and Desert Dunes. Methuen, London.

Barchyn, T.E., Hugenholtz, C.H., 2013a. Dune field reactivation from blowouts: Sevier Desert, UT, USA" (Aeolian Research (2013) 11 (75–84) (S1875963713000700) (10.1016/j.aeolia.2013.08.003)). Aeolian Res. 21, 163–164. https://doi.org/10.1016/j.aeolia.2015.10.003

Barchyn, T.E., Hugenholtz, C.H., 2013b. Reactivation of supply-limited dune fields from blowouts: A conceptual framework for state characterization. Geomorphology 201, 172–182. https://doi.org/10.1016/j.geomorph.2013.06.019

Bo, T.L., Fu, L.T., Zheng, X.J., 2013. Modeling the impact of overgrazing on evolution process of grassland desertification. Aeolian Res. 9, 183–189. https://doi.org/10.1016/j.aeolia.2013.01.001

Brady, N.C., Weil, R.R., 2010. Elements of the Nature and Properties of Soils, 3rd ed, Animal Genetics. Prentice Hall, Upper Saddle River, New Jersey.

Brown, O.W., Hugenholtz, C.H., 2012. Estimating aerodynamic roughness (zo) in mixed grassland prairie with airborne LiDAR. Can. J. Remote Sens. 37, 422–428. https://doi.org/10.5589/m11-051

Chamberlin, T.C., 1897. Supplementary hypothesis respecting the origin of the loess of the

Mississippi Valley. J. Geol. 5, 795–802. https://doi.org/10.1086/607964

Clarke, M.L., Rendell, H.M., 2003. Late Holocene dune accretion and episodes of persistent drought in the Great Plains of Northeastern Colorado. Quat. Sci. Rev. 22, 1051–1058. https://doi.org/10.1016/S0277-3791(03)00024-6

Cook, B.I., Ault, T.R., Smerdon, J.E., 2015. Unprecedented 21st century drought risk in the American Southwest and Central Plains. Sci. Adv. 1, 1–8. https://doi.org/10.1126/sciadv.1400082

Cook, B.I., Cook, E.R., Smerdon, J.E., Seager, R., Williams, A.P., Coats, S., Stahle, D.W., Díaz, J.V., 2016. North American megadroughts in the Common Era: Reconstructions and simulations. Wiley Interdiscip. Rev. Clim. Chang. https://doi.org/10.1002/wcc.394

Cronin, F.D., Beers, H.W., 1937. Areas of intense drought distress, 1930-1936.

Dunn, C.D., Stephenson, M.B., Stubbendieck, J., 2016. Common Grasses of Nebraska 1–178.

Feng, S., Fu, Q., 2013. Expansion of global drylands under a warming climate. Atmos. Chem. Phys. 13, 10081–10094. https://doi.org/10.5194/acp-13-10081-2013

Follmer, L.R., 1996. Loess studies in central United States: Evolution of concepts. Eng. Geol. 45, 287–304. https://doi.org/doi: DOI: 10.1016/S0013-7952(96)00018-X

Forman, S.L., Goetz, A.F.H., Yuhas, R.H., 1992. Large-scale stabilized dunes on the High Plains of Colorado: understanding the landscape response to Holocene climates with the aid of images from space. Geology 20, 145–148. https://doi.org/10.1130/0091-7613(1992)020<0145:LSSDOT>2.3.CO;2

Forman, S.L., Marín, L., Gomez, J., Pierson, J., 2008. Late Quaternary eolian sand depositional record for southwestern Kansas: Landscape sensitivity to droughts. Palaeogeogr. Palaeoclimatol. Palaeoecol. 265, 107–120. https://doi.org/10.1016/j.palaeo.2008.04.028

Forman, S.L., Marín, L., Pierson, J., Gómez, J., Miller, G.H., Webb, R.S., 2005. Aeolian sand depositional records from Western Nebraska: Landscape response to droughts in the past 1500 years. Holocene 15, 973–981. https://doi.org/10.1191/0959683605hl871ra

Forman, S.L., Oglesby, R., Webb, R.S., 2001. Temporal and spatial patterns of Holocene dune activity on the Great Plains of North America: Megadroughts and climate links. Glob. Planet. Change 29, 1–29. https://doi.org/10.1016/S0921-8181(00)00092-8

Galatowitsch, S., Frelich, L., Phillips-Mao, L., 2009. Regional climate change adaptation strategies for biodiversity conservation in a midcontinental region of North America. Biol. Conserv. 142, 2012–2022. https://doi.org/10.1016/j.biocon.2009.03.030

Gremer, J.R., Bradford, J.B., Munson, S.M., Duniway, M.C., 2015. Desert grassland responses to climate and soil moisture suggest divergent vulnerabilities across the southwestern United States. Glob. Chang. Biol. 21, 4049–4062. https://doi.org/10.1111/gcb.13043

Grohmann, C.H., Smith, M.J., Riccomini, C., 2011. Multiscale analysis of topographic surface roughness in the Midland Valley, Scotland. IEEE Trans. Geosci. Remote Sens. 49, 1200–1213. https://doi.org/10.1109/TGRS.2010.2053546

Hack, J.T., 1941. Dunes of the Western Navajo Country. Geogr. Rev. 31, 240. https://doi.org/10.2307/210206

Halfen, A.F., Johnson, W.C., 2013. A review of Great Plains dune field chronologies. Aeolian Res. https://doi.org/10.1016/j.aeolia.2013.03.001

Halfen, A.F., Johnson, W.C., Hanson, P.R., Woodburn, T.L., Young, A.R., Ludvigson, G.A., 2012. Activation history of the Hutchinson dunes in east-central Kansas, USA during the past 2200years. Aeolian Res. 5, 9–20. https://doi.org/10.1016/j.aeolia.2012.02.001

Halfen, A.F., Lancaster, N., Wolfe, S., 2016. Interpretations and common challenges of aeolian records from North American dune fields. Quat. Int. 410, 75–95. https://doi.org/10.1016/j.quaint.2015.03.003

Hanoch, G., Yizhaq, H., Ashkenazy, Y., 2018. Modeling the bistability of barchan and parabolic dunes. Aeolian Res. 35, 9–18. https://doi.org/10.1016/j.aeolia.2018.07.003

Hanson, P.R., Arbogast, A.F., Johnson, W.C., Joeckel, R.M., Young, A.R., 2010. Megadroughts and late Holocene dune activation at the eastern margin of the Great Plains, north-central Kansas, USA. Aeolian Res. 1, 101–110. https://doi.org/10.1016/j.aeolia.2009.10.002

Hanson, P.R., Joeckel, R.M., Young, A.R., Horn, J., 2009. Late Holocene dune activity in the Eastern Platte River Valley, Nebraska. Geomorphology 103, 555–561. https://doi.org/10.1016/j.geomorph.2008.07.018

Hay, J.D., de Lacerda, L.D., Tan, A.., 1981. Soil cation increase in a tropical sand dune ecosystem due to a terrestrial bromeliad. Ecology 62, 1392–1395.

Hesp, P., 2002. Foredunes and blowouts: initiation, geomorphology and dynamics. Geomorphology 48, 245–268. https://doi.org/10.1016/S0169-555X(02)00184-8

Hesse, P.P., Simpson, R.L., 2006. Variable vegetation cover and episodic sand movement on longitudinal desert sand dunes. Geomorphology 81, 276–291. https://doi.org/10.1016/j.geomorph.2006.04.012

Hugenholtz, C.H., Koenig, D.K., 2014. Sand dune stabilization reduces infiltration and soil moisture: A case study from the northern Great Plains. Ecohydrology 7, 1135–1146. https://doi.org/10.1002/eco.1445

Hugenholtz, C.H., Levin, N., Barchyn, T.E., Baddock, M.C., 2012. Remote sensing and spatial analysis of aeolian sand dunes: A review and outlook. Earth-Science Rev. 111, 319–334. https://doi.org/10.1016/j.earscirev.2011.11.006

Hugenholtz, C.H., Wolfe, S.A., 2005. Recent stabilization of active sand dunes on the Canadian prairies and relation to recent climate variations. Geomorphology 68, 131–147. https://doi.org/10.1016/j.geomorph.2004.04.009

Jobbagy, E.G., Jackson, R.B., 2000. The vertical distribution of soil organic carbon and its relation to climate and vegetation. Ecol. Appl. 10, 423–436.

Johnsgard, P.A., 1995. This Fragile Land: A Natural History of the Nebraska Sandhills. University of Nebraska Press, Lincoln, Neb.

Kaul, R.B., Rolfsmeier, S.B., 1994. Diversity of vascular plants and intensity of plant collecting in Nebraska. Trans. Nebraska Acad. Sci. 21, 13–20.

King, D.A., Bachelet, D.M., Symstad, A.J., Ferschweiler, K., Hobbins, M., 2015. Estimation of potential evapotranspiration from extraterrestrial radiation, air temperature and humidity to assess future climate change effects on the vegetation of the Northern Great Plains, USA. Ecol. Modell. 297, 86–97. https://doi.org/10.1016/j.ecolmodel.2014.10.037

Knight, M., Thomas, D.S.G., Wiggs, G.F.S., 2004. Challenges of calculating dunefield mobility over the 21st century. Geomorphology 59, 197–213. https://doi.org/10.1016/j.geomorph.2003.07.017

Ko, J., Ahuja, L.R., Saseendran, S.A., Green, T.R., Ma, L., Nielsen, D.C., Walthall, C.L., 2012. Climate change impacts on dryland cropping systems in the Central Great Plains, USA. Clim. Change 111, 445–472. https://doi.org/10.1007/s10584-011-0175-9

Kocurek, G., Lancaster, N., 1999. Aeolian system sediment state: Theory and Mojave Desert Kelso dune field example. Sedimentology 46, 505–515. https://doi.org/10.1046/j.1365-3091.1999.00227.x

Konen, M.E., Jacobs, P.M., Burras, C.L., Talaga, B.J., Mason, J.A., 2002. Equations for Predicting Soil Organic Carbon Using Loss-on-Ignition for North Central U.S. Soils. Soil Sci. Soc. Am. J. 66, 1878. https://doi.org/10.2136/sssaj2002.1878

Lancaster, N., 1988. Development of linear dunes in the southwestern Kalahari, Southern Africa. J. Arid Environ. 14, 233–244.

Lancaster, N., Baas, A., 1998. Influence of vegetation cover on sand transport by wind: Field studies at Owens Lake, California. Earth Surf. Process. Landforms 23, 69–82. https://doi.org/10.1002/(SICI)1096-9837(199801)23:1<69::AID-ESP823>3.0.CO;2-G

Loope, D.B., Mason, J.A., Dingus, L., 1999. Lethal sandslides from eolian dunes. J. Geol. 107, 707–713.

Loope, D.B., Swinehart, J.B., 2000. Thinking like a dune field: Geologic history in the Nebraska Sand Hills. Gt. Plains Res. 10, 5–35.

Lu, H., Miao, X., Zhou, Y., Mason, J., Swinheart, J., Zhang, J., Zhou, L., Yi, S., 2005. Late Quaternary aeolian activity in the Mu Us and Otindag dune fields (north China) and lagged response to insolation forcing. Geophys. Res. Lett. 32, 1–4. https://doi.org/10.1029/2005GL024560

Lugn, A.L., 1968. The origin of loesses and their relation to the Great Plains in North America, in: Schultz, C., Frye, J.C. (Eds.), Loess and Related Eolian Deposits of the World. pp. 139–182.

Marin-Spiotta, E., Chaopricha, N.T., Plante, A.F., Diefendorf, A.F., Mueller, C.W., Grandy, A.S., Mason, J.A., 2014. Long-term stabilization of deep soil carbon by fire and burial during early Holocene climate change. Nat. Geosci. 7, 428–432. https://doi.org/10.1038/ngeo2169

Mason, J.A., 2001. Transport direction of Peoria Loess in Nebraska and implications for Loess sources on the central Great Plains. Quat. Res. 56, 79–86. https://doi.org/10.1006/qres.2001.2250

Mason, J.A., Jacobs, P.M., Hanson, P.R., Miao, X., Goble, R.J., 2003. Sources and paleoclimatic significance of Holocene Bignell Loess, central Great Plains, USA. Quat. Res. 60, 330–339. https://doi.org/10.1016/j.yqres.2003.07.005

Mason, J.A., Lu, H., Zhou, Y., Miao, X., Swinehart, J.B., Liu, Z., Goble, R.J., Yi, S., 2009. Dune mobility and aridity at the desert margin of northern China at a time of peak monsoon strength. Geology 37, 947–950. https://doi.org/10.1130/G30240A.1

Mason, J.A., Miao, X., Hanson, P.R., Johnson, W.C., Jacobs, P.M., Goble, R.J., 2008. Loess record of the Pleistocene-Holocene transition on the northern and central Great Plains, USA. Quat. Sci. Rev. 27, 1772–1783. https://doi.org/10.1016/j.quascirev.2008.07.004

Mason, J.A., Swinehart, J.B., Goble, R.J., Loope, D.B., 2004. Late-Holocene dune activity linked to hydrological drought, Nebraska Sand Hills, USA. Holocene 14, 209–217. https://doi.org/10.1191/0959683604hl677rp

Mason, J.A., Swinehart, J.B., Hanson, P.R., Loope, D.B., Goble, R.J., Miao, X., Schmeisser, R.L., 2011. Late Pleistocene dune activity in the central Great Plains, USA. Quat. Sci. Rev. 30, 3858–3870. https://doi.org/10.1016/j.quascirev.2011.10.005

May, D.W., 2003. Properties of a 5500-year-old flood-plain in the Loup River Basin, Nebraska. Geomorphology 56, 243–254. https://doi.org/10.1016/S0169-555X(03)00154-5

Meir, A., Tsoar, H., 1996. International borders and range ecology: The case of Bedouin transborder grazing. Hum. Ecol. 24, 39–64.

Miao, X., Mason, J.A., Swinehart, J.B., Loope, D.B., Hanson, P.R., Goble, R.J., Liu, X., 2007. A 10,000 year record of dune activity, dust storms, and severe drought in the central Great Plains. Geology 35, 119–122. https://doi.org/10.1130/G23133A.1

Muhs, D.R., 2017. Evaluation of simple geochemical indicators of aeolian sand provenance: Late Quaternary dune fields of North America revisited. Quat. Sci. Rev. 171, 260–296. https://doi.org/10.1016/j.quascirev.2017.07.007

Muhs, D.R., Holliday, V.T., 2001. Origin of late Quaternary dune fields on the Southern High Plains of Texas and New Mexico. Bull. Geol. Soc. Am. 113, 75–87. https://doi.org/10.1130/0016-7606(2001)113<0075:OOLQDF>2.0.CO;2

Muhs, D.R., Maat, P.B., 1993. The potential response of eolian sands to greenhouse warming and precipitation reduction on the Great Plains of the U.S.A. J. Arid Environ. 25, 351–361.

Muhs, D.R., Reynolds, R.L., Been, J., Skipp, G., 2003. Eolian sand transport pathways in the southwestern United States: Importance of the Colorado River and local sources. Quat. Int. 104, 3–18. https://doi.org/10.1016/S1040-6182(02)00131-3

Muhs, D.R., Stafford, T.W., Cowherd, S.D., Mahan, S. a., Kihl, R., Maat, P.B., Bush, C. a., Nehring, J., 1996. Origin of the late Quaternary dune fields of northeastern Colorado. Geomorphology 17, 129–149. https://doi.org/10.1016/0169-555X(95)00100-J

Muhs, D.R., Swinehart, J.B., Loope, D.B., Been, J., Mahan, S.A., Bush, C.A., 2000. Geochemical evidence for an Eolian sand dam across the North and South Platte rivers in Nebraska. Quat. Res. 53, 214–222. https://doi.org/10.1006/qres.1999.2104

Nield, J.M., Baas, A.C.W., 2008. The influence of different environmental and climatic conditions on vegetated aeolian dune landscape development and response. Glob. Planet. Change 64, 76–92. https://doi.org/10.1016/j.gloplacha.2008.10.002

Omonode, R.A., Vyn, T.J., 2006. Vertical distribution of soil organic carbon and nitrogen under warm-season native grasses relative to croplands in west-central Indiana, USA. Agric. Ecosyst. Environ. 117, 159–170. https://doi.org/10.1016/j.agee.2006.03.031

Peel, M.C., Finlayson, B.., McMahon, T.A., 2007. Updated world map of the K¨oppen-Geiger climate classification. Hydrol. Earth Syst. Sci.

Puta, R.A., Hanson, P.R., Young, A.R., 2013. Late Holocene activation history of the Stanton Dunes, northeastern Nebraska. Gt. Plains Res. 23, 11–23.

Pye, K., Tsoar, H., 2009. Aeolian Sand and Sand Dunes. Springer-Verlag, Berlin.

Ramnarine, R., Voroney, R.P., Wagner-Riddle, C., Dunfield, K.E., 2011. Carbonate removal by acid fumigation for measuring the δ 13 C of soil organic carbon. Can. J. Soil Sci. 91, 247–250. https://doi.org/10.4141/cjss10066

Ray, A., Barsugli, J., Averyt, K., 2008. Climate change in Colorado: a synthesis to support water resources management and adaptation, Intermountain West Climate Summary. https://doi.org/10.1007/s12010-007-8035-9

Reitz, M.D., Jerolmack, D.J., Ewing, R.C., Martin, R.L., 2010. Barchan-parabolic dune pattern transition from vegetation stability threshold. Geophys. Res. Lett. 37, 1–5. https://doi.org/10.1029/2010GL044957

Rhoades, J.D., 1982. Cation exchange capacity, in: Page, A.L., Miller, R.H., Keeney, D.R. (Eds.), Methods of Soil Analysis, Part 2: Chemical and Microbiological Properties. American Society of Agronomy, Inc.; Soil Science Society of America. Inc., Madison, Wisc., pp. 149–157.

Roskin, J., Blumberg, D.G., Katra, I., 2014. Last millennium development and dynamics of vegetated linear dunes inferred from ground-penetrating radar and optically stimulated luminescence ages. Sedimentology 61, 1240–1260. https://doi.org/10.1111/sed.12099

Schaetzl, R., Anderson, S., 2005. Soils: Genesis and Geomorphology. Cambridge University Press, New York.

Schmeisser McKean, R.L., Goble, R.J., Mason, J.B., Swinehart, J.B., Loope, D.B., 2015. Temporal and spatial variability in dune reactivation across the Nebraska Sand Hills, USA. Holocene 25, 523–535. https://doi.org/10.1177/0959683614561889

Schmeisser, R.L., Loope, D.B., Mason, J.A., 2010. Modern and late Holocene wind regimes over the Great Plains (central U.S.A.). Quat. Sci. Rev. 29, 554–566. https://doi.org/10.1016/j.quascirev.2009.11.003

Schmeisser, R.L., Loope, D.B., Wedin, D.A., 2009. Clues to the Medieval destabilization of the Nebraska Sand Hills, USA, from ancient pocket gopher burrows. Palaios 24, 809–817.

Seifan, M., 2009. Long-term effects of anthropogenic activities on semi-arid sand dunes. J. Arid Environ. 73, 332–337. https://doi.org/10.1016/j.jaridenv.2008.10.009

Shay, J.M., Herring, M., Dyck, B.S., 2000. Dune colonization in the Bald Head Hills, southwestern Manitoba. Can. Field-Naturalist 114, 612–627.

Siegal, Z., Tsoar, H., Karnieli, A., 2013. Effects of prolonged drought on the vegetation cover of sand dunes in the nw negev desert: Field survey, remote sensing and conceptual modeling. Aeolian Res. 9, 161–173. https://doi.org/10.1016/j.aeolia.2013.02.002

Smalley, I.J., Vita-Finzi, C., 1968. The formation of fine particles in sandy deserts and the nature Of "desert" loess. SEPM J. Sediment. Res. Vol. 38, 766–774. https://doi.org/10.1306/74D71A69-2B21-11D7-8648000102C1865D

Sridhar, V., Loope, D.B., Swinehart, J.B., Mason, J.A., Oglesby, R.J., Rowe, C., 2006. Large wind shift on the Great Plains during the Medieval Warm Period. Science (80-.). 313, 345–347.

Sridhar, V., Wedin, D.A., 2009. Hydrological behaviour of grasslands of the Sandhills of Nebraska: water and energy-balance assessment from measurements, treatments, and modelling. Ecohydrology 2, 195–212. https://doi.org/10.1002/eco.61

Sweeney, M.R., Loope, D.B., 2001. Holocene dune-sourced alluvial fans in the Nebraska Sand Hills. Geomorphology 38, 31–46. https://doi.org/10.1016/S0169-555X(00)00067-2

Swinehart, J.B., Loope, D.B., 1992. A giant dune-dammed lake on the North Platte River, Nebraska. Geol. Soc. Am. Abstr. with Programs 24, A51.

Thomas, D.S.G., Knight, M., Wiggs, G.F.S., 2005. Remobilization of southern African desert dune systems by twenty-first century global warming. Nature 435, 1218–1221. https://doi.org/10.1038/nature03717

Wang, T., Zlotnik, V.A., Wedin, D., Wally, K.D., 2008. Spatial trends in saturated hydraulic conductivity of vegetated dunes in the Nebraska Sand Hills: Effects of depth and topography. J. Hydrol. 349, 88–97. https://doi.org/10.1016/j.jhydrol.2007.10.027

Wang, X., Dong, Z., Yan, P., Yang, Z., Hu, Z., 2005. Surface sample collection and dust source analysis in northwestern China. Catena 59, 35–53. https://doi.org/10.1016/j.catena.2004.05.009

Wang, Y., Yan, X., Wang, Z., 2016. A preliminary study to investigate the biogeophysical impact of desertification on climate based on different latitudinal bands. Int. J. Climatol. 36, 945–955. https://doi.org/10.1002/joc.4396

Werner, C.M., Mason, J.A., Hanson, P.R., 2011. Non-linear connections between dune activity and climate in the High Plains, Kansas and Oklahoma, USA. Quat. Res. 75, 267–277. https://doi.org/10.1016/j.yqres.2010.08.001

Williams, J.W., Jackson, S.T., Kutzbach, J.E., 2007. Projected distributions of novel and disappearing climates by 2100 AD. Proc. Natl. Acad. Sci. 104, 5738–5742. https://doi.org/10.1073/pnas.0606292104

Winspear, N.R., Pye, K., 1995. Textural, geochemical and mineralogical evidence for the origin of peoria loess in Central and Southern Nebraska, USA. Earth Surf. Process. Landforms 20, 735–745. https://doi.org/10.1002/esp.3290200805

Wolfe, S.A., David, P.P., 1997. Parabolic dunes: Examples from the Great Sand Hills, southwestern Saskatchewan. Can. Geogr. 41, 207–13.

Wolfe, S.A., Hugenholtz, C.H., 2009. Barchan dunes stabilized under recent climate warming on the northern Great Plains. Geology 37, 1039–1042. https://doi.org/10.1130/G30334A.1

Worster, D., 1982. Dust Bowl: The Southern Plains in the 1930s. Oxford University Press, New York.

Xu, Z., Mason, J.A., Lu, H., 2015. Vegetated dune morphodynamics during recent stabilization of the Mu Us dune field, north-central China. Geomorphology 228, 486–503. https://doi.org/10.1016/j.geomorph.2014.10.001

Yan, Y., Xu, X., Xin, X., Yang, G., Wang, X., Yan, R., Chen, B., 2011. Effect of vegetation coverage on aeolian dust accumulation in a semiarid steppe of northern China. Catena 87, 351–356. https://doi.org/10.1016/j.catena.2011.07.002

Yang, Y., Mason, J.A., Zhang, H., Lu, H., Ji, J., Chen, J., Liu, L., 2017. Provenance of loess in the central Great Plains, U.S.A. based on Nd-Sr isotopic composition, and paleoenvironmental implications. Quat. Sci. Rev. 173, 114–123. https://doi.org/10.1016/j.quascirev.2017.08.009

Yizhaq, H., Ashkenazy, Y., Tsoar, H., 2007. Why do active and stabilized dunes coexist under the same climatic conditions? Phys. Rev. Lett. 98, 98–101. https://doi.org/10.1103/PhysRevLett.98.188001